Context Dependent Neural Control of Gaze Shifts

by

Ivan Smalianchuk

B.S. in Neuroscience, University of Pittsburgh, 2013

B.S. in Psychology, University of Pittsburgh, 2013

Submitted to the Graduate Faculty of the

Swanson School of Engineering in partial fulfillment

of the requirements for the degree of

Doctor of Philosophy

University of Pittsburgh

2022

UNIVERSITY OF PITTSBURGH

SWANSON SCHOOL OF ENGINEERING

This dissertation was presented

by

Ivan Smalianchuk

It was defended on

January 13, 2022

and approved by

Neeraj Gandhi, PhD, Professor, Department of Bioengineering

Aaron Batista, PhD, Professor, Department of Bioengineering

Omar El Gharbawie, PhD, Assistant Professor, Department of Neurobiology

Matthew Smith, PhD, Associate Professor, Department of Biomedical Engineering (CMU)

Dissertation Director: Neeraj Gandhi, PhD, Professor, Department of Bioengineering

Context Dependent Neural Control of Gaze Shifts

Ivan Smalianchuk, PhD

University of Pittsburgh, 2022

We explore our environment by looking at objects of interest. In order to precisely direct our visual axis where we intend, we must generate a series of movements with our eyes and head, which shift our gaze to the desired location. A number of neural structures provide control for such behavior, each acting as a unique contributor to either higher- or lower-level movement properties of the action. Some structures, such as the superior colliculus (SC), influence the metrics and kinematics of gaze shifts, e.g., controlling the direction, amplitude, and velocity of a saccade. Others, like the ventral premotor cortex (PMv), monitor the context of the movement, presumably differentiating whether the gaze shift was made to search for food or to locate a threat. Here, we aim to present an overarching view of these neural systems by exploring both the kinematics and context of gaze shifts.

Systematic manipulation of the visual environment was used to explore neural and behavioral features underlying gaze shifts. In the first study, we instructed the subjects to generate saccades to targets on the screen while we recorded single cell spiking activity from the SC. We then utilized statistical techniques to determine instantaneous SC control over saccade velocity. In the second study we recorded from the PMv and instructed the subject to perform gaze shifts that either preceded or followed a head movement. We aimed to establish context-dependent PMv activity modulation. In the last study we explored the ability of the systems to adapt to a predetermined environmental change. We aimed to induce a context (color) dependent saccadic adaptation. In tandem, these studies explore the span of neural control of gaze shifts ranging from low-level kinematics control to high-level context dependency.

Table of Contents

Preface x

Acknowledgements xi

1.0 General Introduction 1

1.1 Gaze Control 3

1.1.1 Superior Colliculus 3

1.1.2 Ventral Premotor Cortex 4

1.2 Mechanisms Of Gaze Shifts 5

1.2.1 Cortical 5

1.2.2 Midbrain 6

1.3 Research Objectives 6

1.3.1 Knowledge Gap 7

1.3.2 Research Strategy 8

2.0 Instantaneous Midbrain Control of Saccade Velocity 10

2.1 Overview 10

2.2 Significance Statement 11

2.3 Introduction 11

2.4 Methods 13

2.4.1 Experimental Design and Statistical Analyses 18

2.5 Results 19

2.6 Discussion 30

2.6.1 Revised View of Neural Control Of Saccades: A Speculation 34

2.7 Acknowledgements 39

3.0 Ventral Premotor Cortex Encodes Task Relevant Features in Eye and Head Movements 40

3.1 Overview 40

3.2 Introduction 41

3.3 Methods 44

3.3.1 Behavioral Tasks 45

3.3.2 Neural Data Collection 48

3.3.3 Data Analysis 50

3.3.4 Decoder 53

3.3.5 Cortical Depth Analysis 55

3.4 Results 56

3.4.1 Single Neuron Analysis 57

3.4.2 Pseudo Population Analysis 61

3.4.3 Classification 64

3.4.4 Depth 66

3.4.5 Summary 66

3.5 Discussion 67

4.0 Color Cannot Act as A Contextual Cue During Monkey Saccadic Adaptation 72

4.1 Overview 72

4.2 Introduction 73

4.3 Materials and Methods 75

4.3.1 Trial Types 76

4.3.2 Target Characteristics and Locations 79

4.3.3 Experimental Sessions 80

4.3.4 Data Acquisition and Analysis 80

4.4 Results 82

4.4.1 General Hypothesis and Predictions 82

4.4.2 Horizontal Concurrent Experiments 86

4.4.3 Horizontal Sequential Experiments 88

4.4.4 Single Target Displacement, Orthogonal and Vector Concurrent Experiments 91

4.5 Discussion 97

4.5.1 Major Observations 97

4.5.2 Context Dependent Adaptation: Comparisons to Previous Observations ... 97

4.5.3 Physiological Implications 99

4.5.4 Superior Colliculus 99

4.5.5 Cerebellum 104

4.5.6 Cortex 105

4.6 Acknowlegements 106

5.0 Discussion and conclusions 107

5.1 Summary 107

5.2 Future Directions 108

5.3 Final Thoughts 110

Bibliography 111

List of Figures

Figure 1: Illustration of across-trial analysis for normal saccades. 17

Figure 2: Temporal profiles of eye velocity and neural activity for normal saccades..... 20

Figure 3: Summary of within- and across-trial correlation analyses for normal saccades. 22

Figure 4: Temporal characteristics of activity-velocity correlation. 24

Figure 5: Analysis of data recorded from laminar probes..... 25

Figure 6: Illustration of across-trial analysis for blink-perturbed saccades. 27

Figure 7: Comparison of correlation analyses for blink-perturbed and normal saccades. . 28

Figure 8: Linear regression features between SC activity and eye velocity. 30

Figure 9: Alternate models of neural control of saccades. 36

Figure 10: Task types..... 47

Figure 11: Track Locations. 49

Figure 12: Example cell which showed significant modulation for every task type. 58

Figure 13: Average neural activity traces by trial type. 59

Figure 14: Cells with significant response to task type. 60

Figure 15: Representative illustrations from PCA and LDA analysis. 63

Figure 16: Naïve bayes performance..... 65

Figure 17: LDA performed on separate layers of the cortex for gaze and head movement epochs during the eye-first task. 66

Figure 18: Delayed Probe probe and backward adaptation trial types and target locations. 78

Figure 19: Predictions based on alternative hypotheses concerning the use of color as a contextual cue during concurrent (Panels A, B) and sequential (C, D) horizontal adaptation experiments. 84

Figure 20: Horizontal Concurrent Experiments..... 87

Figure 21: Horizontal Sequential Experiments..... 90

Figure 22: Backward-Null Experiments..... 92

Figure 23: Orthogonal Concurrent Experiments. 93

Figure 24: Vector Concurrent Experiments..... 96

Preface

The chapters in this dissertation are standalone manuscripts that have been either published in full or are under preparation to be published.

Chapter 2: Smalianchuk, I., Jagadisan, U. K., & Gandhi, N. J. (2018). Instantaneous Midbrain Control of Saccade Velocity. *The Journal of Neuroscience: The Official Journal of the Society for Neuroscience*, *38*(47), 10156–10167. https://doi.org/10.1523/JNEUROSCI.0962-18.2018

Chapter 3: Manuscript under preparation for publication.

Chapter 4: Cecala, A. L., Smalianchuk, I., Khanna, S. B., Smith, M. A., & Gandhi, N. J. (2015). Context cue-dependent saccadic adaptation in rhesus macaques cannot be elicited using color. *Journal of Neurophysiology*, *114*(1), 570–584. https://doi.org/10.1152/jn.00666.2014

Acknowledgements

It is beyond my ability to express in written words my appreciation for all those who have supported and guided me through this process; but I will try nonetheless. First, I must extend the greatest gratitude to Dr. Neeraj Gandhi for putting up with my shenanigans for close to a decade. In all seriousness, I could not imagine a better mentor. His exceptionally high standards forced me to elevate my own abilities to meet them. On the other hand, he never micromanaged and let me do things my own way (and often fail in a dramatic fashion) which nurtured confidence and independence. I don't think I have ever heard him say "no" to any idea that was well thought out. He was always there with a helping hand, or with expert advice. In the laboratory Raj is a strict, demanding, no-nonsense personality with little patience for laziness; while outside the lab he is a relaxed, easy going, happy person. The dichotomy is so stark that my wife, who only met him in social situations, still does not believe me when I tell her about Raj in the lab. Even this showed me a perspective which taught me to compartmentalize and take seriously those things that demand it, while not letting it spill over to those things that don't. I could write pages discussing the lessons I learned under Raj's mentorship, but I must not forget all others that helped me.

I would like to thank Dr. Aaron Batista for everything he has done for me. I joined his lab as an undergraduate student in 2010 and he showed me the ropes of working in a neural lab. There I learned the skills which encompassed the foundation for my graduate career: basics of recording and analyzing neural data, working with NHPs, presenting my work in an effective manner, etc. More than that, Aaron's mentorship opened doors and opportunities for me that I could not obtain by myself. He was the one who recommended me to Raj when I was applying for graduate schools, and he is a major influence in the course my life took after that. Unsurprisingly, he is a part of my

dissertation committee, so he has literally witnessed my academic bioengineering journey from the very beginning to the very end.

I must not forget all the support my lab mates have given me. Specifically, I must thank Dr. Uday Jagadisan: a great friend with whom I just can't seem to find the time to talk. For years, Uday and I were the only two students in Raj's lab and were left completely to our own devices to do science however we saw fit. The lengthy discussions of math concepts around that white board were some of my favorite parts of being in the lab. Also, I would like to thank (soon to be Dr.) Michelle Heusser, who joined the lab a bit later on, and immediately became a good friend. She was (and is) always eager to help, be it with proof-reading manuscripts or listening to practice presentations. And outside of the lab she is probably my last connection to any semblance of a social life.

This is the point where I wish writing was a non-linear method of expression, as I wish that everyone in this section was at the top alongside Raj and Aaron. I will forever be grateful to my family. My mother and my father are incredibly supportive. An 8.5-year graduate path is an absurdly long one, and they have been helping me through it the whole way. Their love and patience got me through this, and I will forever be thankful to them for that. As for my brother, Aleksey, I can't even find the words to express how much his help and friendship meant to me. He has helped me through crisis after crisis (I'm a very crisis prone person apparently) with the stability of a rock. I could lean on him for support 24/7, and without him I would not have finished this program.

With the risk of sounding cliché: last but not least I must thank my wife, Christine. She has been with me before I was a graduate student and has witnessed me at my highest and lowest during this part of my life. Without her daily encouragement and support I would have given up

in this path many years ago. When all went wrong in the lab to the point of critical failure, when all seemed completely hopeless, when things got as dark as they could get, she was the light that got me through that. I love you, Christine, and I will never forget your unrelenting support.

1.0 General Introduction

Accurate exploration of the visual world is key to survival. A monkey that hears a rustling in the leaves must make a quick and accurate gaze shift to examine whether the sound was made by a potential mate, a territorial rival, or a deadly snake. The simple act of orienting gaze to an object of interest can make the difference between life and death. Therefore, those animals that rely on vision to explore their environment (notably primates) have developed complicated neural systems that provide precise and coordinated control over muscle groups that govern gaze shifts. Consequently, trauma or disease-induced disruptions and disorders of these systems severely diminish the quality of life of individuals. Here we aim to advance the knowledge of gaze-shift systems and provide a step towards the progress of treatment and mitigation of these disorders.

We can imagine two opposing scenarios. In one, you are talking to your friend while making polite eye contact, when you hear somebody try to get your attention nearby. You start turning your head towards the sound in preparation to examine who is calling you, while keeping eye contact with your friend until a natural break in the conversation presents itself and you move your eyes to locate the sound. In another scenario, instead of someone trying to get your attention, you hear a sharp, loud noise. Politeness goes out the window as you immediately break eye contact to orient your gaze to the source of the noise. In this scenario, when you are not consciously repressing the eye movement, your eyes will start moving before your head (Goldring et al., 1996). In both scenarios we can imagine that individual components (head and eyes) can share the same kinematics, albeit performed in different order. We hypothesize that this phenomenon is governed, or monitored, by a cortical structure specializing in higher-order movement properties, specifically the ventral premotor cortex.

Conversely, while some structures in the system monitor higher-order properties of movements, some take on the role of governing the lower-order properties such as metrics and kinematics of the behavior. The study of cortical and subcortical control of gaze shifts (specifically eye movements) is one of the oldest categories in neuroscience. Despite the volume of work done in this field, the specifics of the system are yet to be agreed upon. For instance, saccade velocities can be described on average by the main sequence: a relationship between peak eye velocity and saccade amplitude. However, individual saccades show variable velocity profiles. A saccade 10 degrees in amplitude could have a slow rising phase of the velocity profile and a fast drop-off, or a fast rising phase and a slow drop-off, and yet still have the same endpoint. Some speculate that this instantaneous control of saccade velocities happens later in the eye-movement system, perhaps at the level of excitatory burst neurons and further (Van Gisbergen et al., 1981). We, however, propose that a significant part of this control happens as early as in the superior colliculus.

Through examination of the superior colliculus (SC) and the ventral premotor cortex (PMv) we describe both the lower-level motor control properties of saccades, as well as the higher-level monitoring of the context in the execution of head unrestrained gaze shifts. We further explore the context dependency of gaze shifts by evaluating the ability of this system to adapt the kinematics of the gaze shift based on contextual color cues. The work presented in this dissertation examines a subset of many gaze-shift related systems in order to contribute to a more complete understanding of these processes.

1.1 Gaze Control

By and large, one can separate gaze control motor systems into oculomotor and skeletomotor. Barring some extreme examples, movement of the eyes (oculomotor system) is synonymous with movement of gaze. On the other hand, only a small fraction of the skeletomotor system is dedicated to aiding gaze shifts. Taking this into consideration, it is unsurprising to see that vast majority of gaze-related literature examines oculomotor system in isolation. Consequently, we can describe the neural control of eye movements surprisingly well when the head and the body of the subject is restrained. However, once the subject is allowed freedom to move, our description of the neural control of gaze shifts are found lacking. To obtain a complete understanding of neural substrates of gaze shifts, we must take both motor systems into consideration.

1.1.1 Superior Colliculus

The superior colliculus is a midbrain structure that, among other functions, governs the generation of gaze shifts. The SC can be divided into seven distinct layers that have a sensory-motor gradient as you traverse them. The superficial layers, which receive projections from the retina (primary and secondary visual cortex, and frontal eye fields, among others), are responsive to visual stimuli. The middle and deep layers, which receive projections from various motor and sensory cortical areas as well as well as the substantia nigra and the basal ganglia, generate motor commands as well as respond to visual stimuli. The deeper layers tend to have a stronger motor component, in some instances having no visual response at all.

In SC, the motor command is expressed as a "burst" of action potentials in a particular set of neurons. The frequency of that burst is maximal for a particular direction and amplitude of a saccade (Munoz & Wurtz, 1995). Cells that generate similar saccade vectors are grouped together, which creates a topographic map on the surface of the SC. Cells that generate small amplitude saccades are located rostrally in the structure while those that generate larger saccades reside caudally. A larger portion of the population is dedicated to generating smaller saccades than larger, which results in a larger region of the SC being responsible for smaller-amplitude movements.

1.1.2 Ventral Premotor Cortex

The ventral premotor cortex resides posterior to the arcuate sulcus and anterior to the primary motor cortex. It is unique from the primary motor cortex as PMv has a faint granular level, which makes it more akin to the 6-layered prefrontal cortex (Barbas & Pandya, 1987). The cellular activity of PMv is diverse: cells respond to visual as well as tactile stimuli (Fogassi et al., 1996; Graziano et al., 1997; Graziano & Gross, 1998). Motor commands in PMv range from upper skeletal movements to ocular and facial movements (Maranesi et al., 2012; Neromyliotis & Moschovakis, 2017).

The precise role of PMv is not well understood. Electrical microstimulation of the region produces a vast array of both complex and simple behaviors (Grivaz et al., 2017) but lesioning or inactivation of the structure does not produce catastrophic deficits (Kurata & Hoffman, 1994; Schieber, 2000; Schmidlin et al., 2008). This region is established in the coordinated control of several muscle groups—most notably that of the arm, hand, and face/mouth (Bonini et al., 2012; Cooke, 2004; Graziano et al., 2002; Vargas-Irwin et al., 2015). Additionally, PMv is notable for the presence of mirror neurons, a subset of neurons that are active both for the performance of a

certain behavior as well as for an observation of that behavior performed by someone else (Bonini et al., 2013; Coude et al., 2016; Rochat et al., 2010).

1.2 Mechanisms Of Gaze Shifts

1.2.1 Cortical

Within the cortex, the structures that are most noted for generating gaze shifts are the frontal eye fields (FEF), supplementary eye fields (SEF), dorsolateral prefrontal cortex (dlPFC), and the posterior parietal cortex (PPC) (Bruce et al., 1985; Chen & Walton, 2005; Fujii et al., 1995; Galeazzi et al., 2016; Heinze et al., 2014; Knight & Fuchs, 2007). In general, these structures project either to each other, to the midbrain, or to both, and create a complex network that governs gaze shifts. For example, a signal generated in the FEF travels down to the SC, which processes this signal and integrates it into the midbrain mechanisms of gaze shifts (Hanes & Wurtz, 2001). Meanwhile, parallel signals are sent at every step. For instance, the FEF sends signals to dlPFC and SEF, which in turn send their own processed signals to the SC (Gaymard et al., 1998). Describing the specifics of these interactions is well outside of scope of this dissertation, as they are an entire field unto themselves, yet they must be mentioned nonetheless.

A notable absence in this network, however, are non-oculomotor structures that also contribute to gaze shifts. PMv, for instance, rarely enters the domain of gaze shift literature, and more often than not its role is only examined when coupled to another movement, such as a reach or a grasp. Its role in eye-hand and eye-head coupled movements are well-established (Boulanger

et al., 2009; Neromyliotis & Moschovakis, 2017), and yet it is often overlooked in the gaze-shift domain.

1.2.2 Midbrain

Brainstem connectivity for saccade generation has been well documented. A signal in the SC travels to the paramedian pontine reticular formation (PPRF), which contains the excitatory and inhibitory burst neurons that send a signal to the appropriate motoneurons in order to generate a horizontal saccade. The signal from the SC is a burst-like series of action potentials originating from a specific region of the structure.

As discussed above, the SC has a topographic map that dictates the amplitude and the direction of the saccade. An increase of neural activity centered at a particular point on the map indicates a desired displacement of the eye, and it has been suggested that downstream areas receive this information and generate the muscle contractions needed for that desired displacement. This model assumes SC output to be a discrete command, a notion that we challenge in this dissertation.

1.3 Research Objectives

The study of neural control of gaze shifts is one of the oldest disciplines in motor-related neuroscience. Despite the volume of work completed on the subject, gaps in knowledge are fairly prominent. The midbrain models for gaze shifts rely on several assumptions and leave room to be improved upon, and the exploration of cortical control of head-unrestrained gaze shifts is sparse.

Furthermore, the effect of context on the neural control of gaze-shifts is as of yet poorly understood. The objective of the research presented in this document is to close these gaps through systematic exploration of both cortical and subcortical gaze-shift contributors.

1.3.1 Knowledge Gap

The discussion in the general introduction points at several gaps in the field's current knowledge of neural control systems governing gaze-shifts. For instance, there is not a clear agreement on the mechanisms behind even the simplest eye movements such as saccades. Specifically, the details behind the control of gaze-shift kinematics are still debated. We address this shortcoming by proposing an alternative to the traditional model for saccade generation. Specifically, we suggest that the SC plays a direct role in controlling the instantaneous velocity of saccades.

Additionally, there is a notable scarcity of research on head-unrestrained gaze shifts. By virtue of the technical difficulty of recording neural activity in a freely-moving head, most oculomotor studies are performed on head-restrained animals, which reduces gaze shifts to just eye movements. This, in turn, somewhat diminishes the role head movements have in natural gaze shifts and the role oculomotor system has in head-movement control during these tasks. We address this by recording from the PMv of a head-unrestrained animal while it performs gaze shifts.

Finally, the volume of literature describing low-level mechanistic aspects of neural gaze-shift systems far outweighs descriptions of high-level principles behind these movements. We have general models that describe the governance of eye movement properties, but we lack convincing theories about how high-level control affects these models. Specifically, it is not clear how the

context of gaze shifts is represented in the neural code. We close this gap in knowledge by exploring PMv activity while the subject performs gaze shifts under different contexts. Additionally, we determine whether non-volitional gaze shift paradigms (e.g., saccadic adaptation) can be influenced by the context of the task.

1.3.2 Research Strategy

The SC generates a command that determines the desired displacement of the foveation point. However, other parameters of this command, usually expressed as a burst of action potentials, have been linked to properties of movement; specifically, the peak firing rate of the burst is indicative of the peak saccade velocity (Edelman & Goldberg, 2001). We expanded that notion to explore whether the burst affects the eye velocity at any other time period. Specifically, we utilized across- and within-trial statistical techniques to determine to what extent the instantaneous firing rate predicts the instantaneous eye velocity and at what delay.

The activity in the PMv represents the movements of multiple muscle groups. Some anatomical findings show that a particular region of the PMv projects to both eye and neck muscles (Billig & Strick, 2012). We recorded the activity of individual neurons in that region while a subject was performing specific behavioral tasks. We designed the tasks to differentiate the context for the gaze shift as well as temporally separate the movement of individual effectors (eyes and head). Statistical tests were used to indicate correlations between the firing rate and various task-related properties. We then used dimensionality reduction techniques to further investigate the patterns of neural activity as a function of task parameters.

To further assess the effect of context on gaze-shift systems, we explored whether a color-code could influence saccadic adaptation. When the oculomotor system detects a repeated error in

an executed movement, it adjusts to correct for it. For example, if we intend to make a 10 degree saccade, and the visual assessment for accuracy post-movement shows that we generated only an 8 degree saccade, the system will adjust to correct for the error in the future (Albano, 1996; Deubel, 1987). We can manipulate this phenomenon by moving the target on the screen mid-saccade and generate a false error that the system will attempt to correct for. If the system is sensitive to the color-context of the gaze shift, then only introducing this false error when a target is a specific color would induce the correction for this color specifically, and no other color.

These experiments provide insight into the overarching neural mechanisms behind gaze shifts. The results presented in this document span a range of foci from high-level concepts, such as context influence on movement, to lower-level control of movement parameters.

2.0 Instantaneous Midbrain Control of Saccade Velocity

2.1 Overview

The ability to interact with our environment requires the brain to transform spatially-represented sensory signals into temporally-encoded motor commands for appropriate control of the relevant effectors. For visually-guided eye movements, or saccades, the superior colliculus (SC) is assumed to be the final stage of spatial representation, and instantaneous control of the movement is achieved through a rate code representation in the lower brain stem. We investigated whether SC activity in nonhuman primates (*Macaca mulatta*, 2 male and 1 female) also employs a dynamic rate code, in addition to the spatial representation. Noting that the kinematics of amplitude-matched movements exhibit trial-to-trial variability, we regressed instantaneous SC activity with instantaneous eye velocity and found a robust correlation throughout saccade duration. Peak correlation was tightly linked to time of peak velocity, the optimal efferent delay between SC activity and eye velocity was constant at $\sim 12\ ms$ both at onset and during the saccade, and SC neurons with higher firing rates exhibited stronger correlations. Moreover, the strong correlative relationship and constant efferent delay observation were preserved when eye movement profiles were substantially altered by a blink-induced perturbation. These results indicate that the rate code of individual SC neurons can control instantaneous eye velocity and argue against a serial process of spatial-to-temporal transformation. They also motivated us to consider a new framework of saccade control that does not incorporate traditionally accepted elements, like the comparator and resettable integrator, whose neural correlates have remained elusive.

2.2 Significance Statement

All movements exhibit time-varying features that are under instantaneous control of the innervating neural command. At what stage in the brain is dynamical control present? It is well known that, in the skeletomotor system, neurons in the motor cortex employ dynamical control. In the oculomotor system, in contrast, instantaneous velocity control of saccadic eye movements is not thought to be enforced until the lower brainstem. Using correlations between residual signals across trials, we show that instantaneous control of saccade velocity is present earlier in the visuo-oculomotor neuraxis, at the level of superior colliculus. The results require us to consider alternate frameworks of the neural control of saccades.

2.3 Introduction

Even when we want to produce the same movement repeatedly, our action exhibits heterogeneity across repetitions. Thus, variability in intended identical swings of a golf club, for example, yield different trajectories of the club, and therefore the ball. It is possible that variability in the swing could be the result of biological noise in the effectors, although a more likely explanation points to a neural origin (Carmena et al., 2005; Churchland et al., 2006a; van Beers, 2007, 2008). While potential neural sources of movement variability have been extensively studied for hand movements (for a review, see Churchland, 2015), less is known for eye movements, particularly the ballistic type known as saccades.

The superior colliculus (SC), a laminar subcortical structure with a topographic organization of the saccade motor map, is a central node in the oculomotor neuraxis (Gandhi and

Katnani, 2011; Basso and May, 2017). It is intimately linked to the spatiotemporal transformation, in which visuo-oculomotor signals in the SC conform to a space or place code, while recipient structures in the brainstem exhibit a rate code. In a slight modification to this framework - the so-called dual coding hypothesis (Sparks and Mays, 1990; Waitzman et al., 1991) - saccade amplitude and direction are computed from the locus of population activity in the SC, while movement velocity is a "determinant" of the firing rate. The strongest evidence for SC control of saccade velocity comes from causal studies demonstrating that peak eye velocity is correlated with frequency or intensity of electrical microstimulation (Stanford et al., 1996; Katnani and Gandhi, 2012) and that peak velocity is attenuated after inactivation of SC (Lee et al., 1988). However, these results only address the distribution of static saccade descriptors, falling short of explaining dynamic properties of the movement (e.g. instantaneous velocity). Another set of studies has advanced the so-called dynamic vector summation model (Goossens and Van Opstal, 2006; Goossens and van Opstal, 2012), in which the SC controls the desired displacement of the eye through a series of "mini-vectors". Instantaneous control of desired velocity is implicit but not explicitly addressed in this framework.

We tested the hypothesis that SC activity dynamically mediates instantaneous velocity control of saccades. As indicated intuitively, a time-series correlation was first performed by regressing the temporal evolution of SC activity with eye movement profile for each trial, and examining the average of the correlation coefficients. This analysis, by definition, cannot reveal which epoch(s) of the waveforms contributes most significantly to the correlation, and at what transduction time. We addressed these limitations by correlating the instantaneous neural activity and eye velocity across trials, an ensemble approach that calculates the correlation between firing rate and velocity on an individual timepoint basis. Moreover, we focused the analyses only on

amplitude-matched movements for each neuron, thus removing confounds of saccade size in the correlation of across-trials variability. This strategy determines how individual trial differences are reflected in the SC code and differentiates itself from previous efforts that correlated neural activity and behavior as the trial progresses in time (Waitzman et al., 1991; Keller and Edelman, 1994; Goossens and Van Opstal, 2006). It also identifies a putative optimal efferent delay between SC activity and eye velocity. We found that instantaneous residual firing rate strongly correlates with instantaneous residual velocity for both within-trial and across-trials analyses. The peak correlation was best aligned with the time of peak eye velocity, and at a population level, the correlation was significant throughout the movement and at a constant efferent delay of $\sim 12\ ms$. For laminar recording sessions with simultaneously recorded population activity, neurons with the highest firing rates within individual penetrations displayed the strongest correlation. Finally, these relationships were observed not only for ballistic-like, bell-shaped velocity waveforms of normal saccades but also for profiles altered by blink perturbations. Thus, individual SC neurons exhibit a code that can control instantaneous eye velocity, akin to how primary motor cortex controls hand velocity (Ashe and Georgopoulos, 1994; Reina et al., 2001).

2.4 Methods

Three adult rhesus monkeys (*Macaca mulatta*, 2 male and 1 female, ages 8, 10 and 12, respectively) were used for the study. All procedures were approved by the Institutional Animal Care and Use Committee at the University of Pittsburgh and were in compliance with the US Public Health Service policy on the humane care and use of laboratory animals.

Extracellular spiking activity of SC neurons was recorded as head-restrained animals performed a visually-guided, delayed saccade task, with a variable delay of 500-1200ms, under real-time control with a LabVIEW-based controller interface (Bryant and Gandhi, 2005); task design details can be found in a separate study (Jagadisan and Gandhi, 2017). Neural activity was collected with either a multi-contact laminar probe (Alpha Omega; 16 channels, 150 μm inter-contact distance, ~1 MΩ impedance of each contact) or a standard tungsten microelectrode (Microprobes, ~1 MΩ impedance). All electrode penetrations were orthogonal to the SC surface, so that roughly the same motor vector was encoded across the layers. The saccade target was presented either near the center of the neuron's movement field or at the diametrically opposite location. This study reports analyses from 189 neurons, 145 of which were collected with a laminar probe across 18 sessions, and the remaining 44 neurons were recorded with a single electrode (Jagadisan and Gandhi, 2017). All neurons can be classified as visuomotor or motor neurons according to the criterion that activity in the visual epoch (100-250 ms following target onset) or the premotor epoch (-100 to 50 ms around saccade onset) be significantly greater than baseline activity (Wilcoxon rank-sum test, $p<0.01$) (Jagadisan and Gandhi, 2016).

Blink perturbation data were only available for 50 neurons, 43 of which were studied with the single electrode setup and the remaining 7 from a single laminar electrode session. On approximately 15-20% of the trials, an air-puff was delivered to one eye to evoke the trigeminal blink reflex. The puff was timed to induce a blink around the time of saccade onset or even trigger the eye movement prematurely. In this case, blink-triggered saccades provide a valuable control against spurious correlations, as the velocity profile of the saccade is altered compared to that of a normal movement and endpoint accuracy is preserved. Thus, if SC dynamically controls the kinematics of the saccade, the perturbed velocity waveforms should be predicted by the SC activity

as well. For full disclosure, the data from these 50 neurons are the same as those reported in a previous publication (Jagadisan & Gandhi 2017). The key distinction is that the previous study assayed SC activity during the saccade preparation phase, and now the focus is on the peri-saccade period.

Eye and eyelid movements were detected using the magnetic search coil method. Spike trains were converted to a spike density waveform by convolution with a 5 ms Gaussian kernel. All movements were aligned on saccade onset. Standard velocity criteria were used to detect the onset (30 deg/s) and offset (20 deg/s) of normal saccades. For blink-triggered movements, the onset of saccadic component was estimated as the time of a deviation from a spatiotemporal template of a blink related eye movement induced during fixation (Katnani and Gandhi, 2013). The movement profiles were then represented as radial velocity, in which positive values indicate motion towards the movement field and negative values away (Jagadisan and Gandhi, 2017); this differs from the common method in which vectorial velocity representation is always positive and independent of the ideal saccade path towards the target. In other words, vectorial velocity is simply the hypotenuse of the x and y velocities of the eye movement, whereas radial velocity tells us the speed at which the visual axis is moving towards or away from the cell's movement field. This distinction is vital, as we were not able to observe the effects described later when using traditional vectorial coordinates. To remove potential confounds of saccade amplitude on correlations between spiking activity and radial velocity, we additionally limited each neuron's dataset to movements within ±5% of the mean amplitude. Range of mean amplitude across all neurons spanned 8-25 degrees (median: 12 degrees) and, for the analysis comparing normal and blink-perturbed movements, at least 20 trials were available for each condition. All 189 neurons passed the inclusion criteria, 50 of which also had amplitude-matched blink perturbation trials.

This pruning yields amplitude-matched movements that still exhibit trial-by-trial variability in their velocity profiles, which constitute the key data for correlation with the corresponding SC activity.

All computations were performed using MATLAB 2016b (RRID:SCR_001622). To perform the correlation analysis, we started with temporal waveforms of eye velocity and corresponding neural activity for each cell (Figure 1A). We then subtracted the session's mean velocity and spike density waveforms from each trial data to obtain the respective residuals (Figure 1B). This important step removes spurious correlations from generally similar shapes of SC activity and saccade velocity. For within-trial analysis, a Pearson's correlation was determined for each trial's residual velocity and neural activity waveforms. The two residual vectors were shifted relative to each other from $100\ ms$ to $-100\ ms$ in $1\ ms$ increments, and the Pearson's correlation was calculated for each delay (Δt). A zero delay indicates that both vectors are aligned on saccade onset. Negative delays signify instances when the neural activity preceded the velocity, which we refer to as an efferent delay (ED). This analysis was performed for every residual neural activity – velocity waveform pairing for each trial of each cell. For across-trials analysis, we created a vector of activity residuals at time t and a corresponding vector of velocity residuals at time $t + \Delta t$, where the length of the vectors equals the number of trials. The Pearson correlation between these two vectors was determined (Figure 1C). We repeated this procedure for every timepoint in the saccade and for every $1\ ms$ shift, resulting in a correlation coefficient for each combination of time relative to saccade onset and delay (Figure 1D). This technique allowed us to examine the SC effects on eye velocity at every timepoint of the saccade in $1\ ms$ resolution. We repeated both correlational analyses on blink-perturbed trials to see if the results persist even when the saccade properties are altered.

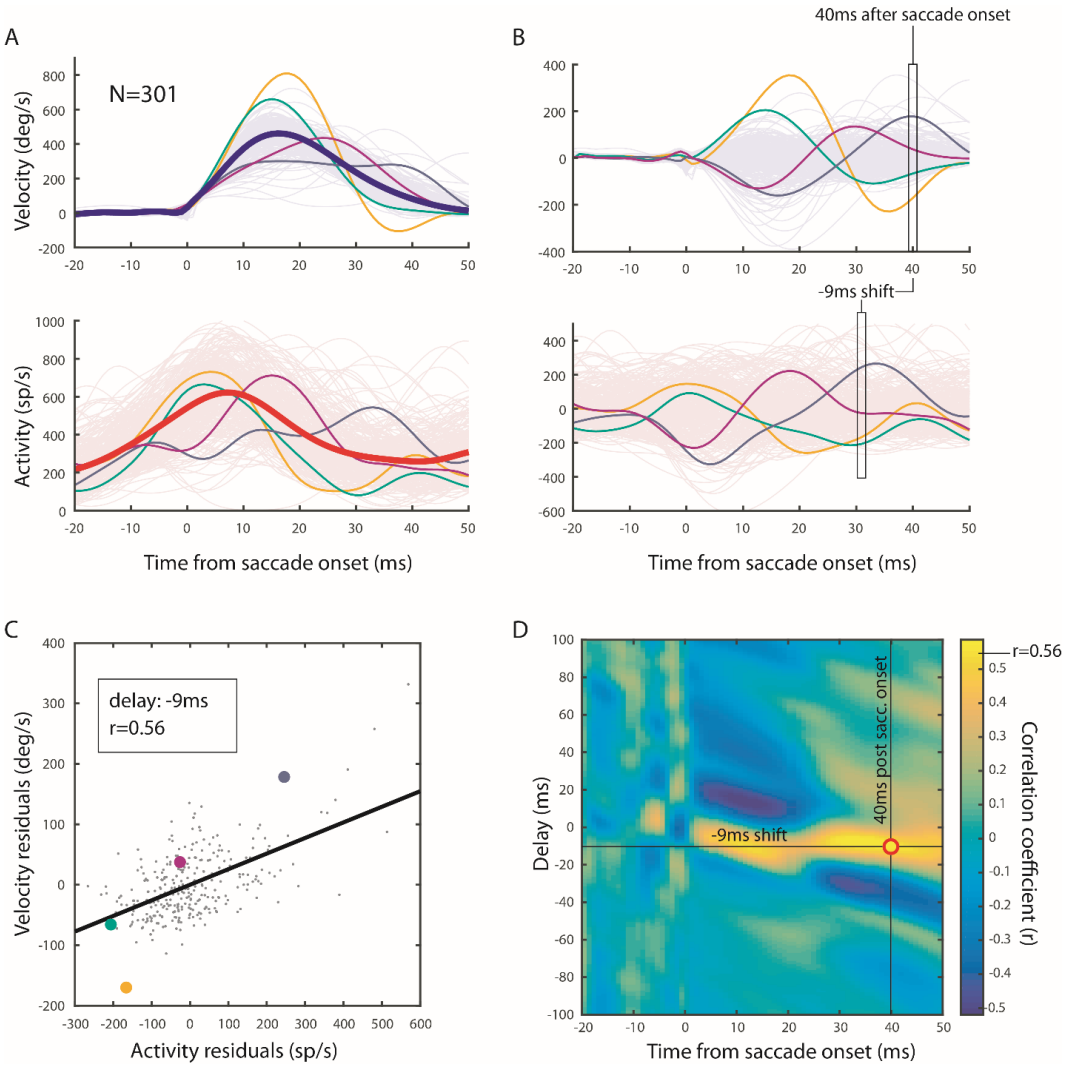

Figure 1: Illustration of across-trial analysis for normal saccades.

A: Radial velocity traces (top) and their corresponding neural activity (bottom) from one example cell. Positive velocity values represent instantaneous eye movement toward the target, while negative values represent movement away. Four traces are highlighted in color to illustrate the fluctuations of individual trials around the mean (thick traces). B: Same traces after subtraction of the mean waveform. Boxed sections show samples of activity and velocity used for regression. While these samples are taken at various delays, only -9ms delay is shown here. C: Velocity samples from box in B are plotted as a function of their corresponding activity sampled at a -9ms delay. Regression line and the correlation coefficient are provided. D: Correlation coefficient values (color) represented as a function of the delay and timepoint of the saccade.

2.4.1 Experimental Design and Statistical Analyses

To determine the significance of the results of within-trial analysis, we randomly paired a residual velocity trace of one trial with residual activity data of another trial from the same session's data and determined the Pearson correlation for the span of delay values. For across-trials analysis, we randomly shuffled the order of elements in each residual vector (instantaneous across-trial shuffle) before determining the correlation coefficient. The shuffling procedures were repeated 100 times for both types of analyses. Deviations of unshuffled correlation results outside 2 standard deviation bounds generated from shuffled data were deemed statistically significant.

To further validate that the influence of the SC on velocity continues throughout the entirety of the saccade, we calculated the duration of significant correlation for each cell. To do this, we determined the confidence threshold by performing the across-trial analysis on shuffled data for each cell one hundred times. Then we determined that the correlation was significant at those points where the real correlation exceeded 2 standard deviations around the mean of the shuffled results. Summing the instances at which correlation was significant gave us the total duration of the correlation.

In a separate analysis we looked at the subset of data which was collected using laminar probes. This subset allowed us to examine the effect of depth of SC neurons on our results. The number of channels with neural data ranged from 4 to 16 per session. Since each session did not have enough channels for sufficient statistical power, we de-meaned the data from each session and combined all channels. We then used linear regression on the de-meaned correlation coefficients of these channels and the corresponding firing rate to establish a trend.

2.5 Results

Figure 1A and Figure 2 show temporal profiles of saccade velocity for many amplitude-matched movements and corresponding spike density signals for one SC neuron. The saccade closely matched the neuron's preferred vector. A within-trial correlation can be readily appreciated by the similar bell-shaped profiles of both velocity and activity waveforms. This relationship can be intuitively queried by correlating the firing rate with velocity for different transduction delays. Figure 3A plots the results of such within-trial analysis for normal saccades across all 189 neurons in our database. The mean peak Pearson correlation ($r = 0.179$) was observed for an efferent delay (ED) of $13\ ms$, equivalently $\Delta t = -13\ ms$. The correlation was significantly different from the pattern observed for shuffled data. This result therefore indicates that the residuals of both SC activity and eye velocity fluctuate around the mean in a coherent fashion and that SC activity can influence saccade velocity.

A major limitation of the within-trial analysis is that it offers no information about the correlation at each instant during the saccade. The correlation coefficient could peak if any sufficiently long sequence of the activity correlates with the corresponding sequence in velocity. One can imagine that SC could, perhaps, encode the accelerating phase of the eye movement and the deceleration phase could be unaffected by SC activity, and rather be guided by muscle viscoelastic properties. In this case, the correlation would peak at a particular ED because the first half of both signals is correlated, but would provide little evidence to support our hypothesis that SC dynamically influences the entire saccade.

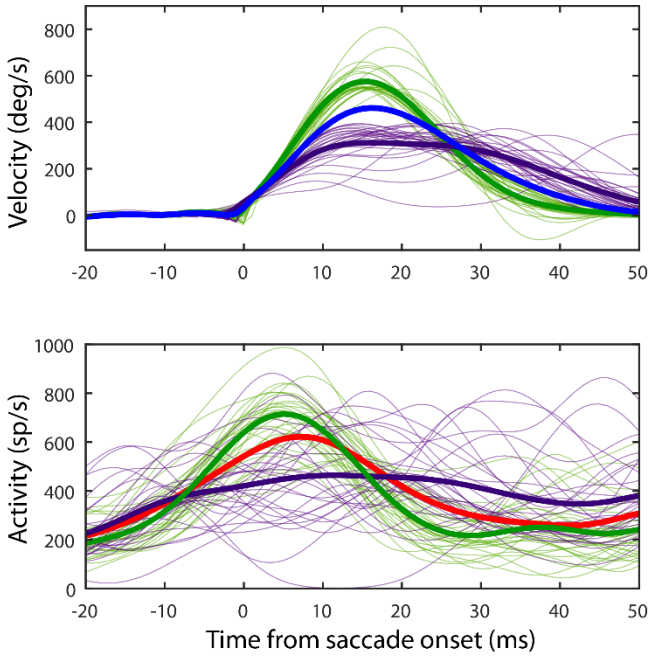

Figure 2: Temporal profiles of eye velocity and neural activity for normal saccades.

Traces shown in green are the 10% of trials with highest peak velocity. Purple traces are the 10% of trials with lowest peak velocity. Thick traces in each subplot are averages. Data are from one session. In additional to the general similarity of waveforms between the velocity (top) and their corresponding activity (bottom), there is also a correlation between the temporal features. Traces with high (low) peak velocity and short (long) deceleration duration are associated with similar profiles in the neural activity.

Figure 2 illustrates a closer inspection reveals a hint of temporal control of eye velocity. The top 10% of trials with highest peak velocities exhibited short shortest deceleration durations, and the associated activity profiles exhibited robust bursts that peaked early in the saccade followed by rapid reduction in firing rates (green traces). In contrast, the 10% of trials with lowest peak velocities, which had long deceleration phases, matched with muted peak rates that continued for prolonged periods (purple traces). Such trends warrant a systematic examination of across-trials analysis to determine precisely the time-course of correlation between activity and velocity (see Figure 1 and Methods section for details). Assembled across trials, the residual firing rates were regressed against residual eye velocities separated by a delay. This procedure was repeated for a large range of delays and for all times points of a saccade. Figure 3B shows the correlation coefficients for all combinations of saccade time points and ED values. A horizontal band of high correlation values is noted for the duration of the saccade for an ED of $12\ ms$. The correlation values in this band (Figure 3C) are even higher (peak: $r = 0.278$) than that found in within-trial analysis. Results from the across-trials analysis therefore provide the strongest evidence that SC dynamically influences eye velocity throughout the entire saccade. Additionally, it is prudent to mention that this analysis is identical whether performed on residuals or unaltered data, thus providing a more direct evidence of correlation as compared to the within-trials analysis.

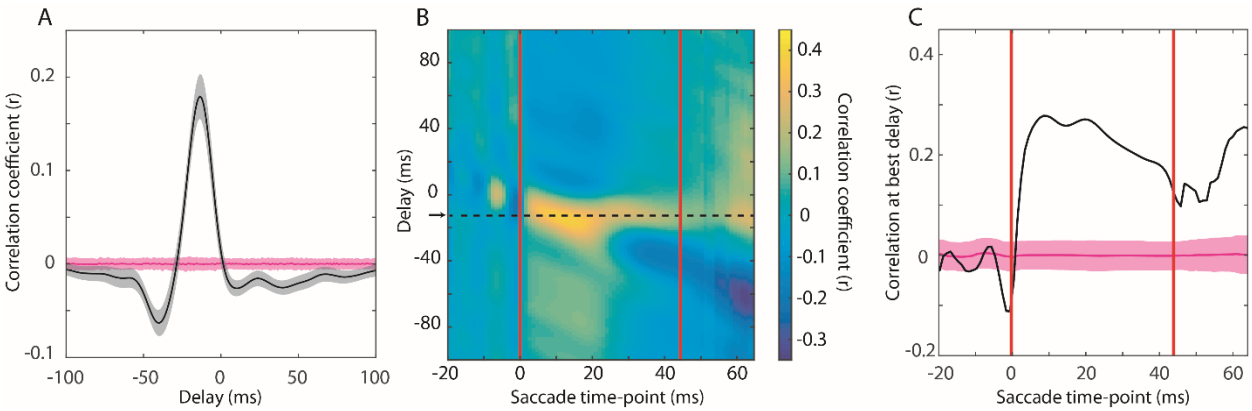

Figure 3: Summary of within- and across-trial correlation analyses for normal saccades.

(A) Within-trial correlation analysis. Black line denotes the correlation coefficient between activity and velocity residuals as a function of the temporal shift. The gray outline is two standard errors around the mean patterns from 189 neurons. Pink line and outline represent the mean correlation coefficients and two standard deviations from the mean of the shuffled data. (B) Across-trials correlation analysis. Heatmap of correlation coefficients between SC activity and eye velocity residuals for each timepoint during the saccade and temporal shift between the two residual vectors ("delay"). Arrow and horizontal dashed line mark the efferent delay at which the average correlation was highest (-12ms). Left and right vertical red lines indicate respectively the beginning and the end of the shortest saccade in the dataset. Data past the rightmost red bar excludes saccades which have terminated prior to the timepoints on the x-axis. (C) Correlation coefficients as a function of saccade timepoints for the optimal efferent delay shown in (B). Pink line and outline represent the mean and two standard deviations for the across-trials analysis performed on shuffled data.

Next, we explored the temporal characteristics of instantaneous activity-velocity correlations. We found that the time of peak correlation was well aligned with the time of peak velocity, after accounting for the efferent delay for each neuron (Figure 4A), although a substantial number of neurons exhibited their strongest correlations before or after peak velocity (negative or positive values on the x-axis, respectively). A paired *t*-test could not reject the null hypothesis that the mean difference was zero ($p = 0.15$). In contrast, the extent of SC's influence over saccade velocity, measured as a proportion of saccade duration, reveals a flat distribution (Figure 4B). Further, cells that had a shorter duration of significant correlation tended to have a lower peak correlation (Figure 4C; $r = 0.53, p = 1.99 \times 10^{-33}, f - test$). The relationship between degree and duration of influence could be explained by cells with higher correlation values having a higher likelihood of rising above the significance level over time. Thus, SC neurons tend to exhibit most influence over eye kinematics around the peak of the saccade velocity profile, and those cells which showed a higher peak correlation continued to influence eye velocity well past the peak, to saccade completion.

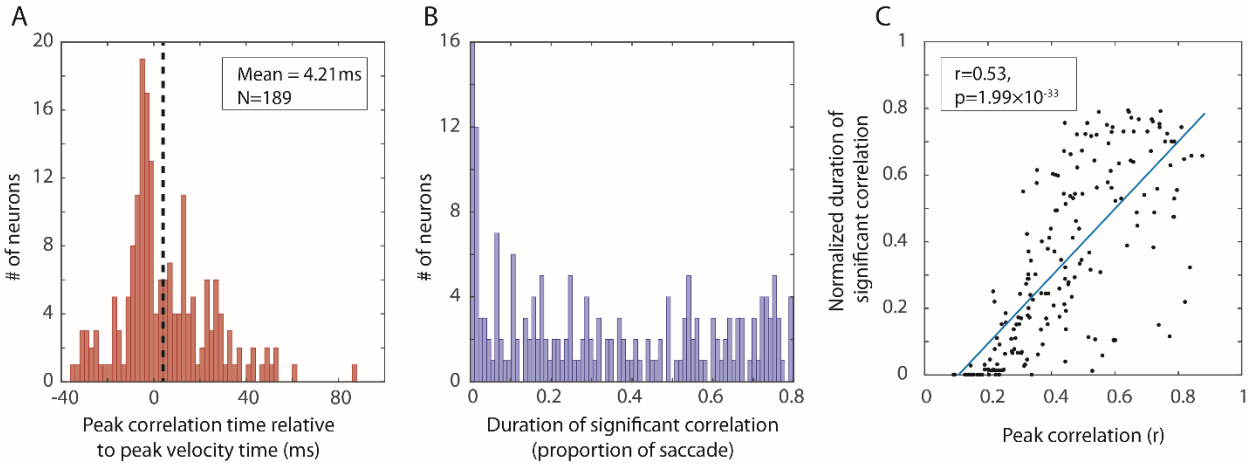

Figure 4: Temporal characteristics of activity-velocity correlation.

(A) Histogram of average peak correlation time relative to average peak velocity time for each neuron. The count on y-axis indicates the number of neurons. (B) Histogram of cumulative duration (as proportion of total saccade length) for which the correlation remained above significance level. (C) Relationship between peak correlation and the duration of the correlation. Each point indicates one neuron. Blue line is the best fit line to the data.

We then identified which properties of the neuronal population contributed to significant correlations. When examining the entire population of cells, simple linear models found no relationship between a cell's peak correlation and its peak firing rate or its location along the rostral-caudal extent of the SC ($p = 0.088, f - test$). However, when we isolated only the cells from a single laminar recording, we observed an increasing trend between the cells firing rate and its peak correlation (Figure 5A). When data from the laminar recordings was pooled by subtracting the average peak firing rate and correlation measures of each session, a statistically significant linear relationship was observed (Figure 5B, $p = 7.4 \times 10^{-6}, f - test$). This suggests that there is a strong relationship between firing rate and instantaneous velocity for neurons along the dorsoventral axis of the SC.

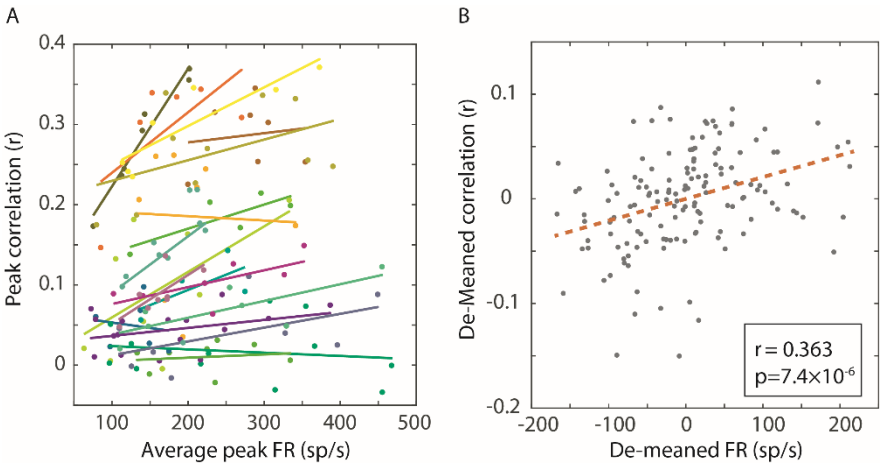

Figure 5: Analysis of data recorded from laminar probes.

(A) Peak correlation of each SC neuron is plotted against the average peak firing rate of that neuron. Neurons recorded in the same penetration are plotted using the same color. Thus, each color represents data from different sessions. The best fit line to each session's data is shown in the matching color. (B) Data from (A) de-meaned and pooled across sessions. Each de-meaned value is obtained after subtracting the respective average across all neurons in its track. The dashed red line is the best fit line.

To assess the robustness of the influence of SC activity over instantaneous eye velocity we turned to the 50 neurons for which we also had blink-perturbation data. Such saccades do not exhibit the stereotypical, bell-shaped profile and therefore offer an opportunity to assess if the correlation persists even in the presence of perturbation. Figure 6 illustrates representative data and the analysis approach in the same format as done for control saccades. The same qualitative features can be noted despite the blink-induced perturbation. The top row of Figure 7 displays the within- and across-trial analyses for normal trials in the 50 neurons. The same general trend persisted even for this subset of neurons. The best EDs for the normal, unperturbed data were 11 ms and 12 ms and the peak correlations were $r = 0.267$ and $r = 0.441$ for within- and across-trial analyses, respectively. For the blink-perturbed data from the same neurons, the peak correlations were $r = 0.210$ and $r = 0.386$ for both within- and across-trial analyses, respectively;

and the ED was 13 for both. Correlative relationship was largely intact despite the blink-induced perturbation.

To further characterize the impact of blink perturbation, we computed for each neuron the linear relationship between residual activity and velocity distributions across the duration of the movement. Assuming the data contained $n\ trials$ and the average duration of the amplitude-matched saccades is $d\ ms$, a single regression was performed across nd points. The activity data were time shifted relative to the velocity distribution to account for the neuron's ED. This was done separately for the normal and blink-perturbed data from each of the 50 neurons. Figure 8A shows a scatter plot of the regression slopes for each neuron in the two conditions. Overall, the slopes tended to be greater during the blink condition (paired t-test p=0.0013). We speculate that reacceleration of saccades in the blink-perturbation condition (Goossens and Van Opstal, 2000; Gandhi and Bonadonna, 2005) produces residuals that likely increase the regression slope. Moreover, we found a strong relationship between each neuron's regression slope and the goodness of fit in both normal (r=0.72, p=2.37×10^{-7}) and perturbation (r=0.35, p=0.02) conditions (Figure 8B). This suggests that although SC activity is updated to reflect the change in velocity, this compensation is likely not complete and that additional temporal control signals are added downstream in the brainstem burst generator.

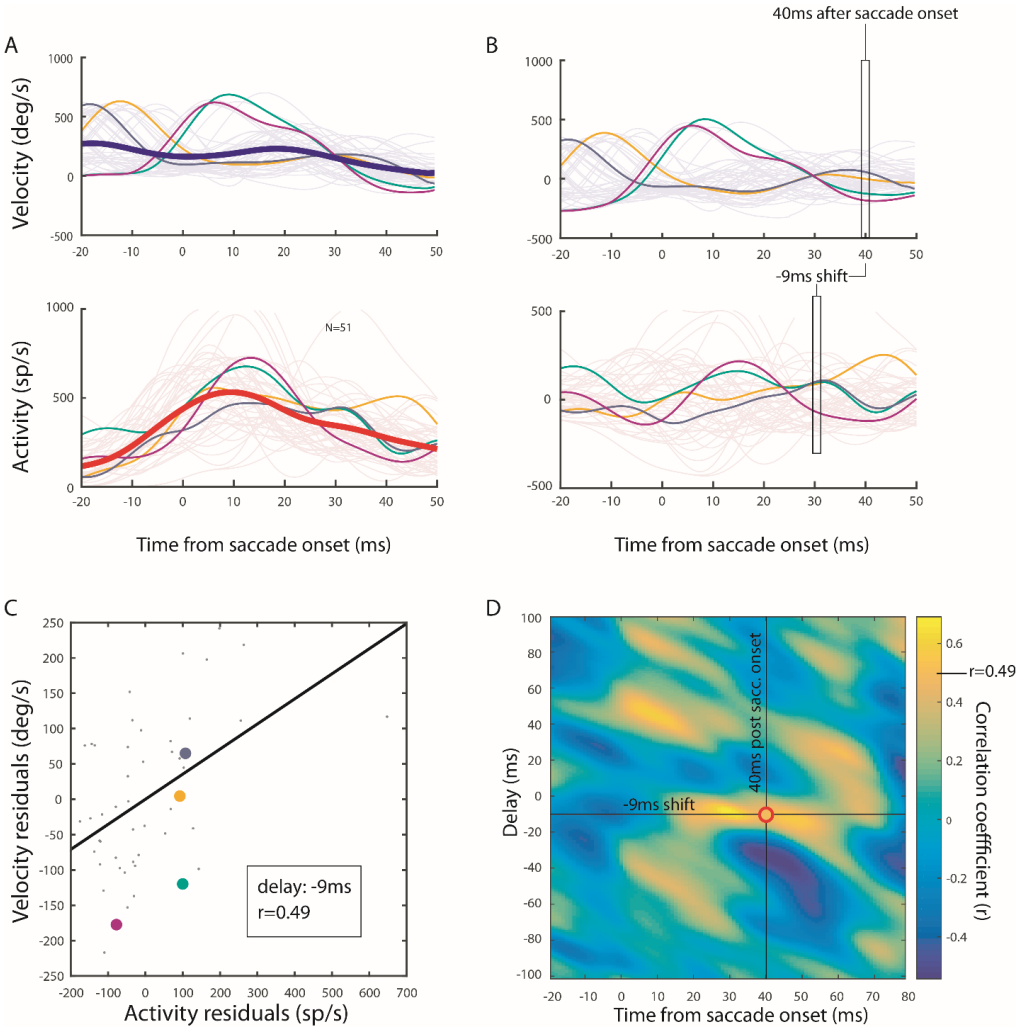

Figure 6: Illustration of across-trial analysis for blink-perturbed saccades.

Same format as Figure 1. A: Velocity and spike density traces. B: Residuals of traces in A. C: Correlation between velocity and activity residuals at -9 ms delay. D: Heatmap of correlations at every delay and at every saccade timepoint.

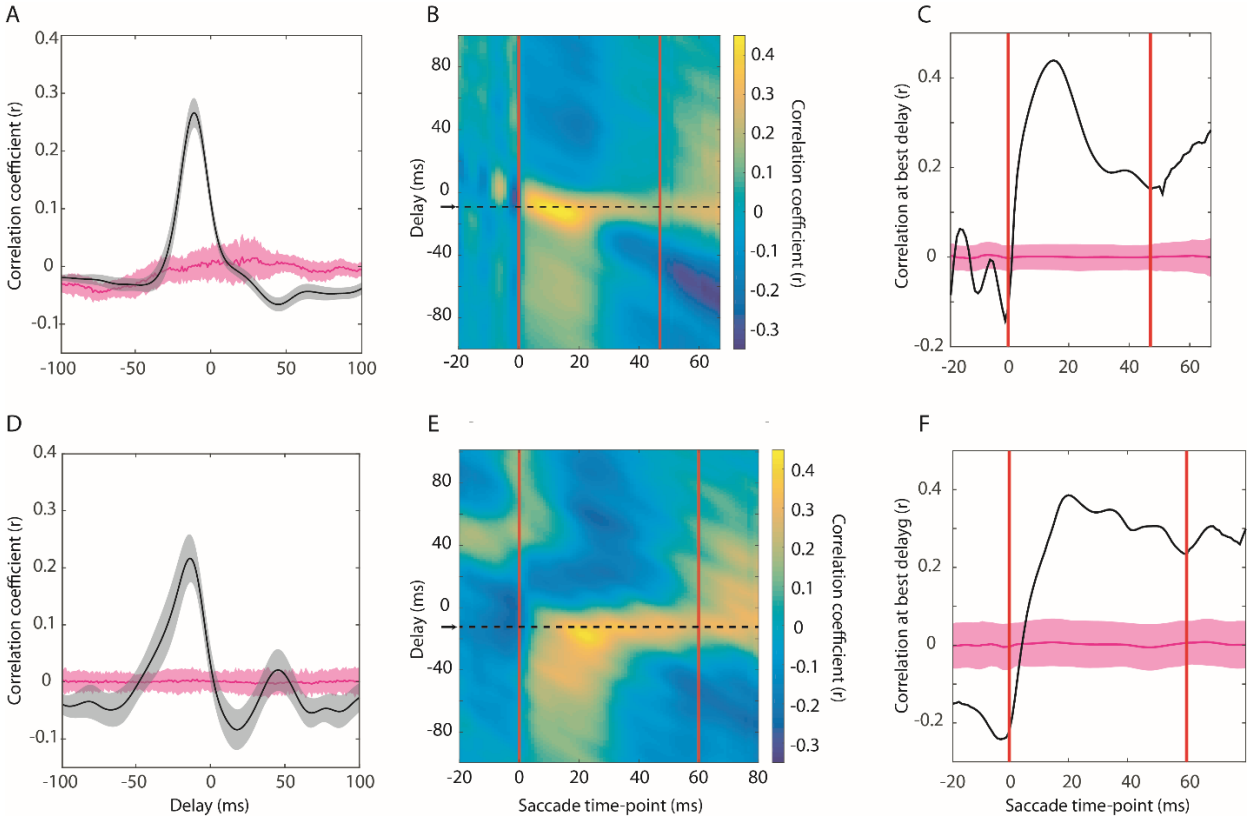

Figure 7: Comparison of correlation analyses for blink-perturbed and normal saccades.

Within-trial correlation between activity and velocity residuals for (A) normal and (D) blink-perturbed saccades available for 50 of 189 neurons. The heatmaps of correlation coefficients obtained from across-trials analysis for (B) normal and (E) blink-perturbed movements. Correlation coefficients as a function of saccade timepoints for the optimal efferent delay for (C) normal and (F) blink-perturbed saccades. The plots follow the same conventions used in Figure 3.

A peculiar finding of our analysis is the statistically significant negative correlation observed just before saccade onset for across-trials regressions (Figures 3C & 7C). This is not a physiological effect but instead a by-product of the data processing, which is why we present it at the end of the Results section. Recall that movement onset is defined as the timepoint when the absolute velocity exceeds 30 deg/s, which means that there must be eye motion prior to reaching this criterion. Consider once again the eye velocity traces in Figure 2. Note that the subset of trials with high (green traces) and low (purple traces) peak velocities actually have the inverse initial velocity relationship just before saccade onset: the green and purple traces exhibit respectively lower and higher initial velocities. The underlying neural activity waveforms before saccade onset, however, do not exhibit this reversal before saccade onset, thus producing the negative correlation. This effect is, as expected, not present when the analysis is performed with data aligned on saccade end (data not shown). A comparable explanation accounts for the negative correlation observed for the large negative delays ($\sim -40\ ms$) of the within-trial analysis (Figure 3A, 7A & 7F). The correlation at such delays are dominated by a regression between the ascending phase of neural activity with the decelerating phase of the eye movement. Of course, these long delays are not reflective of the effective $\sim 12\ ms$ transduction time from the SC to the eye plant.

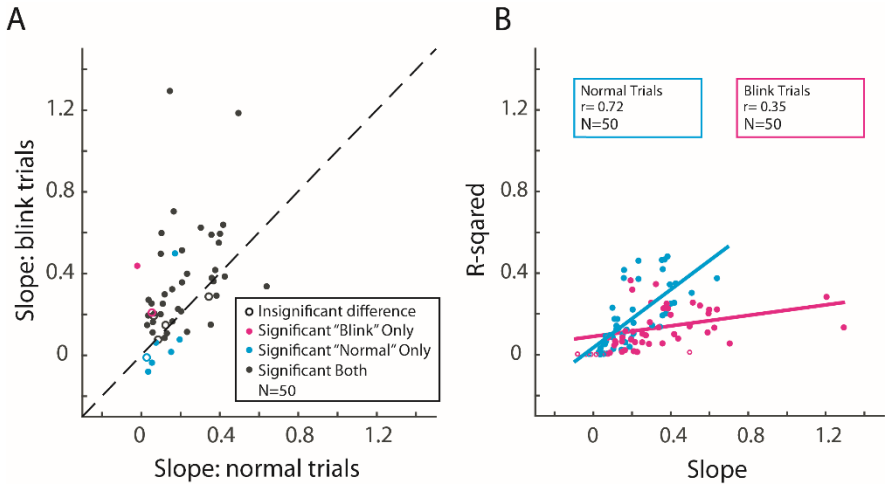

Figure 8: Linear regression features between SC activity and eye velocity.

(A) A pairwise comparison of the regression slopes obtained for normal (x-axis) and blink-perturbed (y-axis) conditions for each neuron. Every neuron had a statistically significant slope for at least one of the two conditions. Cyan: normal trials only; magenta: blink perturbation trials only; black: both types of trials. The dashed line represents the unity relationship. (B) Relationship between slope and R2 values. Cyan: normal trials. Magenta: blink perturbation trials.

2.6 Discussion

We described a previously unreported phenomenon on how SC activity exerts instantaneous control of saccadic eye movements. We found a strong correlation between the motor burst of SC neurons and eye velocity for an efferent delay of approximately 12 ms. The correlation was noted for both within-trial and across-trials analyses. The latter approach, in particular, demonstrated that the correlation remained high for the duration of saccade, lending support for SC control of instantaneous eye speed. It revealed a robust distributed population coding scheme reminiscent of a synfire chain (Diesmann et al., 1999; Shmiel et al., 2006), wherein individual neurons exert influence over saccade dynamics sequentially at different times,

collectively spanning the duration of the saccade. Comparable correlation structure and ED were also observed for blink-perturbed movements, whose velocity profiles deviate significantly from the stereotypical bell-shaped waveforms (Goossens and Van Opstal, 2000; Gandhi and Bonadonna, 2005), although it was particularly important to project the velocity vector onto the preferred vector of the SC neuron (Jagadisan and Gandhi, 2017). We also learned that, within individual electrode penetrations, cells with higher firing rates exhibited a stronger correlation with velocity. This suggests a velocity-activity relationship based on the depth of each cell as well as its spiking properties. Finally, we uncovered the interesting feature that regressions with the largest correlations also had the biggest slopes, implying that eye velocity is more sensitive to firing rates of those neurons that better account for its variance.

While several models of saccade control describe static features of SC activity most likely to influence a saccade, they rarely describe the time course of such influences. The across-trials analysis in our study provides a direct estimate of the efferent delay at which SC activity is most likely to influence the observed movement. The efferent delay is indicative of the transduction time of neural signals from the SC to the extraocular muscles. Studies of SC stimulation have established a 25-30 ms latency for movement initiation (Stanford et al., 1996; Katnani and Gandhi, 2012) and a shorter 10-12 ms delay for influencing an ongoing movement (Miyashita and Hikosaka, 1996; Munoz et al., 1996; Gandhi and Keller, 1999). The ED that yielded the strongest correlation from our neural recording data was approximately 12 ms. Crucially, it remained relatively constant throughout the movement, although we did observe a broader range of ED values with higher correlation coefficients around saccade onset (Figure 3C). While the ED values are different for microstimulation and recordings studies, a direct comparison should be avoided because underlying network level processes associated with movement preparation, which are

implicitly incorporated in neural activity, are likely disengaged when microstimulation is used to trigger a saccade.

We are intrigued by the observation that peak correlation between activity and velocity increased as a function of peak firing rate, but this effect was most notable for neurons within individual electrode tracks and not across the entire SC (Figure 5A). We think this is important because firing rate can vary both as a function of topographic location on the SC map, as well as dorso-ventrally, and the influence of a control signal must ideally not be dependent on topography, i.e., the amplitude and direction of the saccade being executed. Analyses from separate, unpublished work in our laboratory indicate that peak firing rate of the motor burst changes nonlinearly with depth, reaching a maximum in the intermediate layers and decreasing gradually for dorsal and ventral locations (Massot, Jagadisan & Gandhi, Society for Neuroscience, 2018). Neurons with the highest firing rates resemble the classical saccade-related burst neurons, some with buildup activity, and are likely those that project to the gaze centers in the brainstem (May, 2006; Rodgers et al., 2006).

Previous studies have addressed relationships between neural activity and movement parameters in several ways. For SC control of saccades, the focus has been on static parameters. For example, weaker bursts of activity produce saccades with lower peak velocity (Edelman and Goldberg, 2001), peak velocity is correlated with frequency or intensity of microstimulation (Stanford et al., 1996; Katnani and Gandhi, 2012), and peak velocity is attenuated after inactivation of SC (Lee et al., 1988). Modest correlations with SC activity have also been reported for head movements (Walton et al., 2007; Rezvani and Corneil, 2008) and electromyographic activity in proximal limb muscles (Stuphorn et al., 1999). Fewer studies have correlated the temporal profiles

of neural activity and eye movements for indiviual trials or an average across trials (e.g., Waitzman et al., 1991; Keller and Edelman, 1994; Goossens and Van Opstal, 2006), but such analyses do not determine which epoch(s) of the movement are controlled. We instead employed an alternative strategy and computed correlations on across-trials variability of neural activity and eye velocity. By performing the correlation in 1 ms increments during a saccade, we gained insights into instantaneous control without being constrained by the similarity of the temporal features of the two signals. The sliding temporal analysis of across-trials variability affords the ability to infer the efferent delays in communication between SC and extraocular muscles, unlike the aforementioned studies, and the consistency in the estimated delay values speaks to the robustness of the results. Furthermore, by matching saccade amplitude and minimizing endpoint variance, the analysis is able to better capture both moment-by-moment and trial-by-trial variabilities in the signals. Such analyses have been used in skeletomotor research, with significant correlations identified between neural activity waveforms in cortical areas and hand velocity profiles (Ashe and Georgopoulos, 1994; Reina et al., 2001). Trial-to-trial variability in eye and hand velocity has also been attributed to variability in neural activity occurring earlier in the trial, for instance during sensory input (Osborne et al., 2005; Huang and Lisberger, 2009) and motor preparation (Churchland et al., 2006a; Jagadisan and Gandhi, 2017), but this perspective precludes insight into direct dynamic control during ongoing movements.

Our study provides evidence consistent with the hypothesis that SC neurons encode instantaneous saccade velocity. This finding does not conform readily to its standard role in spatiotemporal transformation, that the spatial distribution of population activity in the deeper layers determines the saccade vector and downstream structures generate the firing patterns that reflect the velocity profile of the eye movement. The result that SC activity does influence peak

saccade velocity (cited above) somewhat aligns to a modified framework, the dual coding hypothesis (Sparks and Mays, 1990), in which the level of SC activity acts as a gain factor on the brainstem burst generator (Nichols and Sparks, 1996). However, influencing saccade speed through a global gain is not equivalent to impacting instantaneous motion. Our results agree more with a dynamic vector summation algorithm (Goossens and Van Opstal, 2006; Goossens and van Opstal, 2012) in which the SC controls the desired instantaneous displacement of the eye, although this model abstains from making direct statements about instantaneous velocity control, and it also incorporates a spatiotemporal transformation component. Another framework, which does not employ a spatiotemporal transformation between the SC and lower brainstem, places the duty of dynamic control on the cerebellum, and the SC has secondary roles of providing a directional drive and triggering the movement (Quaia et al., 1999). We do not believe the instantaneous correlation between velocity and neural activity we report here follows from this model, but proponents could render it an epiphenomenon.

2.6.1 Revised View of Neural Control Of Saccades: A Speculation

All extant models of saccade control stipulate the SC output to be a desired displacement signal, which is in position coordinates. How does the notion that SC encodes a velocity signal impact such models? We start by first describing the core elements of an existing framework (Figure 9A). The discharge rate of the active population of SC neurons is decoded into a desired displacement signal (ΔE_d) through a mechanism like weighted vector averaging or summation (see Gandhi and Katnani, 2011 for a review). This signal is the primary input to the comparator of an engineering-inspired, local feedback loop (Robinson, 1975; Jürgens et al., 1981) that subtracts

the instantaneous eye displacement (ΔE) from ΔE_d to compute a dynamic motor error (m.e.), which in turn drives pontine excitatory burst neurons (EBNs). The firing rate of EBNs is a nonlinear function of motor error and reflects an eye velocity signal (E_EBN^' (t); Van Gisbergen et al., 1981) that is further processed downstream by the nucleus prepositus hypoglossi (NPH) and extraocular motoneurons (MN) to generate the saccade. The velocity signal from the EBNs must be integrated into position coordinates to produce the ΔE signal needed at the comparator. Crucially, ΔE must be reset to zero after each saccade so that the model can generate an accurate movement when the next ΔE_d signal is presented by the SC. Thus, the local feedback branch includes a resettable neural integrator (RNI). Finally, the omnipause neuron (OPN) gates the saccadic system by inhibiting the EBN (Keller, 1974). The high frequency burst of SC neurons removes the OPN gate through disynaptic inhibition (Yoshida et al., 2001), which allows the local feedback loop to initiate and control the saccade dynamics until motor error reduces to zero, when the OPN once again inhibits the EBN. This framework, originally proposed by Robinson in 1975, has been tremendously influential, in part because predicted activity profiles by various nodes of the circuit were observed in brainstem neurons in later experiments. However, neural correlates of two essential elements of this circuit, the resettable neural integrator and the comparator (both denoted in red), have remained elusive.

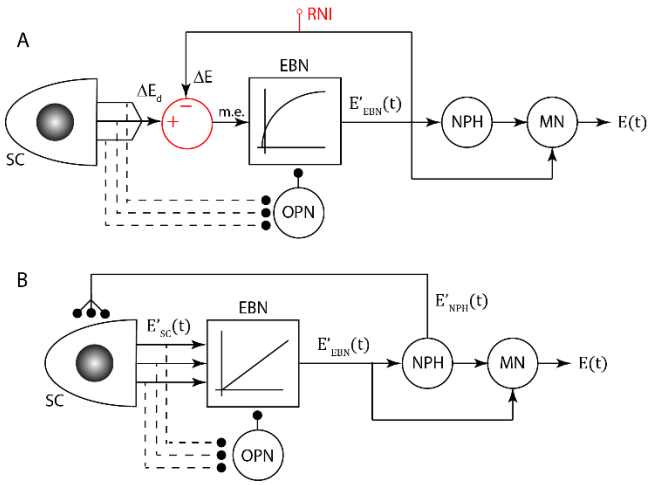

Figure 9: Alternate models of neural control of saccades.

(A) One version of the traditional local feedback loop model. Key elements or processes include computing a desired displacement command (ΔE_d) from SC population activity, using a comparator (red summation symbol) to compute dynamic motor error (m.e.), and employing a resettable neural integrator (RNI; denoted in red text) to convert the eye velocity signal (E_EBN^' (t)) to current eye displacement (ΔE). Also, the excitatory burst neuron (EBN) performs a nonlinear transform on motor error signal to determine eye velocity. (B) Our revised conceptual model is void of the comparator and resettable neural integrator elements and therefore no longer computes dynamic motor error. The EBN output is a linear transform of the SC input. The eye velocity feedback signal (E_NPH^' (t)) projects to the SC. The spatiotemporal pattern of population SC activity is pivotal in determining the instantaneous eye velocity. See text for more details. Additional abbreviations: OPN, omnipause neuron; NPH, nucleus prepositus hypoglossi; MN, motoneuron; SC, superior colliculus; E_SC^' (t), eye velocity signal encoded by SC output; E(t), eye position as a function of time.

To consider the possibility that SC outputs a velocity signal, we offer the speculative framework shown in Figure 9B. The centerpiece is the spatiotemporal distribution of population activity in SC neurons. The Gaussian-like SC population response, in both space and time, produces the stereotypical bell-shaped velocity waveform. We suggest that the intrinsic circuitry in SC, particularly the balance of excitation and inhibition, is essential for molding both the spatial and temporal components of the population response (Kaneda et al., 2008; Phongphanphanee et al., 2014). We speculate that the burst profile effectively also mediates burst duration and that the SC network exhibits refractory dynamics that account for the resettable neural integrator effect (Kustov and Robinson, 1995; Nichols and Sparks, 1995; Schlag et al., 1998). Of course, some of these network features could also be mediated by biophysical properties of SC neurons, which could be implemented through a spiking neural network framework (Morén et al., 2013; Kasap and van Opstal, 2017).

Downstream of the SC, there are also some salient differences from the traditional framework. Most notably, this scheme does not include the elusive resettable neural integrator and comparator, and the EBN therefore does not operate on motor error. Rather, it only scales the SC signal, where the gain (slope) may be a function of the location of active neurons in the SC; this notion of a linear operation by the EBN is credited to previous work (Goossens and Van Opstal, 2006; Van Opstal and Goossens, 2008). Also, the feedback signal now projects to and is distributed across the SC, and it originates from the NPH (E_NPH^' (t); Corvisier and Hardy, 1997) because EBNs do not project to the SC. The majority of NPH neurons exhibit burst-tonic patterns, where the burst component resembles eye velocity (Hardy and Corvisier, 1996). Once the movement is initiated, the velocity feedback signal could attenuate the SC burst and contribute to mediating

saccade duration. Finally, the engagement of EBN by SC activity may involve nonlinearities other than the OPN gate (not depicted in the figure). For example, the neural trajectory defined by SC population activity may need to traverse in an optimal or potent state space (Churchland et al., 2006b; Kaufman et al., 2014) or must exhibit stable temporal structure (Jagadisan and Gandhi, 2018) to recruit the EBN, but once it is online, it obeys the linear transformation.

The legitimacy of our conceptual model will be determined by its ability to account for saccade properties observed under various experimental conditions. While we have not yet simulated the model, our intuition can provide some qualitative predictions. Let's first consider the effect of SC stimulation. Guided by previous studies that recorded neural activity simultaneously during microstimulation of the same region (Histed et al., 2009; Logothetis et al., 2010; Vokoun et al., 2010), we do not expect the SC output to mimic the stimulation train like it appears to do in the pons (Cohen and Komatsuzaki, 1972; Gandhi et al., 2008). Instead, we think the intrinsic connectivity in SC will steer the initial, stimulation-evoked response into an attractor state (Gaussian-like profile) that is similar to the population response associated with an internally generated saccade, thus producing saccades with similar kinematics (Katnani and Gandhi, 2012). We believe the same reasoning applies for chemical inactivation. If the region compromised by the lesion overlaps with the neural tissue activated for a saccade, the intrinsic connectivity will gradually shift the locus, width, and/or firing rate of the spatiotemporal Gaussian pattern (Badler and Keller, 2002), leading to a slower saccade with a potentially different endpoint (Lee et al., 1988). It is also interesting to think about perturbations that alter the trajectory of a saccade or even halt it in midflight. In all cases, the ongoing activity in SC is perturbed through feedback from the NPH, as shown in Figure 9B, or various other methods that are not illustrated (e.g., lateral interactions within the SC, antidromic activation from a site that is stimulated, or through the

cerebellum or cortex). The SC population activity, in turn, is reshaped according to the spatiotemporal and refractory dynamics of the network, and the associated eye velocity reflects the SC activity provided that OPN has released its inhibition on the saccade circuitry.

In summary, we present here compelling evidence that the SC has dynamic influence over each instant of the saccade. The result impacts the notion of spatiotemporal transformation, which is thought to be a serial process of first encoding the movement in a retinotopic reference frame (place code) and then transforming it into a rate code to control its dynamics (Groh, 2001). The SC is considered the last stage of the spatial representation and gaze centers in the lower brainstem employ the temporal algorithm. Our analyses show a clear role of the SC in also exerting temporal control over the saccade throughout the duration of the movement, casting a shadow on a simplistic and serial sensorimotor transformation framework. In doing so, the result aligns well with observations from skeletomotor research, where it was demonstrated decades ago that neurons in the cortex encode velocity of hand movement (Ashe and Georgopoulos, 1994; Reina et al., 2001).

2.7 Acknowledgements

Funding for this research was provided by the following grants: R01 EY022854, R01 EY024831, F31 EY027688, NIH T32 DC011499, and P30 EY008098. We also thank the two anonymous reviewers for their astute insights.

3.0 Ventral Premotor Cortex Encodes Task Relevant Features in Eye and Head Movements

3.1 Overview

Visual exploration of the environment is achieved through gaze shifts or coordinated movements of the eyes and the head. The kinematics and contributions of each component can be decoupled to fit the context of the required behavior, allowing us to shift our gaze without moving our head or move our head without changing our gaze. A neural controller of these effectors, therefore, must show code relating to multiple muscle groups, and it must differentiate its code based on context; after all, a situation in which an optimal gaze shift starts with a head movement is different than the one in which an optimal gaze shifts starts with the rotation of the eye. In this study we tested whether the Ventral Premotor Cortex (PMv) exhibits a population code relating to various features of coordinated head-eye movements. We constructed three different behavioral tasks, each with four variables to explore whether PMv modulates its activity in accordance to these factors. We found task related population code in PMv which differentiates between all task related features. Surprisingly, the evidence of this code was almost absent in single neurons. We conclude that PMv carries information about task relevant features during eye and head movements. Furthermore, this code spans both lower-level information (effector and movement direction) as well as higher-level information (context).

3.2 Introduction

Redirection of the visual axis to an object of interest causes its image to project on the fovea, the part of retina with high photoreceptor density, and allows visual inspection with high spatial acuity. Such changes in gaze are produced typically as a coordinated movement of the eyes-in-orbits and head-on-body (Freedman et al. 1997; Goldring et al. 1996; Crawford et al. 1999; Freedman and Sparks 2000) However, these accounts focus more on the lawful relationship between the two effectors and less on features that allow them to be decoupled. For example, we can keep eye contact and nod our head in agreement when talking to someone; or conversely, we can keep our head still and move just our eyes to scan our environment. Additionally, we can perform the two movements in a sequence: nod first then shift our gaze, or shift our gaze first then nod. In both cases the individual gaze shifts and head movements are comparable, and yet the context for a movement of each is different. Even in conditions where we are not explicitly forcing the dissociation of the movement through conscious means, the interactions between eye and head movements can change depending on context of the movement (Goonetilleke et al. 2015; Haji-Abolhassani et al. 2016; Goossens and Van Opstal 1997; Solman et al. 2017; Corneil and Munoz 1999).

Investigations of the neural control of head movement, particularly when dissociated from an accompanying gaze shift, are rare. The few studies that have examined head movement generation have focused on traditional oculomotor areas such as the superior colliculus (SC),the frontal eye fields (FEF), and supplementary eye fields (SEF) (Chen and Walton 2005; Knight and Fuchs 2007; Elsley et al. 2007; Monteon et al. 2010; Walton et al. 2007; Chen 2006; Corneil et al. 2002; Stryker and Schiller 1975). However, the complexity of coordinated head and eye movements also suggest that perhaps some influence might come from a separate cortical area.

Head movements can be made without accompanied gaze shifts, so it is likely that a region of a brain which is not traditionally viewed as a gaze related area might encode some head movement properties. Here, we consider the role of a non-oculomotor area, the ventral premotor cortex (PMv), in the governance of head and eye movements. Historically, PMv has not been considered a major area in the domain of gaze shift research. Yet, a preliminary, trans-synaptic rabies virus injection study reported that PMv is only 3 or 4 synapses from eye and neck motoneurons (Billig and Strick 2012), suggesting possible control over those muscle groups. Furthermore, stimulation of PMv produces eye and head movements that are often integrated with more complex and seemingly socially meaningful movements of the hands and body (Graziano et al. 2002b; 2002a; Graziano et al. 1994). These results were not presented in a traditional "eye movement" context, since the studies' overall focus was largely skeleto-motor in nature, and yet eye and head movements were produced. Additionally, neurophysiological work has reported modulation of PMv activity during eye and hand movements (Neromyliotis and Moschovakis 2017). Once again, the results here were presented from a hand-eye coordination angle, rather than from an oculomotor perspective, but the parallels between hand-eye coordination and head-eye coordination reinforce our hypothesis. And even more directly, Fujii et. al. reported that saccades can be evoked by the electrical stimulation of the PMv (Fujii et al. 1998). This is one of the few studies which directly labels PMv as a contributor to visuomotor control. Given this set of results, we reasoned that PMv may also mediate movements of the eyes and the head, especially when the two are not coupled together.

Aforementioned works establish that PMv plays some role in certain eye-movements. However, this raises the question: what role does PMv fill that is not already covered by other oculomotor regions? After all, SC has been long recognized as an essential region for producing

gaze shifts, and it is capable of controlling various skeleto-motor systems. For example, deep layers of the SC are well established in orienting movements in rats and mice (Wilson et al. 2018; Dean et al. 1986; Sahibzada, Dean, and Redgrave 1986), as well as arm movements in primates and humans (Philipp and Hoffmann 2014; Pruszynski et al. 2010). One might assume that PMv can act as a redundancy area in the cortex to assist in eye and head movement generation. But other areas fill that role more neatly. FEF, for example, seems to be a parallel eye-movement generation area to the SC. In fact, even when SC is inactivated, FEF signals are enough to still allow the animal to create gaze shifts, although with some deficits (Hanes and Wurtz 2001). And, to complete the parallel, microstimulation of FEF also produces reliable head movements (Knight and Fuchs 2007; Monteon et al. 2010; Elsley et al. 2007). Which brings us back to the original question, what unique feature does PMv provide to eye-head movements?

We hypothesize that PMv carries supplementary information about the context of the task under which the movement is performed. We know that PMv does not exhibit strong direct control over movements, as inactivation or lesioning of this area results in minimal effects on an animal's behavior. Such inactivation shows mild behavioral changes, such as a change in a bias of movement direction or reduced EMG response in the fingers (Schieber 2000; Schmidlin et al. 2008). This leads us to believe that PMv has minimal control over direct kinematics of the movements. However, PMv has been well explored in higher-level properties for behaviors. For example, PMv has been shown to modulate its activity based on the order of motor actions in grasping, where the grip force was indicated by a sequence (Vargas-Irwin et al. 2015), reaching, where the targets for a reach were sequential (Mushiake et al. 1991), and even in linguistic domains, where PMv lesions altered the processing of sequential grammatical structures (Opitz and Kotz 2012). Additionally, PMv has been shown to differentiate between the contexts for

movements. This has been extensively established in grasping domain, where several studies show that PMv modulates differently when a particular grasp has to be made under different contexts; be it while performing the same grip to grasp different objects, or producing the same grip but for different goals such as to eat a treat vs to just grasp (Bonini et al. 2012). Therefore, we propose that PMv shows similar higher-level properties in eye and head movements. In this study we show that this cortical area shows neural activity which differentiates between different task-related features.

Considering all the aforementioned information, we constructed an experimental design through which we establish PMv as an active player in head and eye movements. First, we show correlation between single cell firing rates and task-related properties, which establishes the foundation for PMv role in eye and head movements. We then demonstrate patterns of population activity which code for each individual task feature. And finally, we train a classifier to determine the robustness of this population code. Collectively, these results show that PMv carries a population code for eye and head movement task features, such as the identity of the effector, the order of effector movement, and direction of this movement.

3.3 Methods

Data were obtained from one rhesus macaque (Macaca Mulatta). All procedures were approved by the Institutional Animal Care and Use Committee at the University of Pittsburgh and were in compliance with the U.S. Public Health Service policy on the humane care and use of laboratory animals.

Surgical procedures were performed under aseptic conditions. A stainless-steel head post was affixed to the skull with bone cement and reinforced with titanium screws. A Teflon-coated coil wire was implanted around the sclera of one eye, and the leads of the wire were attached to a plug that was imbedded in the head post. Craniotomies were performed over the left and right PMv coordinates estimated from MRI scans (stereotaxis coordinates: 15mm anterior and 23 lateral to the right and left of the midline), and stainless-steel receptacles were placed over each opening. Behavioral and neural recording sessions were initiated following a recovery period after each surgery.

3.3.1 Behavioral Tasks

The animal sat in a custom primate chair approximately 100cm from an LCD TV. The magnetic field induction method was used to sense gaze position with the scleral search coil implanted around the eye. Head movements were tracked by placing another Teflon-coated coil on a custom-made pedestal on top of the head. To maintain consistency, we define eye and head movements in the external reference frame, which consequently equates an eye movement to a gaze shift. The animal received feedback about his head position via a live cursor on the screen, and after a successful trial completion obtained water or juice reward through a tube which moved with his head. The behavioral data was recorded at 1000 samples/second using custom data acquisition software (MonkeyHost) (Bryant and Gandhi 2005).

We developed a behavioral paradigm with the intent to explore several PMv properties at once. Since we hypothesize that PMv encodes both motor- and context-related signals, we designed the tasks to specifically differentiate these features. They focused on controlling the sequential order of gaze shifts and head movements. This way the characteristics of gaze shifts

and head movements remained relatively equal across different trial types, but the context of the performed movement varied. This allowed us to answer whether PMv activity is associated with movement execution, task type, or a combination of both. In total, we constructed three different task types: “eye-first”, “head-first”, and “together” conditions (Figure 10). These conditions were presented pseudo-randomly to approximately match the number of successful trials between all three types. All trials started with two fixation points 1° in diameter (red for head, white for gaze) appearing next to each other with no space in between. The animal positioned the head cursor within 3°-5° from the red target, and directed the gaze within 3° of the white target to initiate a trial.

In the “eye-first” case, the white point jumped from the center to one of four positions: (r=10°, θ=45°,135°,225°,315°). This jump indicated to the animal to move its gaze to the new location while maintaining the head directed at the initial red point. After a variable delay (150-450ms) the red point jumped to the same eccentric location as the white target (with a slight offset as to not overlap them). This indicated to the animal to align its head with the new location while maintaining gaze on the white point (Figure 10, top). In the “head-first” condition the order of these events was reversed (Figure 10, middle). After fixation, the animal was instructed to first move its head, followed by an eye-only gaze shift. In the “together” condition, both points jumped to the eccentric position together and the animal was required to fixate and align the head cursor with the next location (Figure 10, bottom). No constraints were placed on the relative timing of the two effectors.

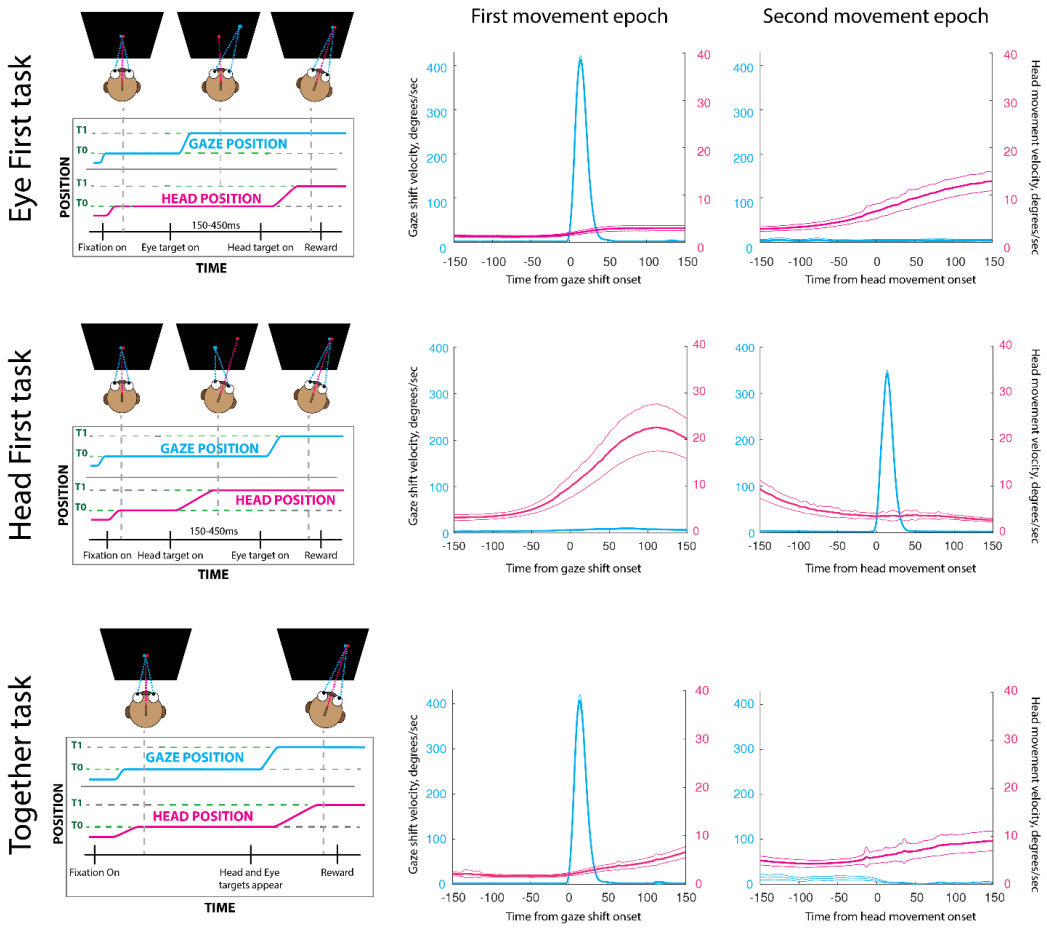

Figure 10: Task types.

Eye-first task. The animal is instructed to move the eye to a target location while keeping the head motionless. After a variable delay time, the animal is instructed to bring the head to the same location as the gaze. Head-first task. The animal is instructed to move the head-cursor to a target in the periphery; after a variable delay the animal is instructed to shift the gaze to the same target. Together task type. The animal is instructed to bring the head marker and gaze to a peripheral target. In this task the animal is not constrained in how he chose to achieve the success condition.

Panels on the right show the average (over all sessions) gaze and head movement velocities during their movement epochs. The thin lines are two standard errors from the mean

Since a natural gaze shift involves both eye and head movements, these tasks were aimed to separate various features of such movements. The role of the "unrestrained" task was to mimic the natural gaze shifts, albeit with an exaggerated head movement. The other two task types temporally separated the movements of the two effectors (eyes and head), allowing us to examine PMv effect on each individually.

3.3.2 Neural Data Collection

Electrophysiology experiments commenced once the animal performed the behavioral tasks consistently. In an initial set of experiments, a tungsten electrode was acutely lowered using Narashige manipulators with an aid of a placement grid, which guided the penetrations through holes separated by 1mm. To locate PMv within the chamber, we inserted the electrode in various locations in the craniotomy, delivered electric pulses (20-100 μA, 50-300ms, 200-400Hz, biphasic pulses) and observed the evoked response, if any. We identified FEF as the region where microstimulation evoked a reliable saccade. We moved posterior one millimeter at a time until we no longer observed reliable FEF-like saccades, which indicated we were in PMv. Figure 11 shows the locations of the tracks that evoked saccades (blue) and those that did not evoke an identifiable movement (x shapes) superimposed over the MRI scans which were used for chamber placement coordinates.

After mapping the regions available within the chamber, we used Plexon™ 16 or 24 channel linear arrays with 200-micron intercontact distance to obtain neural recordings. We acutely lowered electrodes until we observed isolated neurons across a span of about 3mm, or 15 channels. Well isolated neurons were observed on one to eleven separate channels, depending on the session. The locations of the recording sites are indicated in red in Figure 11. Microstimulation

did not evoke saccades at these sites. Data filtering, acquisition, and spike detection was handled by a Grapevine Scout system (Ripple Neuro). Raw signals were filtered with a 750Hz high pass filter to remove spike-irrelevant signal, and spike detection was generally done using a 3RMS above the mean threshold. In some cases, a manual threshold was set to fine tune the detection of the spike. The channels with detected spikes were manually spike-sorted using MKsort (Ripple neuro); only one unit was considered per channel as any additional units in this dataset were indistinguishable from noise.

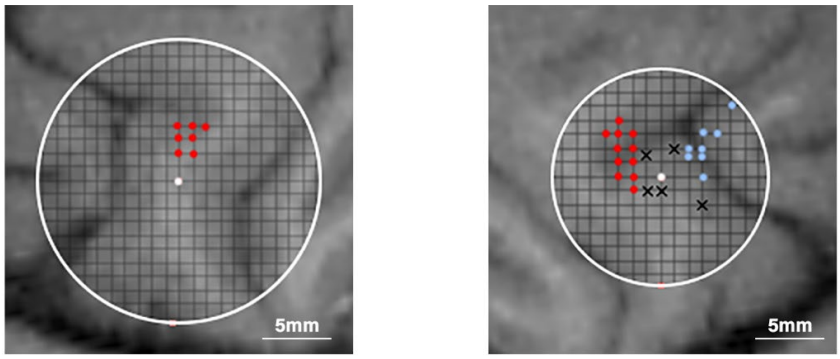

Figure 11: Track Locations.

Left PMv (top left) and right PMv (top right) locations. The center point was positioned using stereotaxic coordinates used in the craniotomy surgery (15mm anterior, 23mm lateral). The size of the perimeter is determined by the chamber used on each side. Inner diameter of the left chamber: 20mm. Inner diameter of the right chamber: 15mm. Red dots represent the sites of the cells used in this study. In blue are the sites where a clear eye movement was evoked with microstimulation. Black "x" marks represent sites where no behavior was evoked by electrical stimulation.

3.3.3 Data Analysis

To successfully establish PMv as a participant in eye and head movements, we first tested for statistically significant firing rate signatures in individual PMv cells to task-related features. We tested whether the firing rates of individual neurons during the movement epoch were different from baseline activity. This analysis showed us whether the cells modulated in relation to either lower-level movement properties (which muscles to engage and which direction to move) or higher-level task properties (task type, for example). We also explored the code as a population by combining the diverse responses of individual cells into one unified signal and explored whether that signal modulated with the higher and lower properties of the behavioral task. Finally, we explored the robustness of this signal by creating a simple naïve Bayes classifier and establishing minimum parameters needed for adequate performance.

All data was analyzed in MATLAB using custom scripts. Eye movement data was smoothed with a 5ms square kernel to remove any equipment noise. Saccade onset was detected when the eye velocity exceeded 35°/s and remained over the threshold for at least 8 consecutive milliseconds. Head movement onset proved to be more challenging, as the head rarely remained perfectly still, and head velocity was generally an order of magnitude slower. To detect head movement, we considered a snippet starting 100ms prior to head go-cue to ~1000ms after. It was then smoothed with a 30ms square kernel and normalized with the range of 0 to 1. Head movement onset was defined when the normalized velocity reached a threshold of 0.3 and remained above it for 15 consecutive milliseconds. A temporal shift of -5ms was added to account for an apparent lag in detection. We then used visual inspection to remove any trials where automatic head or eye movement detection failed. A sample of detected eye and head movement velocities for one session is shown in Figure 10 (middle and right columns).

A total of 86 isolated cells were recorded. Neural data was smoothed using a gaussian kernel with a σ=10. To reduce the number of possible conditions we collapsed across directions by only considering whether the movement was ipsiversive or contraversive. This reduction yielded a total of 12 different conditions: three task types × two directions (ipsi- and contraversive) × two effectors (eye or head). For example, one condition could be that the neural activity is modulated during gaze shifts directed in the contraversive direction for the head-first task only.

Statistical significance of the neural modulation of each neuron was determined by a custom application of a paired t-test. We first grouped alike trials into twelve separate categories, as described above. For each trial, we extracted a baseline period of 0ms to 300ms after the animal aligned both its gaze and head with the initial fixation targets. During baseline the animal was unaware of the context of the task. We then averaged each trial's activity during the baseline period, giving us a $N \times 1$ vector (A) where N is the number of trials. For each trial's movement epoch, we extracted the spike density waveform –80ms to +80ms around its onset. This step yielded $N \times t$ matrix for each gaze and head movement (matrices B and C, respectively), where N has the same trial indices as vector A and t is time in milliseconds. Then we conducted a paired t-test with p threshold of 0.01 comparing each column of either matrix B or C to column vector A. We considered the cell to be significantly modulating for a specific category when the test determined significant difference in distributions for at least 20 consecutive timepoints. Using this method, we identified 74 out of 86 cells which significantly modulated their firing rate during at least one of the conditions.

For population level representation, we used dimensionality-reduction techniques on all 86 cells, including those that did not show significant single-cell modulation. Since these cells were recorded individually and across many sessions, we created a pseudo-population in which we

arranged the data in such a way that the resulting structure is analogous to that of a simultaneously recorded set. For each neuron, we first categorized each trial into one of the three trial-types, as well as by the direction of the movement. Next, we took a snippet of activity centered on each effector movement onset (±150ms), one aligned on the gaze shift and the other aligned on head movement. We then created virtual trials by pulling either gaze-shift or head snippets from 5 random trials from each cell's dataset, and averaging them to create representative activity for the pseudo- trial. The averaging step accomplished three crucial things. It diminished any outlier effects from noisy data, allowed us to increase the number of trials for sessions with low sample sizes, and drastically reduced the possibility of repeated identical pseudo-trials. By repeating this process for each cell in the set, we attained one pseudo-dataset in which all cells can be treated as if they were recorded simultaneously. By repeating this process, we created 500 virtual trials for each of the 12 conditions.

After constructing the pseudo-population, we used principal component analysis (PCA) to determine the first two principal components of the population activity which gave us insight into population activity patterns. To establish the principal components, we concatenated all trials in the pseudo-population, giving us a $(301\ ms * 6000\ trials) \times 86$ neurons matrix. This created a universal space for the entirety of the neural activity, onto which we could project activities of individual conditions to establish whether they reside in unique subspaces. Although through this analysis it is evident that there are differences between conditions, we used PCA mainly as a visualization tool to gain insight into population activity patterns.

To quantify the differences between high dimensional patterns corresponding to each condition, we used linear discriminant analysis (LDA) which determines the dimension of highest separation. We then determined whether there was significant pairwise difference between each

activity along that dimension. To create the linear discriminant model, we used functions provided in MATLAB's Statistics and Machine Learning toolboxes. Since LDA is a pairwise discriminator, we created a separate model for each pair of conditions tested. As in PCA analysis, we concatenated the data across trials, but here we only used the subset of trials corresponding to the two selected conditions; thus, the resulting training matrix was: $(301\,ms * (N\ trials\ condition\ a + N\ trials\ condition\ b)) \times 86$ neurons with the corresponding label vector of $(301 * (N\ trials\ condition\ a + N\ trials\ condition\ b))$ where each value indicates a condition for each ms sample. The resulting linear model maximizes the distance between category means while minimizing within-category variance, thus establishing impressive pairwise separability. We then performed a t-test (p threshold <0.001) on the distributions in the first latent factor to determine whether the means were significantly separable.

3.3.4 Decoder

Although we observe pairwise separation when using linear models, it seems unlikely, that the brain would decode this information in a pairwise fashion, since in the natural environment the number of comparison pairs is well beyond the 12 we examine here. Therefore, our next step was to establish whether the population code carries enough information to classify among the 12 conditions at once. We trained a naïve Bayes classifier to assign one of 12 categories to an input trial and assessed the resulting decoding accuracy. We chose this particular classifier because of its relative simplicity and our own familiarity with it; however, we expect similar results regardless of the classifier chosen. We already showed that even simpler, linear, classifier separates this data between categories; so, it is expected that classification accuracy will not decrease as classifier complexity increases.

To maximize the rigor with which we test the classifier, we created separate 'training' and 'testing' pseudo-populations. In order to remove any possibility of a trial appearing in both 'training' and 'testing' datasets, we only pulled random even numbered trials from individual sessions for the 'training' set and odd numbered trials for 'testing' set. This ensured that when obtaining the 5 random trials needed to create one pseudo-trial, none of these individual trials were duplicated between the two resulting sets. Since this cut our available data in half, we removed all sessions where we had less than 35 trials remaining for any condition. This reduced our resulting population from 86 to 67 cells.

The naïve Bayes classifier was trained in a similar fashion as the LDA classifier, except all conditions were used at once. So, the input matrix was the same structure as the one used for PCA, albeit with less dimensions: (301 ms*6000 trials)×67 neurons and the label vector spanned all the resulting rows: (301 ms*6000 trials). Since every time sample was treated as an independent observation, this allowed us the flexibility to measure the classification accuracy at different timepoints of each epoch. However, the main metric for robustness of this classifier is the minimum cells required for accurate classification. Before discussing these metrics, however, it is prudent to describe the testing of the classifier.

After the classifier has been trained on a full dimensional 'training' set, we used individual pseudo-trials from the 'testing' set as an input to the resulting model. The structure of the input would be: 301ms×67 neurons and the output would be a 301-element vector classifying each millisecond sample of the trial as one of 12 conditions. The mode of the resulting vector indicates the chosen category. We repeated this procedure for 250 pseudo-trials per category from the 'testing' set to gain an average classifier performance.

To establish the minimum number of cells required for accurate classification, we ranked cells by the magnitude of their projection onto the first PC of the population. We repeated our PCA procedure on the 'training' test to obtain this ranking, and then re-trained the decoder first on the data composed on just one highest ranking cell (301 ms*N trials)×1 neuron. Then we tested this classifier with the 'testing' data from the same neuron to obtain classification accuracy. Next, we trained a classifier on the top two best ranked neurons combined ((301 ms*N trials)×2 neurons), then three best neurons, and so on, adding one neuron at a time until we reach full population.

3.3.5 Cortical Depth Analysis

To explore the features of this neural code even further, we asked whether some features varied as a function of depth within the cortex. After all, our linear probes spanned the entirety of the cortex cross-section and therefore we recorded from cells from different layers. It is important to note that this was not a part of the initial hypothesis and therefore the experimental design did not control for the depth of the neural recordings. Regardless, we could estimate the relative depth of each neuron from the channel it was recorded from. Since we attempted to span the entirety of the depth of the cortex when we inserted the electrodes, it is reasonable to assume that superficial channels resided in superficial layers, and deep channels resided in deep layers.

We assigned one of three depth markers to each neuron: 'deep', 'middle', and 'superficial' based on the channel they were recorded on. Most of the recording was done on deep channels, so to keep the number of cells in each group equal, the channel-to-label assignments were not equal. Channels 1-3 were considered 'deep', channels 4-9 were considered 'middle', and channels 10-16 were considered 'superficial'. This gave us relatively the same number of neurons between 'deep'

and ‘superficial’ neurons (24 for ‘deep’, 36 for ‘middle’, and 23 for ‘superficial’), thus allowing for a more direct comparison between the two groups.

For those sessions where 24 channel electrodes were used, only the first 16 channels were considered. Since the channel spacing was the same between 16 and 24 channel electrodes, no transformation of electrode distances was needed to directly compare the two. By and large, channel 1 depth was comparable between different electrodes as they were all lowered to a similar depth (~4000 – 5000 micrometers) as measured by a microdrive (Narashige). It is worth reiterating here that the depth was not controlled, and any variation in scar tissue at the insertion site and cortex deformation would make the depth measurements unreliable.

The primary question we addressed is whether the task relevant information is only present at a certain depth in the cortex. To establish this, we repeated the LDA analysis on the depth relevant subgroups of neurons. We focused on any differences in this separability as a function of depth.

3.4 Results

To establish the role of PMv in coordinated gaze shifts and head movements we analyzed 86 isolated neurons in the context of 12 separate categories. Statistical analysis of individual neurons showed significant, although qualitatively unimpressive, modulation during movement epochs. Examination of these neurons of a population, through LDA and PCA methods, showed a clear separation of the neural code by category, thus showing task relevant PMv activity. The robustness of this code was examined by stressing the parameters of a Naïve-Bayes classifier.

3.4.1 Single Neuron Analysis

We first compared each cell's firing rate during the movement epoch (-80ms to +80ms from movement onset) to that of the baseline period (see Methods). If 20 or more consecutive samples in the movement epoch were outside the baseline distribution (paired t-test, threshold $p<0.05$), the cell was considered to have significant modulation for that condition. An example neuron's spike density waveforms are shown in Figure 12. In this case, the cell reduced its firing rate below baseline for all categories, and no noticeable tuning for any one condition is evident. When examining average firing rates over time for all significantly modulated cells we notice the lack of features common to traditional motor areas; the cells neither exhibit burst-like properties, nor visible suppression signatures, nor any event-locked modulation (Figure 13: left column). Qualitatively, the responses are flat throughout the movement epoch. To further illustrate this lack of apparent modulation, we contrast these cells with those that did not show significant modulation for a given category (Figure 13: right column). One is hard pressed to identify concrete differences between the cells that were significantly active for each category and those that were not. In short, when examining individual cells, we see no obvious or characterizable relationship between the cells' firing rates and the animal's behavior.

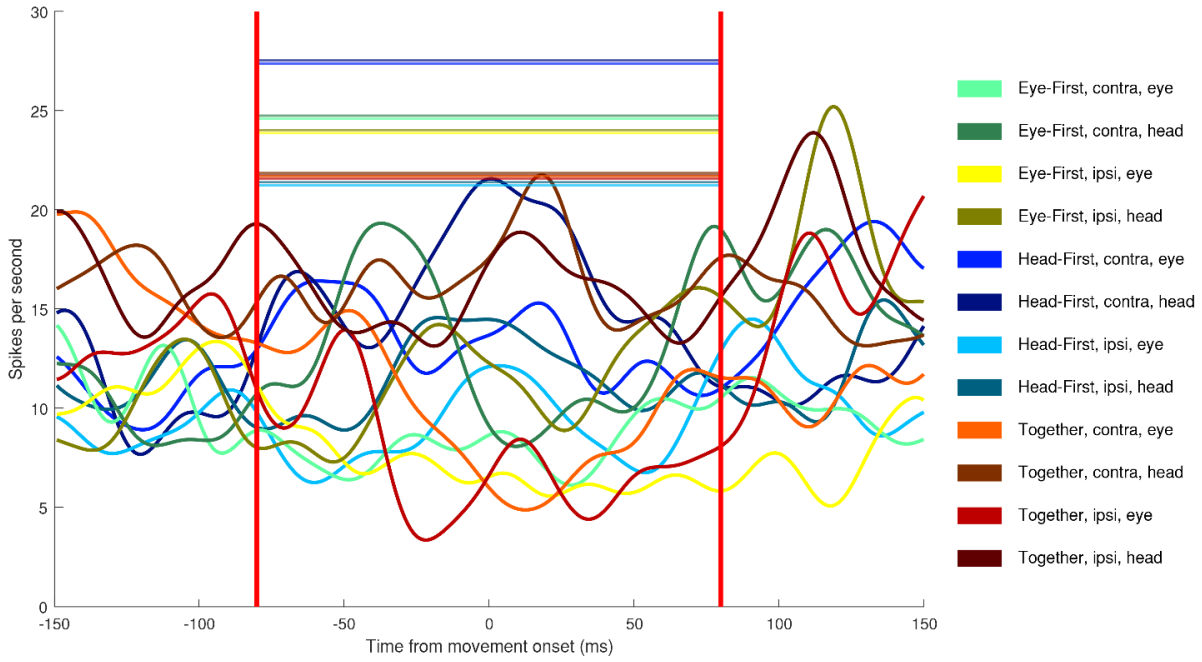

Figure 12: Example cell which showed significant modulation for every task type. The straight lines at the top illustrate the average baseline activity for each condition, against which significance was determined. No clear tuning is identifiable.

We cannot discount statistical results based simply on visual inspection. To gain insight into the validity of the t-test results we plotted the significant activity compared to baseline activity for single cells (Figure 13: middle column, red). We contrasted those results with cells in which the activity was not different from baseline in the same figure (Figure 13: middle column, black). We can see here that all significant firing rate averages and their 95% confidence intervals lay far away from the unity line, thus signifying that this analysis was not overly contaminated with type 1 errors. Overall, we found that 74 out of 86 isolated cells showed a significant firing rate modulation from baseline during the movement epoch for at least one category (modified paired t-test, $p<0.01$) (Figure 14). This indicates that although visual examination of the data does not show any obvious or reliable patterns, the cells do in fact carry some information during the movement epochs.

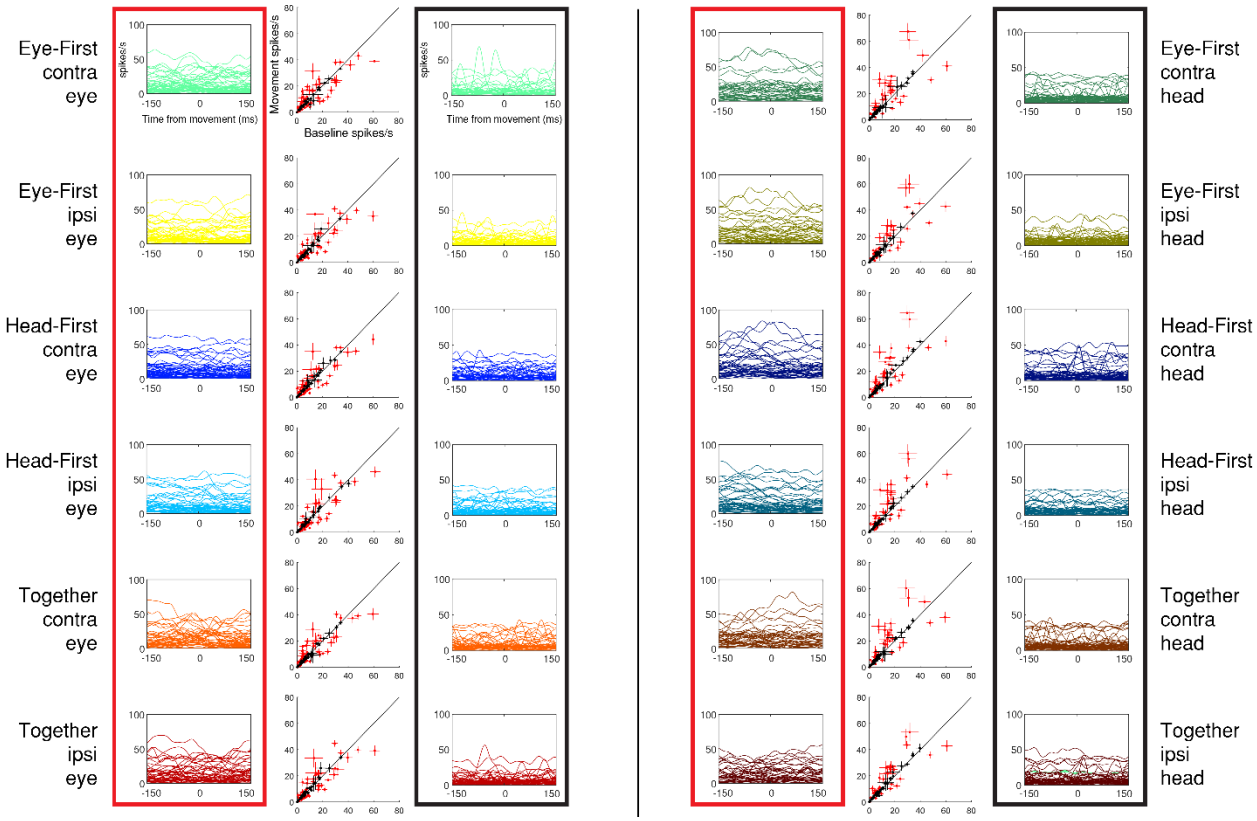

Figure 13: Average neural activity traces by trial type.

Red column: average activity traces corresponding to each category for each cell that was found to have significant modulation. Each line is an average for a single cell. Black column: average activity traces corresponding to each category for each cell that was not found to have significant modulation. Middle column: average firing and 95% confidence intervals for the movement epoch as a function of baseline firing rate. Red markers correspond to those cells which were found significantly modulating.

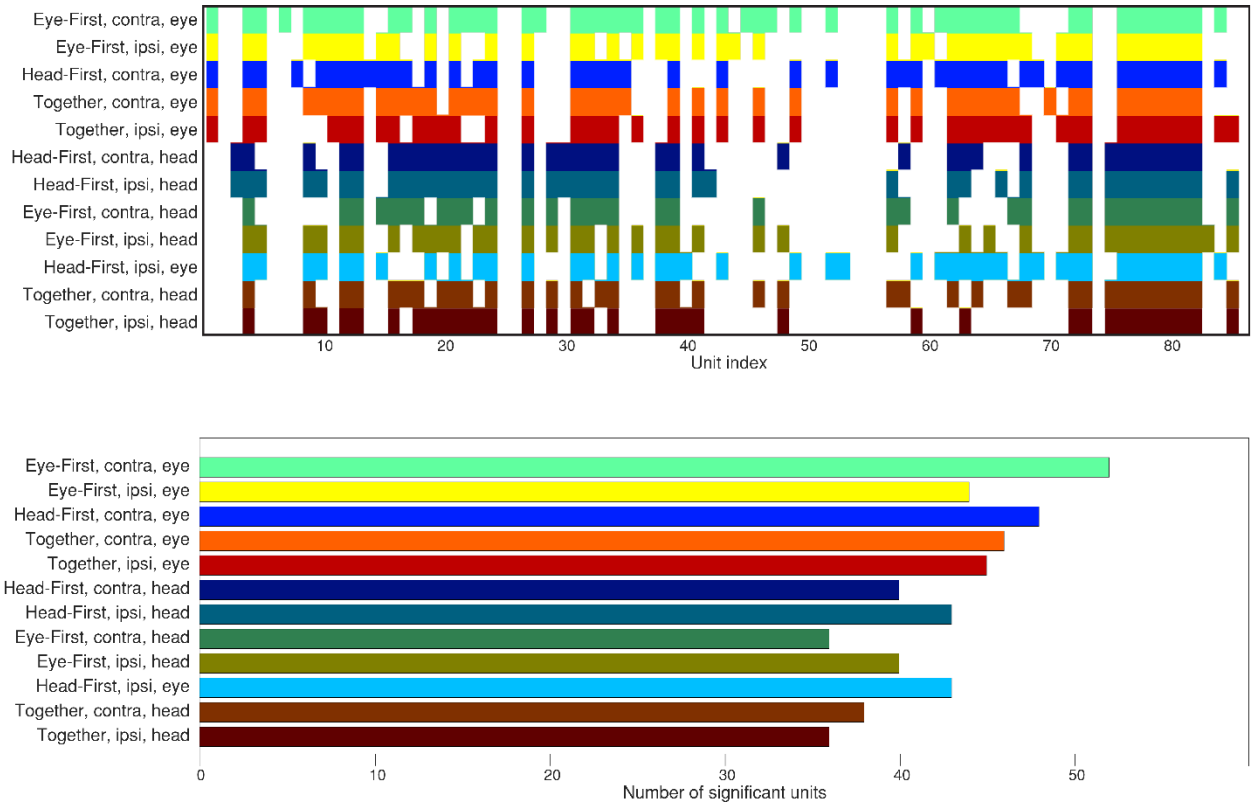

Figure 14: Cells with significant response to task type.

Top: shaded pixels represent tasks for which the cell significantly increased its activity from baseline.

Bottom: histogram of cells which significantly increased their activity from baseline, sorted by category.

To gain a deeper understanding of the role PMv has in eye and head movements, we examined whether a clearer picture could be obtained if we considered the individually recorded neurons as a combined single population.

3.4.2 Pseudo Population Analysis

We did not record all the cells at the same time. Each day the electrode was inserted acutely and therefore sessions across days had separate neurons recorded at different times. Luckily, the homogeneity of the tasks allowed us to restructure the data to simulate simultaneous recordings. We then used this pseudo-population with dimensionality reduction techniques to test for presence of a task-related code.

We constructed a dataset which mimics a simultaneous 86 channel recording (see methods for details). For visualization purposes, we reduced the dimensionality of the data from 86 to 2 dimensions using PCA. Unlike single neuron analysis where the pattern of activity was impossible to characterize, the population activity clearly follows unique trajectories for each category. Although our PCA results are qualitative, we can still assess these patterns by eye (Figure 15). When matching for all factors except trial type, we see that during the movement epoch, the activity traverses a different path during “head-first” task as compared to “eye-first” task. Additionally, the paths for “eye-first” and “together” task types are much more similar (Figure 15, middle). This could be because in natural gaze shifts like the ones we mimicked with the “together” task the eye tends to move before the head, and therefore resembles the “eye-first” task.

We see similar separation when looking at other task properties. For example, when matched for all properties except effector we see a clear separation between the “eye” and “head”

subspaces. Although we chose to show the case where all trials were "eye-first" with contraversive movements (Figure 15, bottom), all combinations of matched factors follow this convention. Neural trajectories between contra- and ipsiversive movements appear to be most similar. However, the similarity between the trajectories is not surprising, as PMv has a large proportion of ipsilateral projections (Dancause et al. 2006; Gerbella et al. 2011) which could imply that a population code would not show a strong laterality preference. Regardless, the trajectories still show some differentiation (Figure 15, bottom).

To quantify the separability of the neural code during each condition we used LDA. We found the dimension of maximum separability between pairwise-matched conditions and determined whether each condition's neural activity was significantly different from the other using a simple t-test. Each pairing of conditions was significantly separable with a p threshold of <0.01. Figure 15 contains LDA results for each PCA example to demonstrate this separability. Even the difference between ipsi- and contralateral movements existed in separate subspaces in the first latent factor dimension (Figure 15, bottom).

Our multi-dimensional analyses demonstrate that even though the single-cell analysis showed no clear pattern, there is a definite population code that becomes apparent when we visualize high dimensional data in lower dimensions. PMv neurons carry a task-relevant code for eye and head movements when considered as a population.

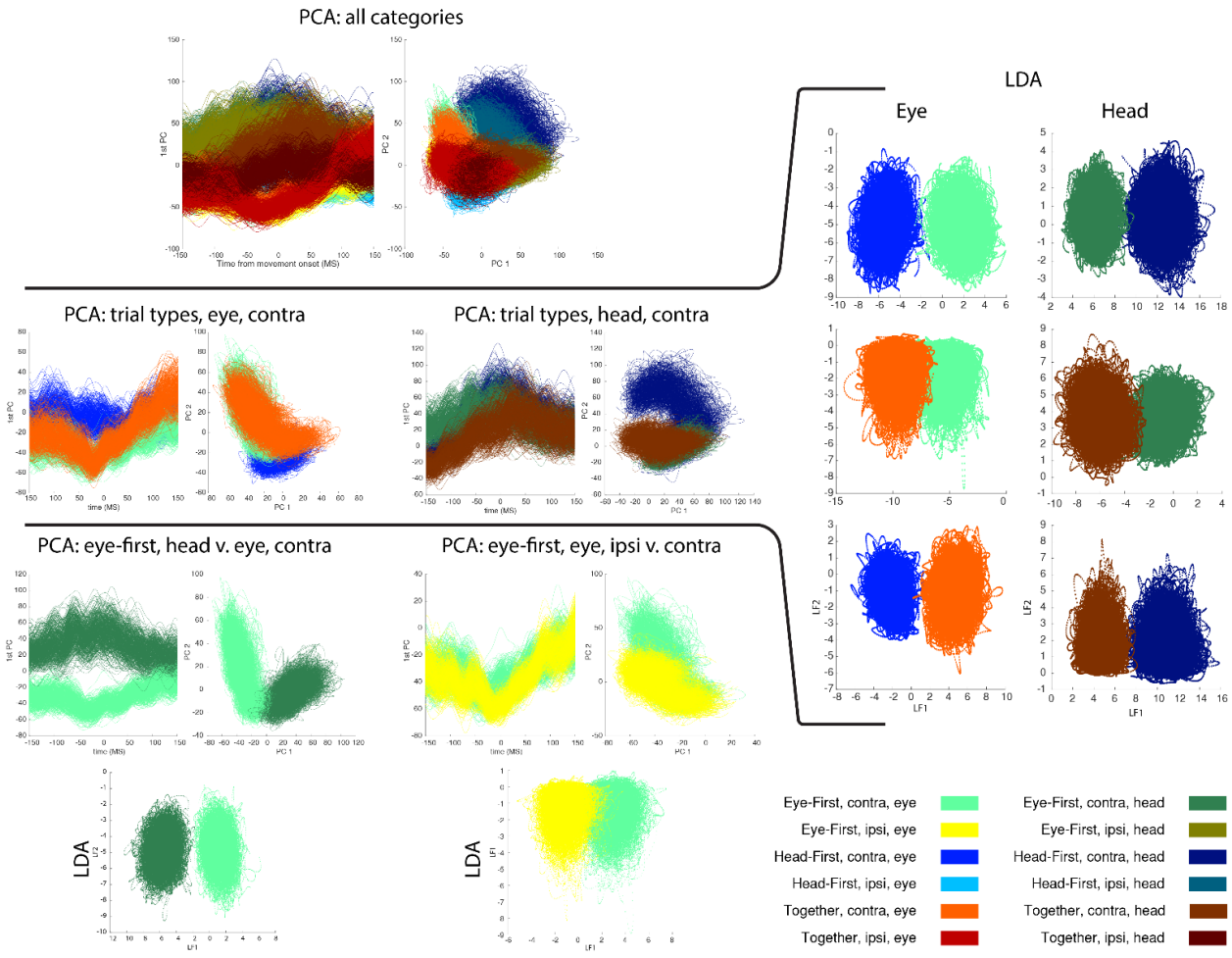

Figure 15: Representative illustrations from PCA and LDA analysis.

Top: first PC as a function of time and first two PCs. Middle: same as above, but only for three trial types; left is the data from the eye movement epoch, right is from the head movement epoch. Corresponding pairwise LDA results are on the right. Bottom left: same as above, but a pairwise comparison between the gaze and the head movement epochs in an eye-first task. Below is the LDA projection on the first two factors. Bottom right: same as bottom left but comparing gaze shifts to ipsi- and contralateral visual space.

3.4.3 Classification

Although LDA shows a clear pairwise separation between different task features, it does not accurately reflect the way these neural signals are used in the brain. It is unlikely that a brain utilizes a pairwise decoder which compares between each pair of conditions individually. Therefore, we wanted to establish that PMv code is robust enough to categorize the activity into one of 12 categories at once. To accomplish this, we trained a relatively simple Naïve Bayes classifier (see methods). When using all c cells for decoding we achieved relatively good results with an average accuracy of ~80%. The decoding accuracy was near 100% for some conditions, while slightly above 50% for others, still well above chance (Figure 16, bottom). We decided to test the robustness of this code by performing the classification on systematically increasing number of neurons.

After sorting the neurons based on their first component weight of the PCA projection, we created a classifier on just one "best" neuron and evaluated its performance. We then continued to add neurons and evaluate subsequent classifiers. We see that it takes 45 neurons to achieve an average classifier performance of ~70%. This suggests this neural code requires a high number of neurons to be usable, which could imply that even though the code is present, it is not very robust. In comparison, some neural classifiers from other cortical motor regions require as little as 15 neurons to achieve this accuracy (Bansal et al. 2012).

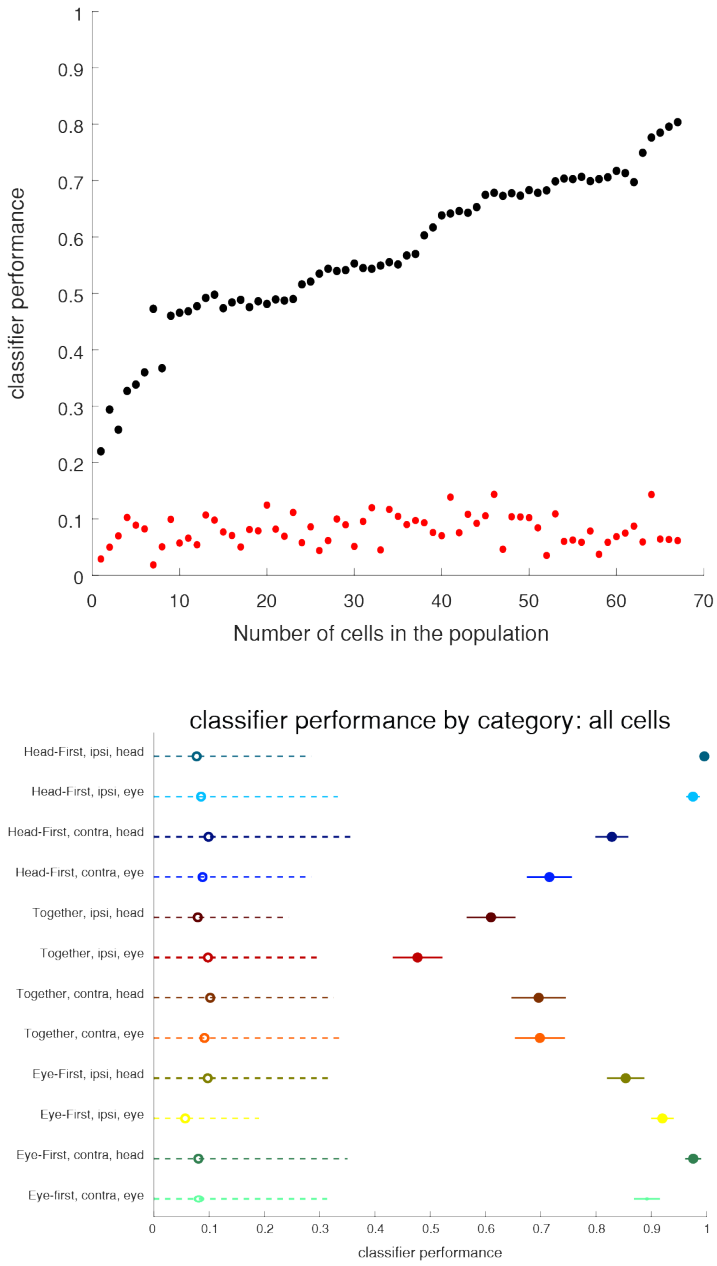

Figure 16: Naïve bayes performance.

Top: black- average decoder performance as a function of size of the training population. Red- same as black, but the training labels were randomized. Bottom: mean decoder performance and two standard deviations at full population separated by category. Open circles are performance from a decoder trained on shuffled data.

3.4.4 Depth

When comparing the ability of PMv code to separate between task-relevant categories as a function of layers, we do not observe a quantifiable result. The separation between categories remains equal regardless of the depth of the recorded neuron; as an example, we show the separation between eye and head subspaces at different depths in Figure 17. However, we cannot make a strong statement about this particular feature of PMv as our control for depth was poor.

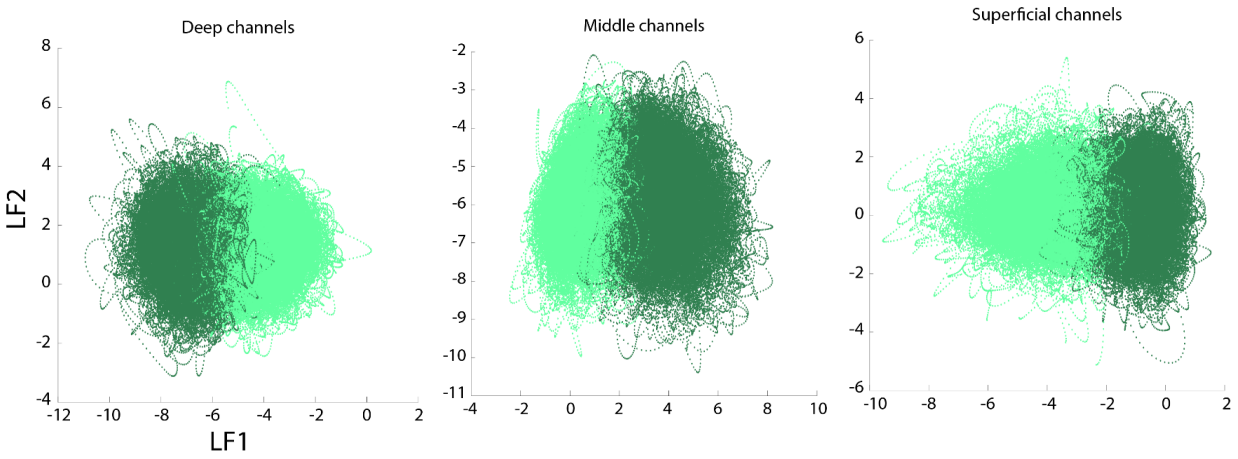

Figure 17: LDA performed on separate layers of the cortex for gaze and head movement epochs during the eye-first task.

3.4.5 Summary

PMv shows a complex relationship with eye and head movements. During the exploration of the region via microstimulation, we observed no notable or repeatable eye or head movements (methods). Furthermore, research shows that inactivation on PMv has little concrete effect on behavior; reported effects show either lack of awareness of motor deficits in humans (Berti 2005)

or a bias in a motor choice in animals (Schieber 2000). However, here we show that PMv carries a clear code for shifting gaze and moving the head. This code is present in single neuron firing rate properties, albeit not in a clear form. And this code emerges clearly when analyzed as a population of neurons. Furthermore, a simple decoder can access this code and determine both the action performed (gaze shift or head movement) and the context under which this muscle group was recruited (eye-first, head-first, or together). On the other hand, this firing-rate code lacks many of the familiar features present in traditional motor areas, such as clear movement-locked modulation, or burst-like properties (Figure 13: left column).

Overall, we can confidently conclude that PMv activity carries features related to different eye and head movements. The precise implementation of this code in a brain will require further investigation.

3.5 Discussion

We rely on vision to explore our surroundings. Despite this, the mechanisms of controlled, natural gaze shifts remain largely unexplored. Difficulties in head-unrestrained neural recordings have limited the scope at which head movements have been studied; and majority of gaze related research relies mainly on saccadic movements of the eyes in a head-restrained environment. In reality, our gaze shifts rely on precise coordinated movements of eyes and head. Known for influencing coordinated movements of separate body parts, PMv is a great candidate to influence these eye-head movements.

Previous microstimulation-based exploration of the premotor cortex shows several key features; mainly, the region is not specialized in the control of one particular motor function.

Although the majority of work in the region relies on hand and arm movements, representations of virtually all skeletomotor effectors are present in the PM cortex (Graziano et al. 2002b; Godschalk et al. 1995; Fujii et al. 1998). But unlike other cortical motor regions which represent multiple effectors, e.g., the primary motor cortex, the topographic organization is far coarser in PMv. This lack of organization is even more stark when approaching the exploration of PMv from an oculomotor perspective, where neural structures are exceptionally organized. The SC and FEF are so well organized, in fact, that you can predict the evoked movement just by mapping the electrode site in the region (Sommer and Wurtz 2000; Klier et al. 2001). By contrast, the coordinates in PMv are rarely predictive of the evoked movement. Regardless, a categorization of PMv topography would provide an invaluable asset to conduct research in this region. Several studies have been conducted which describe the evoked behavior from microstimulation of various regions in PMv (Godschalk et al. 1995; Graziano, Taylor, and Moore 2002b; Fujii et al. 1998). In general, it seems that as one traverses the superior to inferior PMv, the body representation moves from inferior to superior. In other words, the superior portion of PMv has large representations of forelimbs and shoulders, and inferior PMv contains a large orofacial representation. However, we can still identify sites in superior PMv where orofacial and forelimb movements are represented, which indicates that this organization is quite scattered. This, however, played to our advantage as we were able to locate a region where both eye and neck representations converged. In fact, this coarse organization might be the key contributor to PMv's role in coordinated movements, and therefore a strict topography would be detrimental to its role.

Additionally, overall PMv control over motor actions cannot be easily stereotyped. For contrast, the activity in other oculomotor areas like SC, or FEF produces such predictable behaviors that one can describe not only the direction or amplitude of the movement, but even the

kinematics with which the movement occurred (Freedman and Sparks 2000; van Opstal and Goossens 2008; Goossens and Van Opstal 2006; Smalianchuk et al. 2018; Thompson et al. 1996; Walton et al. 2007; Bruce et al. 1985). Even the activity of a non-oculomotor cortical region like M1 produces movements that are precisely characterized by the produced kinematics, or by muscle-constriction properties (Morrow et al. 2007; Vargas-Irwin et al. 2010; Sergio et al. 2005). However, movements produced by PMv are rarely described with such precision. Generally, the behaviors produced through the microstimulation of PMv are too complex for parametric description, so descriptors such as "coordinated", "complex", or "defensive" have to be used in leu of precise measurements (Cooke 2004; Graziano et al. 2002b). When examining eye movements specifically, results once again showed qualitative descriptors, one of which being a "centering" behavior in which the saccades occurred towards a central point in the visual field (Fujii et al. 1998). Once again, this corroborated our hypothesis; complex coordinated context-dependent movements such as head unrestrained gaze shifts are not well suited for parametric descriptions.

All the above PMv features led us to an examination of its role in specific coordinated movements, namely eye and head. These movements involve multiple muscle groups, and specific movement properties change with context, which places these movements well within the possibility of PMv influence. We first approached this examination through the lens of traditional oculomotor studies. More precisely, we expected to see behavior- or stimulus-locked firing rate features in the average firing rate for each condition. However, no such features were present in the data. On visual inspections, cells did not seem to modulate the activity regardless of any experimental factor. Contrary to our initial intuition, the results of statistical analyses showed a strong effect of trial features on the neural activity. Despite this statistical significance, we could

not extract a satisfactory description of PMv involvement in gaze shifts. Each individual cell seemed to have its own unique code that vaguely described the observed behavior.

The lack of characterizable single-cell results was unexpected to us given that other PMv studies have reported discernable movement related properties. Moschovakis et. al. showed exceptionally clear eye-movement-locked responses in PMv cells (Neromyliotis and Moschovakis 2017). In fact, all previous literature led us to expect neurons that burst for a movement, and perhaps modulate the properties of that burst based on context. Instead, we were confronted with an indescribable, yet statistically significant, firing rate code. A possible explanation for this phenomenon might be analogous to some findings in the prefrontal cortex (PFC), where the neural code only emerged when analyzed as a population, and was obscured when looking at individual cells (Elsayed and Cunningham 2017). The notion that if cells respond to multiple task parameters at once, their single-cell code might be obscured and only a population response will show the full picture aligned with our hypothesis. We expected the cells in PMv to respond to multiple effectors, at the least. Hence, the logical next step in our data analysis was to examine the cells as a unified population. When the cells are active together, a clear code is easily discerned. After a simple PCA dimensionality reduction, we could see the separation of neural trajectories as a function of task properties in the first two principal components. This effect was even more obvious in an LDA projection of the data.

For completeness' sake we tested the robustness of this population code by examining how well a classifier could use it. We wanted to see how large this population has to be to reliably differentiate between task related properties. We knew that it had to be more than a single cell, since if that were the case, we would see the representations in single units. We also determined that all 67 cells were more than enough, as the classifier performance was adequate. Through

systematic variation of the population size, we found that about 45 was sufficient for accurate classification.

The results of this study ascribe interesting properties to PMv neural code. Our results show this code to carry usable motor information, similar to traditional motor-related regions. Conversely, the single neuron activity features are very different from traditional motor areas. They do, however, seem to share many properties with the PFC: low firing rates which respond in an unclear manner to several features at once (Elsayed and Cunningham 2017). The functional aspect of this region also seems to straddle this separation. On one hand, we can decode motor properties of the action, such as which effector to move; on the other, PMv population code carries higher-level concepts. In our case, we could determine the task type that the animal was asked to perform. And historically, PMv has been studied in its role in determining context for actions, order of events, and decision making (Schieber 2000; Opitz and Kotz 2012; Hepp-Reymond et al. 1999): all roles which would not be out of place for PFC. This may corroborate the proposed functional connectivity between dorsolateral PFC, the PC, and M1 (Spedden et al. 2020). Findings in our study might add another piece of evidence to this possibility.

This work provides an invaluable insight into the execution of coordinated head and eye movements. We demonstrate a presence of gaze-related signals in an area previously not traditionally seen as a gaze-related structure. Additionally, PMv code differentiates between high order features, such as task-type as well as lower order features, like effector identity; which indicates a unique role from other gaze-related brain areas during eye and head movements.

4.0 Color Cannot Act as A Contextual Cue During Monkey Saccadic Adaptation

4.1 Overview

When the head does not move, rapid movements of the eyes called saccades are used to redirect the line of sight. Saccades are defined by a series of metrical and kinematic (evolution of a movement as a function of time) relationships. For example, the amplitude of a saccade made from one visual target to another is roughly 90% of the distance between the initial fixation point (T_0) and the peripheral target (T_1). However, this stereotypical relationship between saccade amplitude and initial retinal error ($|T_1-T_0|$) may be altered, either increased or decreased, by surreptitiously displacing a visual target during an ongoing saccade. This form of saccadic adaptation has been described in both humans and monkeys. We tested the hypothesis that a contextual cue (target color) could be used to evoke differential gain (actual saccade/initial retinal error) states in rhesus monkeys. We did not observe differential gain states correlated with target color during horizontal adaptation regardless of whether these targets were displaced simultaneously, sequentially, along the same vector as the primary saccade or perpendicular to it. These results are consistent with hypotheses that state that color cannot be used as a contextual cue and are interpreted in light of previous studies of saccadic adaptation in both humans and monkeys.

4.2 Introduction

Primates coordinate movements of the eyes, head, arms, and/or legs in order to gather information from, and efficiently interact with, their local environment. Saccadic eye movements have been frequently studied in an attempt to uncover the neural mechanisms underlying the maintenance of movement accuracy and precision as well as the ability to pair arbitrary sensory stimuli (e.g. a visual object's color, shape, orientation, and/or motion properties) with a specific motoric response in both humans and monkeys (for examples see: Hopp and Fuchs, 2004; Iwamoto and Kaku, 2010; Pélisson et al. 2010; Herman et al. 2013; Liversedge et al. 2011; Gold and Shadlen, 2007; Shadlen and Kiani, 2013). Saccades are rapid, conjugate eye movements that may be used to reorient the line of sight such that the high-resolution region of the retina (the fovea) can be aligned with objects of interest (Leigh and Zee, 1999). Primate saccades are defined by a series of stereotypical metrical relationships between amplitude, peak velocity, and duration. For example, saccade duration is linearly related to movement amplitude (Bahill et al. 1975; Baloh et al. 1975), peak eye velocity and movement amplitude are described by a saturating exponential function (vanGisbergen et al. 1984), and primary saccade gain (movement amplitude/initial retinal error) is approximately 0.90-0.95 (Hyde, 1959; Becker & Fuchs, 1969; Becker, 1972; Henson, 1978, 1979; Prablanc et al. 1978; Kowler & Blaser, 1995). Modifications to these relationships may result from neuromuscular disease (Leigh & Zee, 1999) or, in the case of saccade gain, by experimental manipulations.

Under laboratory conditions, motor learning in the saccadic system ("saccadic adaptation") has mostly been studied by surreptitiously introducing a visual error at the end of a saccade that was aimed at a target located at a particular vector relative to where the subject was fixating (Albano, 1996; McLaughlin, 1967; Deubel, 1987, 1991; Deubel et al., 1986; Miller, et al., 1981;

Noto et al. 1999; Robinson et al. 2003; Scudder et al. 1998; Semmelow et al. 1987; Straube et al. 1997). Under these circumstances: 1) changes in primary saccade amplitude follow a roughly exponential time course with "rate constants" around 30–60 saccades in humans (Albano, 1996; Deubel et al., 1986; Deubel, 1987) and 100-800 saccades in monkeys (Straube et al., 1997); 2) the change in primary saccade vector is proportional to the visual error induced at the end of the movement, but is rarely large enough to consistently place the fovea on the desired target; 3) the magnitude of backward adaptation is larger than forward adaptation in response to the same post-saccadic visual error; 4) adaptation effects transfer to saccades with vectors similar to those initially adapted ("adaptation fields"; Noto et al, 1999); and 5) a corrective movement need not be executed by the subject in order for learning to progress (Wallman & Fuchs, 1998), which indicates that a visual error signal is sufficient enough to drive this form of motor learning.

There has recently been a great deal of interest in "context dependent" saccadic adaptation (see Pélisson et al., 2010, Herman et al., 2013 for reviews). In this type of experiment a cue, either internal (e.g. proprioceptive feedback of eye position) or external (e.g. visual target properties), is used during and after the learning process to elicit different gain states. For example, Alahyane & Pélisson (2004) have shown that human horizontal saccade amplitude can simultaneously be reduced and increased to the same initial target displacement (T_1-T_0) depending upon the vertical orbital eye position (either 12.5° up or 25° down) at which a subject initiates the primary saccade. Interestingly, this eye position contingent gain behavior has proven difficult to elicit in rhesus monkeys under similar conditions (Figures 2 & 8 in Tian & Zee, 2010).

The use of external visual cues to drive different gain states during saccadic adaptation has led to a mixture of results in human subjects. Deubel (1995), in a few human subjects, was unable to elicit distinct gain states during horizontal adaptation using colored, static targets (red crosses

and green circles) that were displaced along the same axis as the primary saccade by a few degrees of visual angle. Subsequent investigations of human saccadic adaptation were also unable to elicit context dependent adaptation using either static shapes (diamonds versus squares; Bahcall & Kowler, 2000) or moving visual targets with different shapes and colors (Azadi & Harwood, 2014). However, other explorations of saccadic adaptation have shown that visual cues such as flickering versus non-flickering targets (Madelain et al., 2009) and other properties of moving targets (speed and direction) (Azadi & Harwood, 2014) can be used to elicit different gain states.

Given the different behaviors of human subjects in context cue adaptation experiments using different visual stimuli, and the potential for monkeys to have different behavior to the same stimuli that elicited context dependent adaptation behavior in humans, we designed the current study to test the hypothesis that color can be used as a contextual cue in a saccade adaptation task. Although our results concur with those observations made by Deubel (1995) and Azadi & Harwood (2014), our experiments provide a more extensive data set to support the assertion that the saccadic adaptive control system does not differentiate between color targets. These data are interpreted in the light of previous context dependent adaptation studies, our knowledge of the anatomical substrate underlying saccadic eye movements, and physiological investigations of the neural substrate underlying the generation of saccades and saccadic adaptation.

4.3 Materials and Methods

All procedures were approved by the Institutional Animal Care and Use Committee of the University of Pittsburgh and were in compliance with the guidelines set forth in the United States Public Health Service Guide for the Care and Use of Laboratory Animals. Two male rhesus

monkeys (BB and WE) weighing 9.0-13.0kg served as subjects. Both monkeys had a small head-restraint device secured to the skull during an aseptic surgery. In an additional aseptic surgery, monkey BB had a scleral coil implanted for monitoring gaze position (Judge et al. 1980). After full recovery, both animals were trained to sit in a primate chair with their head restrained and a sipper tube was placed near the mouth for reward delivery. Both subjects were subsequently trained to make gaze shifts to visual targets.

For monkey BB, visual stimuli, behavioral control, and data acquisition were controlled by a custom-built program that uses LabVIEW architecture on a real-time operating system supported by National Instruments (Austin, TX) (Bryant and Gandhi, 2005). The animal sat inside a frame containing two alternating magnetic fields that induced voltages in the eye coil and thus permitted measurement of horizontal and vertical eye positions (Robinson, 1963). Visual targets were displayed on a 55 inch, 120 Hz resolution LED monitor. For monkey WE, eye movements were monitored using an eye tracker (Eye Link 1000, SR Research Ltd, Mississauga, Ontario, Canada), and visual targets were presented on a 21 inch, 100 Hz resolution CRT monitor.

4.3.1 Trial Types

Subjects performed two tasks (probe and adaptation trials; Figure 18A,B) that each began with the illumination of an initial fixation target (T0). Subjects were required to look at and maintain fixation of T0 for a variable duration (500-1000ms, 50 or 100ms increments). Trials were aborted if the line of sight deviated beyond a computer-defined window (3° radius) surrounding T0. However, if fixation was maintained, a peripheral target (T1) was illuminated. T0 and T1 overlapped between 0 to 750ms in 250ms increments. If the subject continued to maintain fixation of T0 for the duration of this overlap period, then T0 was extinguished, cuing the animal to make

a saccade to T1. To this point both probe and adaptation trial types were identical. During "probe" trials (Figure 18A), T1 remained illuminated until the position of the line of sight exited the computer window centered on the location of the no longer visible T0. T1 was never re-illuminated after the line of sight crossed this position criterion during probe trials; therefore, no visual feedback was available on these trials. "Adaptation" trials (Figure 18B) were similar to probe trials except that after T1 was extinguished, a target (T2) was immediately illuminated in a new spatial location. The new location could be further away from (horizontal forward adaptation) or closer to (horizontal backward adaptation) T0 along the horizontal meridian during trials attempting to elicit adaptation of the horizontal component of the primary saccade vector (Figure 18C). In experiments attempting to elicit changes in the vertical component of the primary saccade vector, targets could be displaced above (upward adaptation) or below (downward adaptation) the horizontal meridian (Figure 18D). The latter experiments are hereafter referred to as "orthogonal adaptation" experiments.

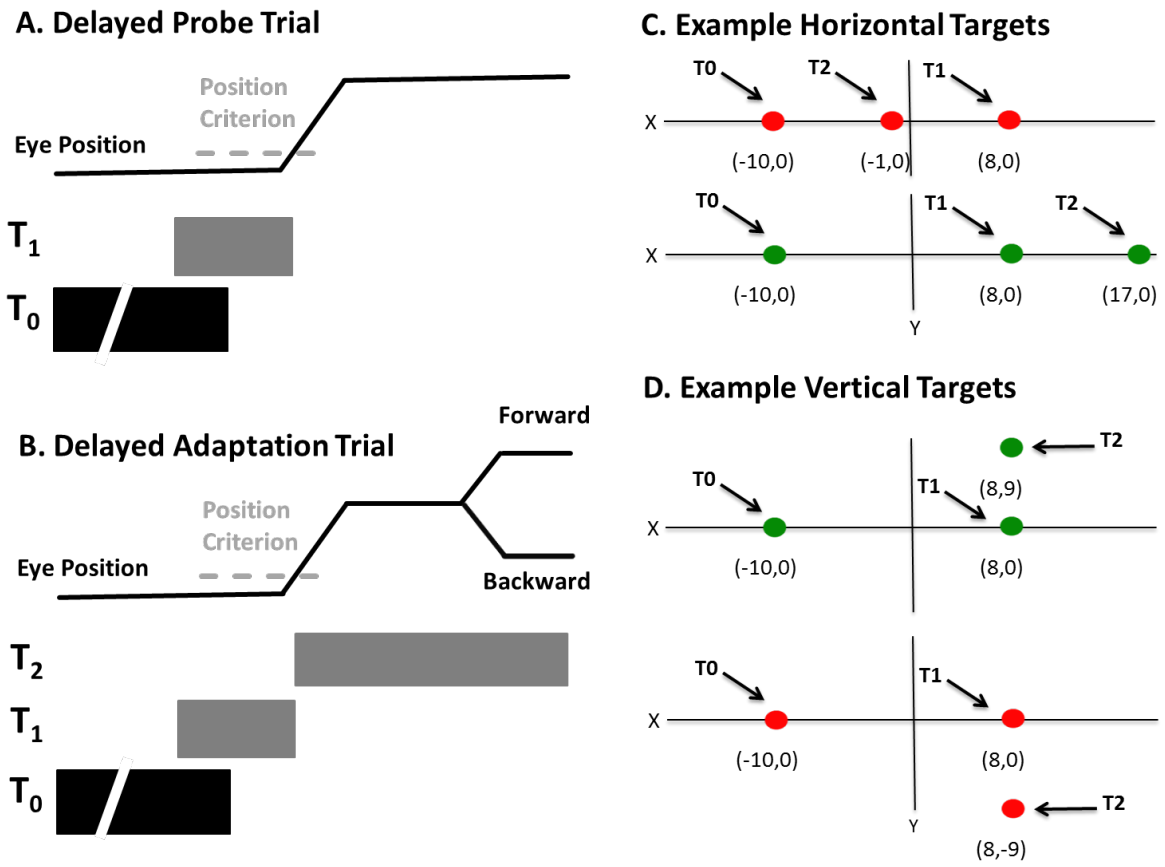

Figure 18: Delayed Probe probe and backward adaptation trial types and target locations.

Probe (A) and adaptation (B) trials begin in the same fashion. Subjects are initially required to fixate a target (T0) for a variable duration within a computer-defined window. A peripheral target (T1) is then presented and the subject must maintain fixation of T0 for a variable "delay period" during which T0 and T1 overlap. If the subject maintains fixation to the end of the delay period, then T0 is extinguished, cuing the subject to produce a saccade to T1. When the subject produces a saccade towards T1 they will leave the computer defined window and trigger the offset of T1. In probe trials, this target is never illuminated again. In backward adaptation trials, another target (T2) is presented at a location between T0 and T1. During a forward adaptation experiment T2 would be presented at a more eccentric location. Although not shown here, note that the color of the target remains constant within a trial. However, the target color may be red, green, or yellow between trials. Panels C and D illustrate the location of targets during horizontal and vertical adaptation experiments. Colors correspond to those used during adaptation trials in the adaptation phase (See Materials and Methods for further details).

4.3.2 Target Characteristics and Locations

Targets (T0, T1, T2) were red, green, or yellow dots subtending ~1° of visual angle. Target color remained constant within a given trial. Therefore, during adaptation trials, the fixation point color could indicate forward or backward adaptation. Target locations during probe and adaptation trials remained fixed within a data collection session. The fixation target (T0) was fixed at either (-10º, 0º) in some sessions and at (10º, 0º) in other sessions. As illustrated in Figure 18C, if a subject began horizontal adaptation trials by fixating a T0 located at (-10º, 0º), then T1 during these trials was always located at (8º, 0º). T2 could be located at (-1º, 0º) or (17º, 0 º) during horizontal backward (red targets) and forward (green targets) adaptation trials, respectively. The mirror images (as reflected through the ordinate) of these targets were used during adaptation trials that began at (10º, 0º). Orthogonal adaptation sessions used the same T0 and T1 as horizontal experiments. However, during these sessions T2 was located either 9° above (green targets) or below (red targets) T1 during upward and downward adaptation trials, respectively (Figure 18D).

The position of T1 during probe trials was randomly selected from four possible locations during each data collection session. These locations included the T1 and T2 positions used during adaptation trials as well as a location that would elicit a saccade in the opposite direction of the primary saccade made during adaptation trials; for example, if T0 was (-10º,0º) then this target would be located at (-18º,0º). The direction of the primary saccade during adaptation trials was pseudorandomly alternated (left or right) between sessions. For illustrative purposes, all targets and data are discussed as if primary saccades were always directed to the right and only probe trials at the T1 location of adaptation trials are presented.

4.3.3 Experimental Sessions

Adaptation sessions were carried out in one of two general patterns: concurrent or sequential (Figure 18). Each session began with a block of probe trials, hereafter referred to as the "pre-adaptation phase", whose target colors and locations were randomly interleaved. During concurrent sessions (top row), the pre-adaptation phase was immediately followed by an "adaptation phase" in which only adaptation trials using two of the three colors (red and green) were randomly interleaved. Note that during both concurrent and sequential adaptation sessions, red targets were associated with trials meant to elicit backward or downward adaptation and green targets were associated with trials meant to elicit forward or upward adaptation. The adaptation phase of concurrent sessions was followed by a "post-adaptation" phase in which only probe trials using all three colors were randomly interleaved.

During sequential sessions (bottom row), the pre-adaptation phase was followed by a block of red adaptation trials. This block of adaptation trials was immediately followed by a brief block of (20-40) red probe trials using only the T1 location used during adaptation trials in the previous adaptation block. The red-only probe phase was followed immediately by a block of green adaptation trials. A post-adaptation phase, identical to the post adaptation phases in the concurrent experiments, followed the block of green adaptation trials.

4.3.4 Data Acquisition and Analysis

For both animals, each trial was digitized and stored on the computer's hard disk for off-line analysis in MATLAB (R2013b; Natick, Massachusetts, U.S.A). Horizontal and vertical eye positions were stored with a resolution of 1ms. Component velocities were obtained by

differentiating the eye position signals. The onset and offset of saccades were identified using a velocity criterion of 40°/second. Saccade amplitude was defined as the change in eye position from the beginning to end of the eye movement based on this velocity criterion. All of the data reported here are the result of measuring the first ("primary") saccade made towards T1 that was associated with the adaptation trials for a particular session. This has traditionally been used to assess the subject's motoric state at various time points during adaptation experiments (see Hopp & Fuchs (2004) for review). The primary saccade needed to occur within 500ms after the offset of T0 and have a horizontal amplitude greater than 5° in order to be considered for further analysis. Saccade gain was defined by the following formula:

$$Saccade\ Gain = \frac{|Saccade\ Amplitude|}{|(T_1 - Initial\ Eye\ Position)|}$$

By definition a saccade with a gain that is less than 1.0 is hypometric whereas a saccade with a gain greater than 1.0 is hypermetric. Trials were then parsed based on whether the target color within a trial was red, green, or yellow. For each color group, the average gain or amplitude of saccades made during all pre-adaptation phase probe trials using the T1 that was used during adaptation trials ("pre-probe trials") was compared with average of all probe trials presented after a particular adaptation segment ("post-probe" trials). All values are reported as means (± SD) and comparisons of means were made using a two-tailed t-test or one-way ANOVA in the MATLAB Statistical Toolbox; significance was determined using a criterion of $p < 0.05$. Lastly, the relationship between saccade gain and trial number during the adaptation phases of each session data was assessed by fitting (MATLAB Curve Fitting Toolbox) this data with an exponential, saturating function ($y = a \pm b*\exp(-x/c)$), where x represents trial number, y indicates saccade gain,

c is the time constant, and a and b are constants. In the case where adaptation occurs, the time (trial) constants from this exponential fitting should be on the order of hundreds of trials (Straube et al., 1997). In the case where gain remains relatively constant throughout the adaptation phase, the time constants should be very short (less than 10 trials) or undefined (i.e. fit did not converge to a solution).

4.4 Results

4.4.1 General Hypothesis and Predictions

The two alternative hypotheses being tested by our experiments, and their predictions during the concurrent and sequential adaptation paradigms, are illustrated for the reader in Figure 19. Hypothesis #1 states that color does not act as a contextual cue. Hence, no changes in saccade gain are predicted during the interleaved forward and backward jumps that occur in concurrent sessions. It follows that saccade gains to all three colored targets in the post-adaptation probe epoch will not differ from each other or the pre-adaptation gains. During sequential sessions (Figure 19C), we expect the saccade gain to decrease when the red target steps backward during a block of adaptation trials. Some recovery could occur during the brief block of red probe trials that follows or gain could remain stable because there is no visual feedback during these trials. The gain should be less than the pre-adaptation value at the beginning of the next block of green adaptation trials (in which the target jumps forward), but it should increase gradually as forward adaptation takes effect. For the probe trials presented during the post-adaptation phase, the gains

of all three colors should be comparable and similar to the pre-adaptation gain values. Collectively, saccade gains are similar regardless of the color and context of the targets.

Hypothesis #2 proposes that color does act as a contextual cue. For concurrent sessions (Figure 19B), both backward and forward adaptation can be induced simultaneously, which persists within the post-adaptation period. Note that probe trials with the yellow target should show no adaptation. In sequential sessions (Figure 19D), backward adaptation should occur with red target trials. When forward adaptation trials follow with green target trials, the initial saccade gain should match the pre-adaptation value, not the gain observed at the end of the red-probe trials; thus, there could be a discontinuity is saccade gain as we switch from red to green trials. In the post-adaptation phase, saccade gains observed toward the end of the backward and forward adaptation trials should be observed during red and green probe trials, respectively. The gain for yellow probe trials should match the corresponding pre-adaptation value.

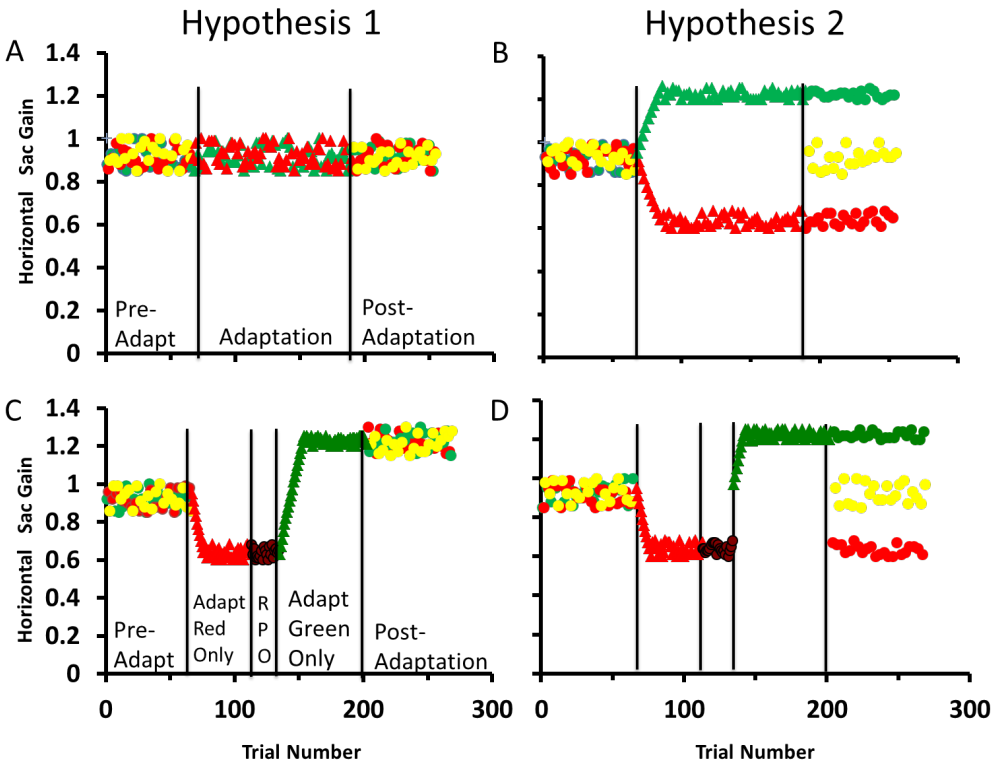

Figure 19: Predictions based on alternative hypotheses concerning the use of color as a contextual cue during concurrent (Panels A, B) and sequential (C, D) horizontal adaptation experiments.

Circles represent probe trials whereas triangles represent adaptation trials. Colors represent the color of all targets within a given trial. Hypothesis #1, that color cannot act as a contextual cue, predicts that gain will remain constant throughout the three phases (pre-adapt, adaptation, post-adapt) of a sequential experiment (A). Hypothesis #2, that color can act as a contextual cue, predicts that gain will decrease in response to red (backward) adaptation trials and increase in response to green (forward) adaptation trials during a sequential experiment (B). These gain changes will carry over into the post-adaptation phase, but the gain on yellow trials will be equivalent to the gain during the pre-adaptation phase. (C,D) Both hypotheses predict changes in gain during the adaptation phases of sequential experiments. Hypothesis #1 predicts a decrease in saccade gain during red adaption trials, carryover of this gain state during the red probe only phase ("RPO"), an increase in gain during green adaptation trials, and a carryover of the gain at the end of the green adaptation phase into the post-adaptation phase for probe trials using all three colored targets.

Hypothesis #2 predicts a decrease in saccade gain during red adaption trials and the carryover of this gain state to the red probe only phase. However, at the beginning of the green adaptation phase, the gain of the primary saccades will be the same as that during green probe trials in the pre-adaptation phase. The gain of saccades during the green adaptation phase will increase and this gain will carry over to only green probe trials in the post-adaptation phase. During the post-adaptation phase the gain of red adaptation trials will be the same as that during the red only probe phase whereas the yellow probe trials will have the same gain as those yellow trials in the pre-adaptation phase.

4.4.2 Horizontal Concurrent Experiments

Figure 20A portrays data from an exemplar horizontal concurrent experiment (BBHC5). As illustrated in this figure, during the pre-adaptation phase of this experiment the mean ± SD gains of saccades made to T1 were similar regardless of color (green = 0.95 ± 0.05; red = 0.99 ± 0.05; yellow = 0.97 ± 0.04). Interestingly, the gain of primary saccades during red (backward) and green (forward) adaptation trials did not change during the adaptation phase. This qualitative assertion is supported by the observation that the time (trial) constants for the exponential fits of adaptation trials were very short (green = 0.08; red = 0.04). Furthermore, this gain state was maintained into the post-adaptation phase in which the monkey made saccades during probe trials using the three different colors (post-probe green = 0.98 ± 0.05; red = 0.96 ± 0.05; yellow = 0.99± 0.05).

Figure 20B displays the pre-adaptation probe (solid bars) and post-adaptation probe mean (striped bars) for each of the three different colors for each of the 10 horizontal concurrent experiments. As shown, in no case was the pre-adaptation probe mean of a particular color different than the post-adaptation probe mean (two-tailed t-test, $p > 0.05$). Furthermore, the time (trial) constants from the exponential fits of adaptation trials in these sessions was either undefined (green trials: 8/10 sessions; red trials: 2/10 sessions) or was less than 6 trials (green trials: 2/10 sessions; red trials: 8/10 sessions). These observations support the assertion that no adaptation based on color cues occurred during the adaptation epoch of horizontal concurrent experiments.

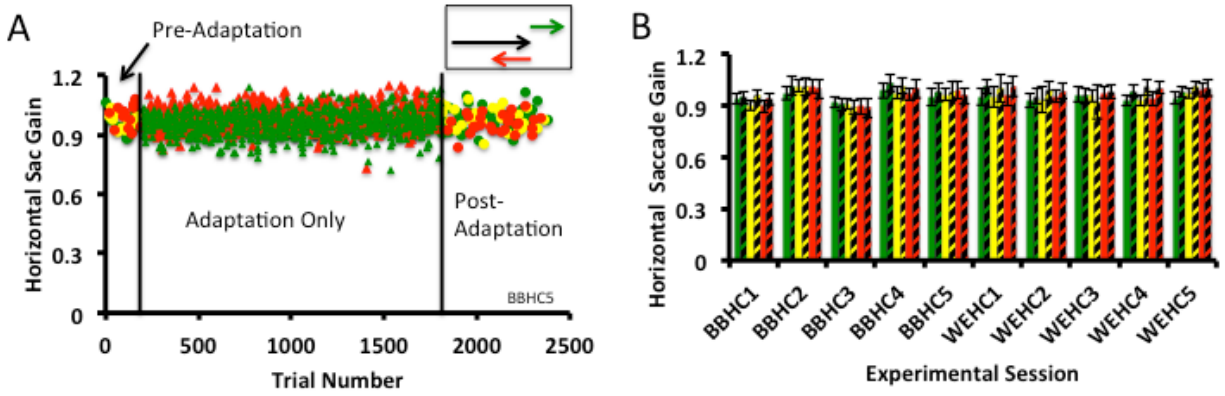

Figure 20: Horizontal Concurrent Experiments.

(A) Horizontal, primary saccade gain during the preadaptation, adaptation, and post-probe segments of experiment BBHC5. Each symbol (circle or triangle) represents data from a single trial. Circles represent probe trials; triangles represent adaptation trials; symbol colors represent the color of the targets within a given trial. Inset portrays the direction of the primary saccade (black arrow), the direction of the intrasaccade target displacement during red (red arrow) and green (green arrow) adaptation trials. (B) Summary of the saccade gain values for 10 horizontal concurrent sessions.The mean (±SD) of the preadaptation probe (solid bars) and post adaptation probe (oblique striped bars) for each target color (green, yellow, red) is illustrated. No significant differences between pre- and post-probe means were observed in these experiments (two-tailed t-test, $p > 0.05$).

4.4.3 Horizontal Sequential Experiments

Figure 21A portrays data from an exemplar horizontal sequential experiment (BBHS3). The gains of saccades made to T1 were also similar regardless of color in the pre-adaptation phase of this experiment (green = 0.94 ± 0.06; red = 0.94 ± 0.05; yellow 0.92 ± 0.04). During the first adaptation block (red trials, backward adaptation), the gain of the primary saccades gradually declined such that the gain of the red probe trials that immediately followed this adaptation block was significantly smaller than the red probe trials from the pre-adaptation phase (post probe mean ± SD = 0.80 ± 0.05; two-tailed t-test, $p < 0.001$). During the ensuing green (forward) adaptation block, the gain of saccades produced gradually increased such that the gain of the last 15 green adaptation trials at of this segment was qualitatively similar to that of the pre-adaptation green probe trials (mean ± SD 1.00 ± 0.03). In fact, the gain of the pre-adaptation probe trials for green, red, and yellow targets were not different than the post-adaptation probe trials of that same color (post probe green = 0.95 ± 0.06, red = 0.95 ± 06, yellow = 0.96 ± 0.05; two-tailed t-test, $p < 0.05$).

Figure 21B compares the gain of pre-adaptation (solid bars) to post-adaptation (striped bars) probe trials based on color across all sequential adaptation sessions. Note that the gain of red post-adaptation probe trials was not significantly different than pre-adaptation probe trials in the majority (7/8) of cases; in other words, saccades made during trials with red targets during the post-adaptation probe phase had regained their baseline gain state after it reduced in the red adaptation block. In the majority of cases (6/8), pre-and post-adaptation probe trials using green and yellow targets were not different. In the remaining two cases (BBHS2, WEHS2), green and yellow post-adaptation probe trials were significantly smaller than pre-adaptation probe trials. In both cases, this is most likely the result of incomplete recovery from the gain reduction that occurred during the red adaptation segment.

Unlike the outcome of concurrent sessions, changes in saccade gain were observed during the red-only and green-only adaptation phases in sequential blocks. Figure 21C illustrates this point by plotting the gain across the different epochs. Each session was divided into six epochs. Mean (± SD) gain during "Pre-Adapt Probe", "Red Probe Only", and "Post-Adapt Probe" epochs was assessed by averaging all probe trials within these segments regardless of color. Mean gain during the adaptation epochs was assessed by averaging 15 adaptation trials at either the beginning ("Begin Green Adapt") or end ("End Red Adapt" and "End Green Adapt") of a particular adaptation segment. In this figure, each session is represented by a different color and each monkey by a different symbol (BB = ●; WE = ▲). Lastly, the mean (± SD) across all sessions for a particular epoch is represented by a grey square and dotted line.

Generally, the changes in gain observed across phases in the exemplar session (Figure 21A) were present across all experimental sessions (Figure 21C). For example, saccade gain decreased significantly between Pre-Adapt Probe and End Red Adapt epochs within each session and was maintained throughout the Red Probe Only and Begin Green Adapt epochs (two-tailed t-test, bonferroni correction, $p < 0.001$). By the last 15 trials of the green adaptation phase (End Green Adapt) gain had returned to baseline levels in 6/8 experiments (two-tailed t-test, bonferroni correction, $p < 0.05$). Gain was not significantly different between pre- and post-adaptation probe trials in 5/8 experiments (two-tailed t-test, bonferroni correction, $p < 0.05$). In those experiments in which differences in gain were observed between pre- and post-adaptation phases (BBHS2, WEHS2, WEHS4), the gain was always smaller in the post-adaptation phase.

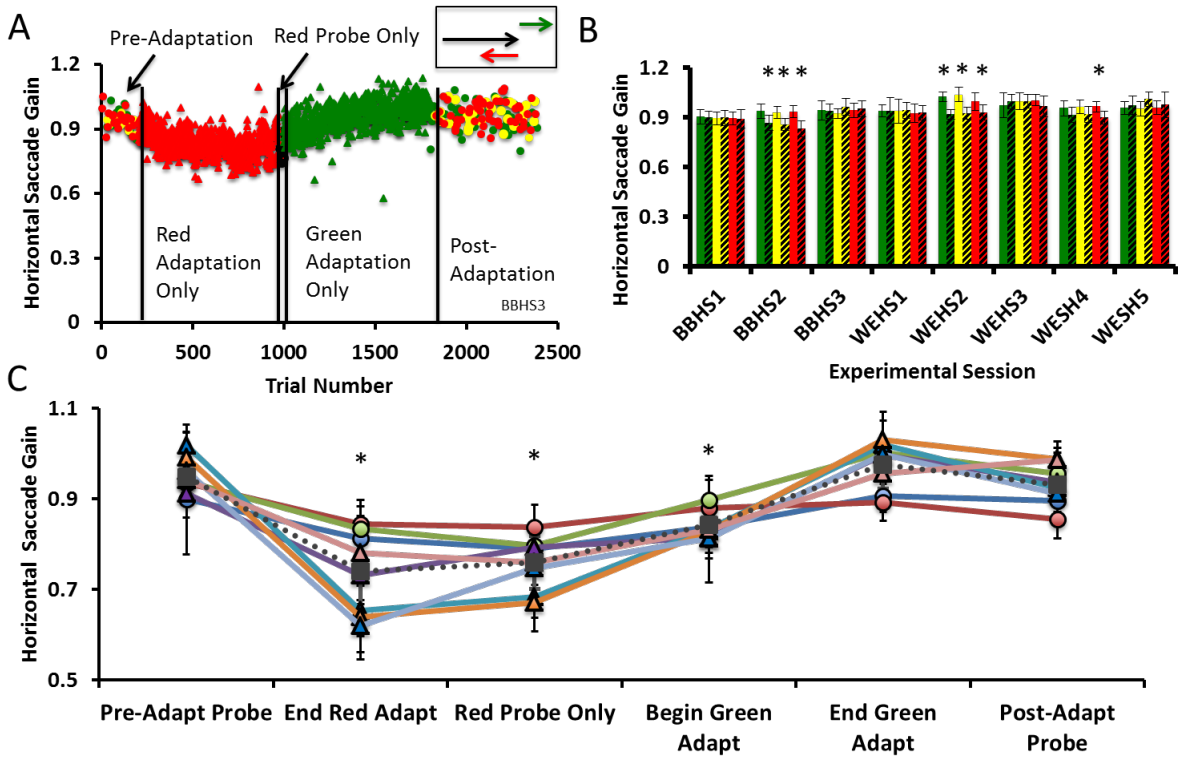

Figure 21: Horizontal Sequential Experiments.

(A) Horizontal, primary saccade gain during the preadaptation, red and green adaptation, red probe only, and post-probe segments of experiment BBHS3. Symbols, colors, and inset are the same as described for figure 20. (B) Summary of the saccade gain values for 8 horizontal sequential sessions. The mean (±SD) of the preadaptation probe (solid bars) and post adaptation probe (striped bars) for green, yellow and are presented. (*) denotes a significant change in saccade gain between pre- and post- adaptation phases (two tailed t-test, $p < 0.05$). (C) Saccade gain as a function of session epoch (Pre-Adapt, End Red Adapt, Red Probe Only, Begin Green Adapt, End Green Adapt, and Post-Probe) during all Horizontal Sequential Experiments. Circles and triangles represent data from monkeys BB and WE, respectively. Pre-, Red Only, and Post-Probe mean gain was taken from all trials in that epoch regardless of color. Gains from the adaptation phases were calculated using either the last 15 (End Red Adapt and End Green Adapt epochs) or the first 15 (Begin Green Adapt epoch) adaptation trials. Grey squares represent the grand mean (±SD) across all sessions for that epoch. (*) denotes a significant change in the grand mean between an epoch and the pre-adaptation phase (two-tailed t-test, bonferroni correction, $p < 0.05$).

Like previous examples of monkey saccade amplitude adaptation, we also fit adaptation trials with a saturating exponential function (see methods). In brief, the time (trial) constants of green (mean = 827.6 ± 647.9; range = [152, 1698]; mean R2 = 0.985 ± 0.002) and red (mean = 969.4 ± 1081; range = [53, 2785]; mean R2 = 0.799 ± 0.235) adaptation trials were not significantly different (two-tailed t-test, p =0.27) and were in the range of those previously reported (e.g. Straube et al., 1997).

4.4.4 Single Target Displacement, Orthogonal and Vector Concurrent Experiments

The experiments reported thus far lend support to the hypothesis that color cannot be used as a contextual cue. However, it was possible that during these experiments the saccadic adaptation mechanism was averaging the visual errors between red (backward) and (green) adaptation trials thereby canceling out any contextual effects. Therefore, we decided to perform three additional control experiments. Figure 22 portrays data collected from an exemplar backward-null experiment in monkey BB and a summary of pre- and post-adaptation probe gains for each color target. The pre-adaptation phase, and the monkey's behavior during this phase, was similar to that of the horizontal concurrent and sequential experiments (compare figures 20, 21, and 22). During the adaptation phase of this experiment, red and green target trials were randomly interleaved. Importantly, the red stimulus jumped backward, while the concurrent green stimulus was never displaced and remained lit at the same location for the remainder of the trial. If the colors can act as a contextual cue in these experiments, then saccade gain should decrease during red adaptation trials and remain constant during green probe trials. However, if the saccade adaptation mechanism was averaging between the two targets, then saccade gain should decline for both red and green trials, albeit at a slower rate and/or a reduced magnitude. Neither of these patterns were observed

in the exemplar experiment (Figure 22A) or in the summary data (Figure 22B), which suggests that the adaptive control mechanism may not be using the visual error during red adaptation trials in this circumstance.

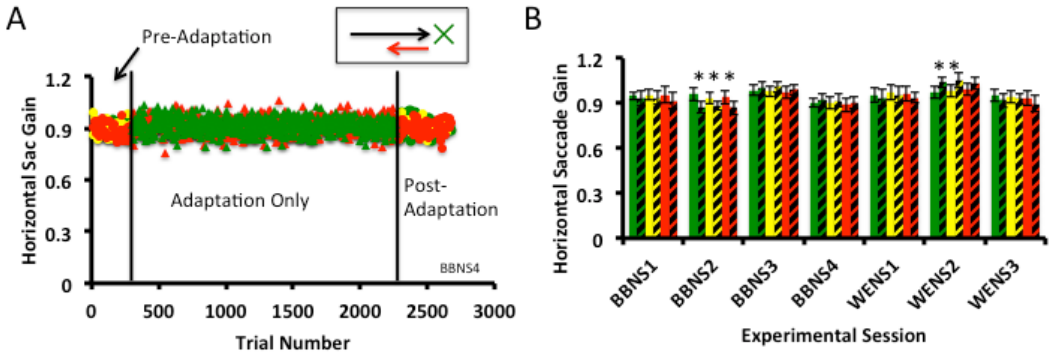

Figure 22: Backward-Null Experiments.

(A) horizontal, primary saccade gain during the preadaptation, adaptation, and post-probe segments of experiment BBNS4. (B) Summary of the saccade gain values for 7 single target displacement sessions. The mean (±SD) of the preadaptation probe (solid bars) and post adaptation probe (oblique striped bars) for each target color (green, yellow, red) is illustrated. (*) denotes a significant change in saccade gain between pre- and post- adaptation means (two-tailed t-test, $p < 0.05$).

Figure 22B displays the pre-adaptation probe (solid bars) and the post-adaptation probe mean (striped bars) for each of the different colors for each of the eight horizontal concurrent experiments. In the majority of experiments (5/7), the pre-adaptation probe mean of a particular color was not different than the post-adaptation probe mean. In one experiment (BBNS2), saccade gain was significantly smaller during post-adaptation probe trials than pre-adaptation probe trials for every color. In the remaining experiment (WENS2), saccade gain increased between pre- and post-adaption probe trials for two (green and yellow) out of three colors. Lastly, the exponential time (trial) constants were either undefined (green trials: 4/7 sessions; red trials: 1/7) or less than 9 trials (green trials: 3/7 sessions; red trials: 6/7) in these sessions. These observations are not

consistent with hypotheses that state that color can act as a contextual cue or that the adaptation mechanism will take an average between the two targets across multiple trials.

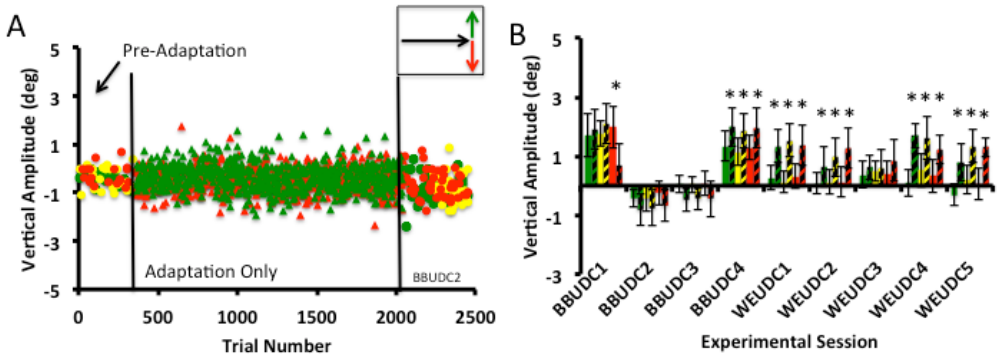

Figure 23: Orthogonal Concurrent Experiments.

(A) vertical, primary saccade amplitude during the preadaptation, adaptation, and post-probe segments of experiment BBUDC2. (B) Summary of the vertical amplitude values for 9 orthogonal concurrent experiments. The mean (±SD) of the preadaptation probe (solid bars) and post adaptation probe (oblique striped bars) for each target color (green, yellow, red) is illustrated. (*) denotes a significant change in saccade amplitude between pre- and post- adaptation means (two-tailed t-test, $p < 0.05$).

Figure 23 describes the amplitude of the vertical component of the primary saccade from 9 (4 in monkey BB; 5 in monkey WE) orthogonal concurrent experiments in which T2 during adaptation trials was displaced either 9° upwards (green) or downwards (red) relative to the T1 target. During the exemplar experimental session (BBUDC2), the amplitude of the vertical component remained relatively constant throughout the adaptation phase and was not different between the pre- and post-adaptation phases of the experiment. This observation was made in 3/9 of the experiments. In one experiment (BBUDC1), two out of the three colors (green and yellow) did not change significantly between the pre- and post-adaptation phases. In the remaining 5 experiments, significant changes occurred for all three colors such that the post-adaptation trials

had an upward displacement. This variable behavior resulted in time (trial) constants that were undefined (green trials: 6/9 sessions; red trials: 5/9 sessions) or less than 3 trials (green trials: 2/9 sessions; red trials: 3/9 sessions) in the majority of sessions. In only one session (BBUDC4) were the time constants greater than 10 trials (green trials = 12.84, R2 = 0.01; red trials = 97.4, R2 = 0.05).

The results from each of the aforementioned experiments suggest that the adaptive control system does not use color as a contextual cue. If this is true, then error signals provided on adaptation trials using one color should transfer to both adaptation and probe trials that use other colors. We tested this prediction by concurrently intermixing backward (red) and upward (green) adaptation trials during the adaptation phase of our concurrent experiments. Figure 24A shows the vertical amplitude versus trial plots for one of these experiments in subject BB (BBVAC1). The vertical amplitude was similar between probe trials using different colors in the pre-adaption phase. During the adaptation phase, the vertical amplitude of saccades increased (was deviated upwards) during adaptation trials using both red and green targets even though target displacement in the vertical direction only occurred during green adaptation trials. This increase in vertical amplitude was also observed in the post-probe phase such that probe trials using red, green, and yellow targets were significantly larger than that of comparable trials in the pre-adaptation phase. Significant changes in vertical amplitude were seen in 3 of 4 experiments (Figure 24C). Lastly, the time (trial) constants from exponential fits of vertical green (203.6 ± 198.6; R2 = 0.18 ± 0.05) and red (114.4 ± 73.6; R2 = 0.56 ± 0.41) adaptation trials were similar.

Figure 24B shows the horizontal amplitude versus trial plots for the same experiment as Figure 24A. The horizontal amplitude of saccades was similar between probe trials using different colors. During the adaptation phase, the horizontal amplitude of saccades decreased during

adaptation trials using both red and green targets even though target displacement in the horizontal direction only occurred during red adaptation trials. This reduction in horizontal amplitude was also observed in the post-probe phase such that probe trials using red, green, and yellow targets were significantly smaller than that of comparable trials in the pre-adaptation phase. Significant changes in horizontal saccade amplitude were seen for all three colors in all four experiments (7D). Lastly, the time (trial) constants from exponential fits of horizontal green (120.8 ± 19.7; R2 = 0.81 ± 0.30) and red (131.0 ± 44.4; R2 = 0.83 ± 0.28) adaptation trials were also similar. Although in the same range, it is not clear why the trial constants during vector concurrent experiments were, on average, qualitatively faster that the horizontal sequential experiments stated above; however, note that these values are still in the same range of those previously reported (e.g. Straube et al., 1997) and may be due to the use of large intra-saccade target displacements (Cecala & Freedman, 2009). Regardless, the observation that saccade amplitude did not vary as a function of trial color in any of the aforementioned experiments is consistent with the hypothesis that color cannot be used as a contextual cue.

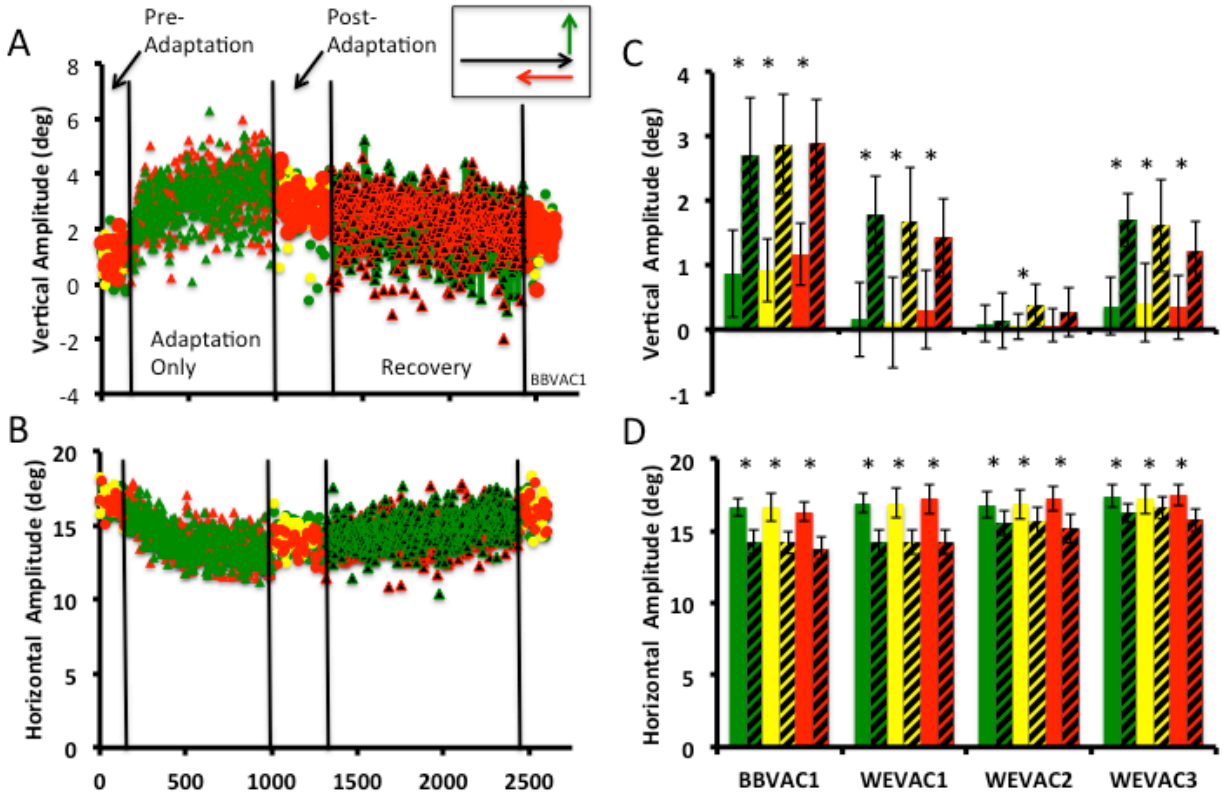

Figure 24: Vector Concurrent Experiments.

Horizontal (A) and vertical (B) primary saccade amplitude during the preadaptation, adaptation, and post-probe segments of experiment BBVAC1. A circle or triangle represents data from a single trial. Solid colored circles represent probe trials; solid colored triangles represent adaptation trials; Black triangles with colored borders represent recovery trials. Symbol/outline colors (red, green, or yellow) represent the color of the targets within a given trial. Inset portrays the direction of the primary saccade (black arrow), the direction of the intrasaccade target displacement during red (red arrow) and green (green arrow) adaptation trials. (C,D) Summary of the vertical (C) and horizontal (D) values for 4 vector concurrent experiments. The mean (±SD) of the preadaptation probe (solid bars) and post adaptation probe (oblique striped bars) for each target color (green, yellow, red) is illustrated. (*) denotes a significant change in saccade amplitude between pre- and post- adaptation means (two-tailed t-test, $p < 0.05$).

4.5 Discussion

4.5.1 Major Observations

In each of the aforementioned experiments we attempted to elicit distinct saccade gain states using static, colored targets as the contextual cue. In our experiments the intra-saccade target displacement during adaptation trials was large (9° or ~50% of primary saccade amplitude) and was either along the same axis as (Figures 20, 21), or orthogonal (Figure 23) to, our subjects' primary saccades. Under these conditions, subjects were unable to elicit distinct gain states based on color regardless of whether the color cues were presented simultaneously (Figures 19, 23), sequentially (Figure 21), or when only one (red) of the three possible color cues had an intra-saccade target displacement (Figure 22). Furthermore, we observed complete transfer between trials meant to reduce horizontal amplitude (using red targets) and those trials that were meant to increase the vertical component of the primary movement (using green targets; Figure 24). These observations were consistent with those hypotheses that state that color cannot be used as a visual cue for adaptation and are in line with prior observations made in humans (Deubel, 1995; Azadi & Harwood, 2014; Benjamin et al., in review). These results are interpreted below in the context of prior behavioral and physiological studies of gaze adaptation.

4.5.2 Context Dependent Adaptation: Comparisons to Previous Observations

Attempts to elicit context dependent saccadic adaptation have been primarily been made using human subjects (Pélisson et al, 2010; Herman et al, 2013, but see Tian & Zee, 2010). To the best of our knowledge, the experiments discussed in the current report were the first attempt to

elicit context dependent saccade adaptation in the rhesus monkey using a visual cue of any type. Furthermore, our report improves and extends the human experiment performed by both Deubel (1995) and Azadi & Harwood (2014) in several ways: 1) Deubel made his observations in two human subjects with very few trials and only two experiments. Our dataset therefore represents a much more powerful assessment of Deubel's preliminary observations using colored, static targets; 2) we used large intra-saccade target displacements (50% of target eccentricity) which have been successful at eliciting large gain changes in head-restrained monkey subjects (Figure 11 from Cecala & Freedman, 2009). This should have increased the likelihood of observing even a small, color dependent change in saccade gain; 3) both Deubel (1995) and Azadi & Harwood (2014) attempted to simultaneously increase and decrease saccade gain within the same axis of the primary saccade, which is much like the "horizontal concurrent" experiments in the current report (Figure 20). Our "horizontal sequential" (Figure 21), "single target displacement" (Figure 22), "orthogonal concurrent" (Figure 23), and "vector concurrent" (Figure 24) experiments represent novel tests of the stated hypotheses (Figure 19) and are novel contributions to our understanding of the adaptive mechanism underlying primate adaptation. What remains unclear is why the saccadic adaptive control system would take into account some internal and external cues (initial eye position: Alahyane & Pélisson, 2004; target flicker: Madelain et al., 2009; moving target direction and/or speed: Azadi & Harwood, 2014), but not others (target shape, color: Deubel, 1995; Bahcall & Kowler, 2000; Azadi & Harwood, 2014)? In order to address this question, we must provide a brief overview of what is known regarding the anatomy and physiology underlying saccade generation with particular emphasis on those circuits that have been investigated using permutations of the McLaughlin (1967) task.

4.5.3 Physiological Implications

The McLaughlin (1967) task has been used to investigate the role of the superior colliculus (SC) (Frens and Van Opstal, 1997; Takeichi et al., 2007; Quessy et al., 2010), oculomotor brainstem (Takeichi et al., 2005; Kojima et al., 2008), and midline cerebellum (for reviews, see Robinson & Fuchs, 2001; Iwamoto & Kaku, 2010) in the adaptive control of saccades. The following physiological discussion will focus on the superior colliculus and the midline cerebellum since these are the regions of the primate brain that have been studied the most during saccadic adaptation. We would like to caution the reader that there is still a paucity of information regarding the role of the aforementioned, and countless other, brain structures in saccadic adaptation. Therefore, the following prose should be viewed as speculative, but hopefully a useful framework upon which to begin thinking about the neural mechanism that may underlie context dependent saccadic adaptation.

4.5.4 Superior Colliculus

The SC has long been implicated in the orienting movements of primates. It can be functionally divided into the superficial visual and the sensorimotor intermediate and deep layers. The superficial layers receive direct, achromatic input from the retina (Schiller & Malpeli, 1977) and are retinotopically organized (Goldberg & Wurtz, 1972). The intermediate and deep layers (hereafter referred to as the "deeper layers") of the SC are sites where auditory, visual, and somatosensory signals converge and an area where motor commands for orienting movements of the line of sight are generated (Sparks & Groh, 1995; Gandhi & Katnani, 2011). The locus of motor-related activity in the deeper layers specifies the amplitude and direction of changes in the

direction of the line of sight and activity is topographically organized such that small movements are represented in the rostral pole and larger movement vectors are located caudally (Wurtz and Goldberg, 1971; Sparks and Mays, 1981; Freedman & Sparks, 1997; Gandhi & Katnani, 2011). Single unit recordings in the SC during the McLaughlin task (Quessy et al., 2010; Frens and Van Opstal, 1997) suggest that the SC motor command appears to specify a desired movement to the location of the first peripheral (T1) target, not the subject's actual movement (but see Takeichi et al., 2007). This suggests that some additional signal must modify or bypass the collicular output (at least as assessed at the single cell level) to alter the gain of saccades observed during this task. However, this result does not exclude the possibility that slight differences (e.g. changes in the peak or average firing rate or number of spikes) in the SC movement command could be recognized by the adaptive control mechanism and then be paired with a specific, modified gain value during the adaptive process. In fact, this may be a necessary condition in order for context dependent adaptation to occur since saccades produced in response to similar static visual targets would presumably have very similar populations of activity in the SC motor map and therefore be associated very similar gain states at any given time. This assertion is supported by the observation that saccadic adaptation transfers to saccades/targets within a localized region of retinotopic space (Noto et al, 1999).

In our experiment, the use of chromatic cues (red, green, or yellow visual targets) was unable to drive contextual adaptation. Chromatic modulation of sensory activity has been observed in the deep layers (White et al. 2009; White & Munoz, 2011) and is most likely the result of inputs to these layers from V4 (Fries, 1984; Lock et al., 2003) and/or the frontal eye fields (FEF; Schall et al., 1995). However, the chromatic visual responses of neurons in the SC show "strong sensitivity, but only moderate selectivity, for color" (White et al., 2009) and the motor responses

of visuomotor cells may not be significantly different under the conditions used in our, and previous, context cue experiments using color (White et al. 2009; White & Munoz, 2011; Deubel, 1995; Azadi & Harwood, 2014). Based on these physiological observations, and the assumption that an efference copy of the color invariant SC motor command is provided to the adaptive control mechanism, we would not expect target color would be able to drive context dependent adaptation.

Using human subjects, Madelain and colleagues (2009) were able to elicit context dependent adaptation using flickering (a square wave at a rate of 5 Hz) versus non-flickering visual targets. To our knowledge no one has contrasted the effects of this exact stimulus on the motor activity produced by single units in the deeper layers of the SC. However, neuronal adaptation in the visual response has been observed in the superficial and deep layers of the SC to sequentially presented stimuli at time intervals similar to that used by Madelain and colleagues (e.g. 1.25-59Hz, Mayo & Sommer, 2008; 0.8-20Hz, Fecteau and Munoz, 2005). Therefore, it is possible that flickering and non-flickering stimuli are represented differently within the SC and that the motor commands associated with these stimuli can be differentiated by the adaptive control mechanism. This hypothesis can account for the context dependent learning that has been observed in human subjects and can be addressed empirically with neuronal recordings in the deep layers of the SC of monkeys.

Azadi & Harwood (2014) were able to use the speed and direction (clockwise or counter-clockwise) of circularly moving targets as a contextual cue in humans. Unfortunately, very little is known regarding the neural substrate underlying the planning and execution of primate saccades initiated from fixation to a moving visual target. Keller et al. (1996) compared the movement fields of deep layer SC neurons of monkeys when they produced saccades to stationary targets versus when they made interceptive saccades to targets moving at either 45 or 60°/sec outwardly along

the optimal vector (as defined by describing the movement field using static targets) from a central fixation point. These authors observed a systematic shift in the center of the movement field in the direction of target motion and a reduction in the firing rate for the optimal vector. Unfortunately these authors did not collect neural data under conditions where their subjects made saccades to intercept targets moving inward along the optimal vector. If the populations of SC activity during these contexts (outward vs. inward) are different, then the adaptive control system could use this information to recognize two distinct "contexts" and pair these contexts with specific gains. Again, this hypothesis can be addressed empirically with single unit neuronal recordings.

In human subjects, initial orbital eye position has been shown to be a useful contextual cue (Alahyane & Pélisson, 2004). In contrast, Tian & Zee (2010), in most of their experiments, were able to decrease saccade gain from one eye position, but observed little or no increase in gain from the other eye position. Therefore, it is not clear whether initial eye position can be useful for the study of context dependent adaptation in the monkey model. Regardless, if we do assume that initial eye position can drive context dependent adaptation in primates, could the SC provide an eye position signal to the adaptive mechanism that can be useful in distinguishing saccades initially of equal magnitude initiated from the different orbital positions?

Eye position signals have been reported in several studies of the primate SC (van Opstal et al., 1995; Krauzlis et al. 2000; Pare & Munoz, 2001; Campos et al., 2006). However, there is some controversy as to whether or not this signal affects the motor activity in the deeper layers. For example, while viewing natural images, van Opstal and colleagues (1995) described gain field-like modulations of peri-saccadic activity related to initial eye position whereas Campos and colleagues (2006) noted an effect of initial eye position during only the intersaccade interval. Regardless, it is clear from each of the aforementioned reports that the magnitude of the initial eye

position signal, relative to the visual and movement related bursts, is quite small and does not affect the tuning of the neuron's movement field. Furthermore, studies of the SC during head-unrestrained gaze shifts have not reported eye position related signals (e.g. Freedman & Sparks, 1997) even though the head and eye contributions to primate gaze shifts are correlated strongly with the initial position of the eyes at gaze onset (Freedman, 2008). It should also be noted that initial eye position in some cases of gaze adaptation need not act as a contextual cue. In head-unrestrained primates, Cecala & Freedman (2008, 2009) have shown that modifications in gaze amplitude from one orbital eye position with specific eye and head contributions transfers to gaze shifts at other orbital eye positions with vastly different eye and head contributions. This is not to say that unique gain states couldn't be elicited from the different eye positions, but rather that it seems not to be the default in this context.

Nagy & Corneil (2010) have reported gain field effects in the SC related to horizontal head position that scale task-related SC activity without changing the location of a neuron's response field. The effect of horizontal head position on gaze adaptation has not been investigated in head-unrestrained primates. However, static head position cues have been used as contextual cues in saccadic adaptation. For example, Shelhamer & Clendaniel (2002) have shown that head position ("roll tilt of the head") can be used as a contextual cue for saccadic adaptation. It is not clear whether vestibular or proprioceptive cues related to head position are used by the adaptive control mechanism in this case.

In summary, although the SC could provide initial eye or head position signals to the adaptive control mechanism, there are other regions of the oculomotor, cephalomotor, and proprioceptive systems that could provide much more robust position signals. Many of these

structures project to the medioposterior cerebellum, a region that has been implicated in the adaptive control of saccadic eye movements (Robinson and Fuchs 2001).

4.5.5 Cerebellum

The deeper layers of the SC are connected to the medioposterior cerebellum (caudal fastigial nucleus and oculomotor vermis; Ohtsuka and Noda 1990) via nucleus reticularis tegmenti pontis (NRTP; May et al. 1990; Ohtsuka and Noda 1990). Lesions to the medioposterior cerebellum impair rapid saccadic adaptation (Barash et al. 1999; Robinson et al. 2002; Takagi et al. 2000; Kojima et al, 2011; Xu-Wilson et al, 2009; Panouillères et al. 2013) and the burst metrics of neurons in NRTP (Takeichi et al. 2005), caudal fastigial nucleus (Inaba et al. 2003; Scudder and McGee 2003), and oculomotor vermis (Catz et al. 2005, 2008; Soetedjo & Fuchs 2006; Soetedjo et al, 2008a,b; Prsa et al, 2009; Kojima et al, 2010) are altered along with saccade amplitude during the McLaughlin task. Interestingly, Noda and colleagues observed eye position modulation of firing rate in a small number of Purkinje cells (Kase et al, 1980) and mossy fibers (Ohtsuka & Noda, 1992) in the oculomotor vermis. The origins of these signals are unclear, but could arise from the SC (via the SC-NRTP/DLPN-Vermal circuit; Yamada & Noda, 1987), the prepositus hypoglossi (Yamada & Noda, 1987; Cannon & Robinson, 1987), or directly proprioceptive input from the extraocular muscles (Donaldson, 2000). Therefore, it is possible that the eye position dependent contextual adaptation is the result of the adaptive mechanism having access to eye position information at this level of the cerebellar circuit. Interestingly, eye position does not seem to modulate saccade related bursts (Ohtsuka et al, 1994) or tonic firing rates during fixation (Ohtsuka & Noda, 1991) in the caudal fastigial nucleus even though this structure receives may of

the same inputs as the oculomotor vermis (Noda et al, 1990) and transient inactivation this structure with muscimol does produce a predictable fixation offset (Guerrasio et al, 2010).

Unfortunately, there is a dearth of data regarding visual responses in the medioposterior cerebellum. However, Kojima et al. (2010), in the only study of the oculomotor vermis to use saccade tasks that could dissociate visual from motor responses, were unable to observe visual related signals in response to static targets. It is unclear whether other visual signals (e.g. moving visual targets) would impact the adaptive control circuitry at this level.

4.5.6 Cortex

Recent fMRI investigations in humans have suggested that the cortex may be involved in saccadic adaptation (Blurton et al, 2012; Gerardin et al, 2012). To our knowledge, there has been only one physiological study of the cortex's contribution to saccadic adaptation in monkeys (Steenrod et al, 2013). Steenrod and colleagues described visual, delay, and presaccadic activity in the lateral intraparietal area that, much like the superior colliculus (Quessy et al, 2010), encoded the location of T1, not the changes in saccade amplitude elicited by the McLaughlin task. Lastly, there has not been a study of cortical neural activity during contextual saccadic adaptation. Future studies such as these will undoubtedly lead to new insights into the adaptive mechanism controlling saccades and possibly other effectors.

4.6 Acknowlegements

This work was supported in part by NIH grants EY022854 (NJG), EY018894 (MAS), EY008098 (NJG, MAS), DC0025205 (NJG), and DC011499 (IS). ALC would like to thank Elizabethtown College for continued financial support through the college's Faculty Grant program.

5.0 Discussion and conclusions

5.1 Summary

We rely on sight to explore our world, and our ability to accurately direct our gaze to objects of interest is instrumental in our ability to do so. Primates have developed extraordinary neural systems to precisely control our gaze shifts, and we are just beginning to unravel the mechanisms by which they operate. These systems must control both the parameters of these movements as well as monitor the motivations behind them. There are structures that seem to prefer one of these functions over the other.

In this document we established that the SC exerts close control over saccade kinematics, specifically the velocity of the eye movement. It was previously believed that SC commands are a static set of parameters for a preferred saccade, governing the direction, amplitude, and to some degree the peak velocity of the movement. Traditional models rely on this structure, as they ascribe the control of instantaneous velocity to lower structures from the SC. However, we see that instantaneous SC activity closely correlates with instantaneous eye velocity.

Pivoting from subcortical control of gaze, we examine the influence of PMv on gaze shifts. We see that this area readily identifies the task parameters under which the movement was performed. The neural code in PMv can distinguish lower-level properties, such as which muscle group is engaged and which direction the movement is made, as well as higher-level task conditions such as the order of movements that need to be made.

Although we see context-relevant code in cortical areas like PMv, it does not always mean that this information is used in all instances. When we attempt to manipulate saccadic adaptation

by introducing endpoint error under only one condition (equivalently, one color) but not the other, we see that the system is unable to usefully differentiate between them. Perhaps color-based cueing requires a structure which plays no role in saccadic adaptation. Or maybe color is simply not a salient-enough cue to adequately engage the system to differentiate between the conditions.

Overall, it is clear that the description of the neural control of gaze shifts depends on the lens through which you examine it. Each structure prioritizes either lower- or higher-level movement properties based on its role in the system, with some showing aspects of both. It is, however, clear that a complete understanding of the system will require an examination of all systems in tandem.

5.2 Future Directions

In the first chapter of this dissertation, we propose a revised model of saccade generation. We show compelling evidence for this revision, especially regarding the new role of collicular signals, but we only present anatomical justification for some aspects of the model. For example, the feedback pathway we propose has not been explored in this particular paradigm. Understandably, we could not perform rigorous experimentational exploration of every aspect of the model, as such an act would span a lifetime of work. This limitation, however, presents a multitude of future directions for further research. It is my hope that our proposed model would inspire others to rigorously explore every aspect of it, as that would either validate our findings or demonstrate the shortcomings of the model. Either outcome would be a boon to the field of oculomotor research.

Additionally, our claim that SC asserts some control over instantaneous eye velocity can be examined further. You will notice that although our correlation values are statistically significant, they are far from a perfect correlation. This implies that other mechanisms may be involved in controlling the instantaneous velocity. This leaves several routes of possible future action. One is to further explore the SC role in this context. Perhaps the nature of recording from single neurons omits a portion of the signal, thus reducing the correlation values. Maybe a population of neurons, recorded from multiple sites at the same time, could indicate a stronger SC contribution to velocity control. Another possible direction is the exploration of other brain areas during the same behavioral paradigm. Does FEF show similar properties to the SC in this regard? A repetition of the same experiment and analyses would indicate whether other oculomotor regions participate in this mechanism. And if they do, what does the combined neural code look like for instantaneous velocity control?

It is also my hope that this dissertation can be the stepping stone for future research into the role of context in head-unrestrained gaze shifts. With the advancement of technology, recording neural signals in head-unrestrained subjects is becoming easier every year. Wireless data acquisition, head-unrestrained eye tracking, and virtual-reality headsets are just some examples of technologies that would have made my own experiments more approachable, and perhaps would have led me to a more controlled and sophisticated experimental design.

That being said, from a scientific perspective (rather than technological one), the future directions are almost limitless. The way context affects the neural code is a relatively new field of study. If I were to continue to do research, I would use my second chapter as a basis for future exploration on how PMv monitors the context of performed actions. Knowing that it has representations of both lower- and higher-level movement properties would lead to an

experimental design that precisely controls for these factors. The resulting findings would significantly improve our understanding of neural control of context-dependent behaviors, and the role of PMv in such conditions.

5.3 Final Thoughts

It is often prudent to examine specific parts of the neural system in very granular, isolated parts. In order to advance our knowledge in any one domain, such approaches are necessary; it is often impossible to accurately and appropriately describe a facet of the system without isolated focus on such parts. However, a complete understanding of the system requires consideration of all components. In this document we examined isolated parts of the oculomotor system spanning a wide range of modalities to glimpse at a larger picture behind the neural mechanisms of gaze shifts. Although we do not propose a unifying model, we do add a perspective that combines the higher-level properties of movements with lower-level kinematic control by examining in detail structures that control these components.

Bibliography

Alahyane, N., & Pe´lisson, D. (2004). Eye Position Specificity of Saccadic Adaptation. *Investigative Opthalmology & Visual Science*, *45*(1), 123. https://doi.org/10.1167/iovs.03-0570

Albano, J. E. (1996). Adaptive changes in saccade amplitude: Oculocentric or orbitocentric mapping? *Vision Research*, *36*(14), 2087–2098. https://doi.org/10.1016/0042-6989(96)89627-1

Ashe, J., & Georgopoulos, A. P. (1994). Movement Parameters and Neural Activity in Motor Cortex and Area 5. *Cerebral Cortex*, *4*(6), 590–600. https://doi.org/10.1093/cercor/4.6.590

Azadi, R., & Harwood, M. R. (2014). Visual cues that are effective for contextual saccade adaptation. *Journal of Neurophysiology*, *111*(11), 2307–2319. https://doi.org/10.1152/jn.00894.2013

Badler, J. B., & Keller, E. L. (2002). Decoding of a motor command vector from distributed activity in superior colliculus. *Biological Cybernetics*, *86*(3), 179–189. http://www.ncbi.nlm.nih.gov/pubmed/12068785

Bahcall, D. O., & Kowler, E. (2000). The control of saccadic adaptation: implications for the scanning of natural visual scenes. *Vision Research*, *40*(20), 2779–2796. https://doi.org/10.1016/s0042-6989(00)00117-6

Bahill, A. T., Clark, M. R., & Stark, L. (1975). The main sequence, a tool for studying human eye movements. *Mathematical Biosciences*, *24*(3–4), 191–204. https://doi.org/10.1016/0025-5564(75)90075-9

Baloh, R. W., Sills, A. W., Kumley, W. E., & Honrubia, V. (1975). Quantitative measurement of saccade amplitude, duration, and velocity. *Neurology*, *25*(11), 1065–1070. https://doi.org/10.1212/wnl.25.11.1065

Bansal, A. K., Truccolo, W., Vargas-Irwin, C. E., & Donoghue, J. P. (2012). Decoding 3D reach and grasp from hybrid signals in motor and premotor cortices: spikes, multiunit activity, and local field potentials. *Journal of Neurophysiology*, *107*(5), 1337–1355. https://doi.org/10.1152/jn.00781.2011

Barash, S., Melikyan, A., Sivakov, A., Zhang, M., Glickstein, M., & Thier, P. (1999). Saccadic dysmetria and adaptation after lesions of the cerebellar cortex. *The Journal of Neuroscience : The Official Journal of the Society for Neuroscience*, *19*(24), 10931–10939. https://doi.org/10.1523/JNEUROSCI.19-24-10931.1999

Barbas, H., & Pandya, D. N. (1987). Architecture and frontal cortical connections of the premotor cortex (area 6) in the rhesus monkey. *The Journal of Comparative Neurology*, *256*(2), 211–228. https://doi.org/10.1002/cne.902560203

Basso, M. A., & May, P. J. (2017). Circuits for Action and Cognition: A View from the Superior Colliculus. *Annual Review of Vision Science*, *3*, 197–226. https://doi.org/10.1146/annurev-vision-102016-061234

Benjamin, B., Macomb, C., Martin, A., & Cecala, A. L. (2016). Preliminary Report: Can color act as a contextual cue in human saccadic adaptation? *BIOS*, *87*(1), 9–20. https://doi.org/10.1893/bios-d-14-00011.1

Berti, A. (2005). Shared Cortical Anatomy for Motor Awareness and Motor Control. *Science*, *309*(5733), 488–491. https://doi.org/10.1126/science.1110625

Billig, I., & Strick, P. (2012). *Anatomical Evidence for Overlap of Neck and Oculomotor Control Systems in Ventral Premotor Cortex* (p. 1). Society for Neuroscience.

Blurton, S. P., Raabe, M., & Greenlee, M. W. (2012). Differential cortical activation during saccadic adaptation. *Journal of Neurophysiology*, *107*(6), 1738–1747. https://doi.org/10.1152/jn.00682.2011

Bonini, L., Ferrari, P. F., & Fogassi, L. (2013). Neurophysiological bases underlying the organization of intentional actions and the understanding of others' intention. *Consciousness and Cognition*, *22*(3), 1095–1104. https://doi.org/10.1016/j.concog.2013.03.001

Bonini, L., Ugolotti Serventi, F., Bruni, S., Maranesi, M., Bimbi, M., Simone, L., Rozzi, S., Ferrari, P. F., & Fogassi, L. (2012). Selectivity for grip type and action goal in macaque inferior parietal and ventral premotor grasping neurons. *Journal of Neurophysiology*, *108*(6), 1607–1619. https://doi.org/10.1152/jn.01158.2011

Boulanger, M., Bergeron, A., & Guitton, D. (2009). Ipsilateral head and centring eye movements evoked from monkey premotor cortex. *NeuroReport*, *20*(7), 669–673. https://doi.org/10.1097/wnr.0b013e328329c3c6

Bruce, C. J., Goldberg, M. E., Bushnell, M. C., & Stanton, G. B. (1985). Primate frontal eye fields. II. Physiological and anatomical correlates of electrically evoked eye movements. *Journal of Neurophysiology*, *54*(3), 714–734. https://doi.org/10.1152/jn.1985.54.3.714

Bryant, C. L., & Gandhi, N. J. (2005). Real-time data acquisition and control system for the measurement of motor and neural data. *Journal of Neuroscience Methods*, *142*(2), 193–200. https://doi.org/10.1016/j.jneumeth.2004.08.019

Campos, M., Cherian, A., & Segraves, M. A. (2006). Effects of Eye Position upon Activity of Neurons in Macaque Superior Colliculus. *Journal of Neurophysiology*, *95*(1), 505–526. https://doi.org/10.1152/jn.00639.2005

Cannon, S. C., & Robinson, D. A. (1987). Loss of the neural integrator of the oculomotor system from brain stem lesions in monkey. *Journal of Neurophysiology*, *57*(5), 1383–1409. https://doi.org/10.1152/jn.1987.57.5.1383

Carmena, J. M., Lebedev, M. A., Henriquez, C. S., & Nicolelis, M. A. L. (2005). Stable ensemble performance with single-neuron variability during reaching movements in primates. *The Journal of Neuroscience : The Official Journal of the Society for Neuroscience*, *25*(46), 10712–10716. https://doi.org/10.1523/JNEUROSCI.2772-05.2005

Catz, N., Dicke, P. W., & Thier, P. (2005). Cerebellar Complex Spike Firing Is Suitable to Induce as Well as to Stabilize Motor Learning. *Current Biology*, *15*(24), 2179–2189. https://doi.org/10.1016/j.cub.2005.11.037

Catz, N., Dicke, P. W., & Thier, P. (2008). Cerebellar-dependent motor learning is based on pruning a Purkinje cell population response. *Proceedings of the National Academy of Sciences of the United States of America*, *105*(20), 7309–7314. https://doi.org/10.1073/pnas.0706032105

Cecala, A. L., & Freedman, E. G. (2008). Amplitude changes in response to target displacements during human eye-head movements. *Vision Research*, *48*(2), 149–166. https://doi.org/10.1016/j.visres.2007.10.029

Cecala, A. L., & Freedman, E. G. (2009). Head-unrestrained gaze adaptation in the rhesus macaque. *Journal of Neurophysiology*, *101*(1), 164–183. https://doi.org/10.1152/jn.90735.2008

Chen, L. L. (2006). Head movements evoked by electrical stimulation in the frontal eye field of the monkey: evidence for independent eye and head control. *Journal of Neurophysiology*, *95*(6), 3528–3542. https://doi.org/10.1152/jn.01320.2005

Chen, L. L., & Walton, M. M. G. (2005). Head Movement Evoked By Electrical Stimulation in the Supplementary Eye Field of the Rhesus Monkey. *Journal of Neurophysiology*, *94*(6), 4502–4519. https://doi.org/10.1152/jn.00510.2005

Churchland, M. M. (2015). Using the precision of the primate to study the origins of movement variability. *Neuroscience*, *296*, 92–100. https://doi.org/10.1016/j.neuroscience.2015.01.005

Churchland, M. M., Santhanam, G., & Shenoy, K. V. (2006). Preparatory Activity in Premotor and Motor Cortex Reflects the Speed of the Upcoming Reach. *Journal of Neurophysiology*, *96*(6), 3130–3146. https://doi.org/10.1152/jn.00307.2006

Churchland, M. M., Yu, B. M., Ryu, S. I., Santhanam, G., & Shenoy, K. V. (2006). Neural variability in premotor cortex provides a signature of motor preparation. *The Journal of Neuroscience : The Official Journal of the Society for Neuroscience*, *26*(14), 3697–3712. https://doi.org/10.1523/JNEUROSCI.3762-05.2006

Cohen, B., & Komatsuzaki, A. (1972). Eye movements induced by stimulation of the pontine reticular formation: evidence for integration in oculomotor pathways. *Experimental Neurology*, *36*(1), 101–117. http://www.ncbi.nlm.nih.gov/pubmed/4558412

Cooke, D. F., & Graziano, M. S. A. (2004). Sensorimotor Integration in the Precentral Gyrus: Polysensory Neurons and Defensive Movements. *Journal of Neurophysiology*, *91*(4), 1648–1660. https://doi.org/10.1152/jn.00955.2003

Corneil, B. D., & Munoz, D. P. (1999). Human Eye-Head Gaze Shifts in a Distractor Task. II. Reduced Threshold for Initiation of Early Head Movements. *Journal of Neurophysiology*, *82*(3), 1406–1421. https://doi.org/10.1152/jn.1999.82.3.1406

Corneil, B. D., Olivier, E., & Munoz, D. P. (2002). Neck Muscle Responses to Stimulation of Monkey Superior Colliculus. II. Gaze Shift Initiation and Volitional Head Movements. *Journal of Neurophysiology*, *88*(4), 2000–2018. https://doi.org/10.1152/jn.2002.88.4.2000

Corvisier, J., & Hardy, O. (1997). Topographical characteristics of preposito-collicular projections in the cat as revealed by Phaseolus vulgaris-leucoagglutinin technique. A possible organisation underlying temporal-to-spatial transformations. *Experimental Brain Research*, *114*(3), 461–471. https://doi.org/10.1007/PL00005655

Coudé, G., Festante, F., Cilia, A., Loiacono, V., Bimbi, M., Fogassi, L., & Ferrari, P. F. (2016). Mirror Neurons of Ventral Premotor Cortex Are Modulated by Social Cues Provided by Others' Gaze. *The Journal of Neuroscience : The Official Journal of the Society for Neuroscience*, *36*(11), 3145–3156. https://doi.org/10.1523/JNEUROSCI.3220-15.2016

Crawford, J. D., Ceylan, M. Z., Klier, E. M., & Guitton, D. (1999). Three-Dimensional Eye-Head Coordination During Gaze Saccades in the Primate. *Journal of Neurophysiology*, *81*(4), 1760–1782. https://doi.org/10.1152/jn.1999.81.4.1760

Dancause, N., Barbay, S., Frost, S. B., Plautz, E. J., Stowe, A. M., Friel, K. M., & Nudo, R. J. (2006). Ipsilateral connections of the ventral premotor cortex in a new world primate. *The Journal of Comparative Neurology*, *495*(4), 374–390. https://doi.org/10.1002/cne.20875

Dean, P., Redgrave, P., Sahibzada, N., & Tsuji, K. (1986). Head and body movements produced by electrical stimulation of superior colliculus in rats: Effects of interruption of crossed tectoreticulospinal pathway. *Neuroscience*, *19*(2), 367–380. https://doi.org/10.1016/0306-4522(86)90267-8

Deubel, H. (1987). ADAPTIVITY OF GAIN AND DIRECTION IN OBLIQUE SACCADES. In *Eye Movements from Physiology to Cognition* (pp. 181–190). Elsevier. https://doi.org/10.1016/b978-0-444-70113-8.50030-8

Deubel, H. (1991). Adaptive Control of Saccade Metrics. In *Presbyopia Research* (pp. 93–100). Springer US. https://doi.org/10.1007/978-1-4757-2131-7_11

Deubel, H. (1995). Is Saccadic Adaptation Context-Specific ? In *Studies in Visual Information Processing* (pp. 177–187). Elsevier. https://doi.org/10.1016/s0926-907x(05)80016-9

Diesmann, M., Gewaltig, M. O., & Aertsen, A. (1999). Stable propagation of synchronous spiking in cortical neural networks. *Nature*, *402*(6761), 529–533. https://doi.org/10.1038/990101

Donaldson, I. M. (2000). The functions of the proprioceptors of the eye muscles. *Philosophical Transactions of the Royal Society of London. Series B, Biological Sciences*, *355*(1404), 1685–1754. https://doi.org/10.1098/rstb.2000.0732

Edelman, J. A., & Goldberg, M. E. (2001). Dependence of saccade-related activity in the primate superior colliculus on visual target presence. *Journal of Neurophysiology*, *86*(2), 676–691. https://doi.org/10.1152/jn.2001.86.2.676

Elsayed, G. F., & Cunningham, J. P. (2017). Structure in neural population recordings: an expected byproduct of simpler phenomena? *Nature Neuroscience*, *20*(9), 1310–1318. https://doi.org/10.1038/nn.4617

Elsley, J. K., Nagy, B., Cushing, S. L., & Corneil, B. D. (2007). Widespread Presaccadic Recruitment of Neck Muscles by Stimulation of the Primate Frontal Eye Fields. *Journal of Neurophysiology*, *98*(3), 1333–1354. https://doi.org/10.1152/jn.00386.2007

Fecteau, J. H., & Munoz, D. P. (2005). Correlates of Capture of Attention and Inhibition of Return across Stages of Visual Processing. *Journal of Cognitive Neuroscience*, *17*(11), 1714–1727. https://doi.org/10.1162/089892905774589235

Fogassi, L., Gallese, V., Fadiga, L., Luppino, G., Matelli, M., & Rizzolatti, G. (1996). Coding of peripersonal space in inferior premotor cortex (area F4). *Journal of Neurophysiology*, *76*(1), 141–157. https://doi.org/10.1152/jn.1996.76.1.141

Freedman, E. G. (2008). Coordination of the eyes and head during visual orienting. *Experimental Brain Research*, *190*(4), 369–387. https://doi.org/10.1007/s00221-008-1504-8

Freedman, E. G., & Sparks, D. L. (1997). Eye-Head Coordination During Head-Unrestrained Gaze Shifts in Rhesus Monkeys. *Journal of Neurophysiology*, *77*(5), 2328–2348. https://doi.org/10.1152/jn.1997.77.5.2328

Freedman, E. G., & Sparks, D. L. (2000). Coordination of the eyes and head: movement kinematics. *Experimental Brain Research*, *131*(1), 22–32. https://doi.org/10.1007/s002219900296

Freedman, E. G., & Sparks, D. L. (1997). Activity of Cells in the Deeper Layers of the Superior Colliculus of the Rhesus Monkey: Evidence for a Gaze Displacement Command. *Journal of Neurophysiology*, *78*(3), 1669–1690. https://doi.org/10.1152/jn.1997.78.3.1669

Frens, M. A., & Van Opstal, A. J. (1997). Monkey Superior Colliculus Activity During Short-Term Saccadic Adaptation. *Brain Research Bulletin*, *43*(5), 473–483. https://doi.org/10.1016/s0361-9230(97)80001-9

Fries, W. (1984). Cortical projections to the superior colliculus in the macaque monkey: A retrograde study using horseradish peroxidase. *The Journal of Comparative Neurology*, *230*(1), 55–76. https://doi.org/10.1002/cne.902300106

Fujii, N., Mushiake, H., Tamai, M., & Tanji, J. (1995). Microstimulation of the supplementary eye field during saccade preparation. *NeuroReport*, *6*(18), 2565–2568. https://doi.org/10.1097/00001756-199512150-00028

Fujii, N., Mushiake, H., & Tanji, J. (1998). An oculomotor representation area within the ventral premotor cortex. *Proceedings of the National Academy of Sciences of the United States of America*, *95*(20), 12034–12037. https://doi.org/10.1073/pnas.95.20.12034

Galeazzi, J. M., Navajas, J., Mender, B. M. W., Quian Quiroga, R., Minini, L., & Stringer, S. M. (2016). The visual development of hand-centered receptive fields in a neural network model of the primate visual system trained with experimentally recorded human gaze changes. *Network (Bristol, England)*, *27*(1), 29–51. https://doi.org/10.1080/0954898X.2016.1187311

Gandhi, N. J., & Keller, E. L. (1999). Comparison of saccades perturbed by stimulation of the rostral superior colliculus, the caudal superior colliculus, and the omnipause neuron region. *Journal of Neurophysiology*, *82*(6), 3236–3253. https://doi.org/10.1152/jn.1999.82.6.3236

Gandhi, N. J., & Bonadonna, D. K. (2005). Temporal interactions of air-puff-evoked blinks and saccadic eye movements: insights into motor preparation. *Journal of Neurophysiology*, *93*(3), 1718–1729. https://doi.org/10.1152/jn.00854.2004

Gandhi, N. J., & Katnani, H. A. (2011). Motor functions of the superior colliculus. *Annual Review of Neuroscience*, *34*(1), 205–231. https://doi.org/10.1146/annurev-neuro-061010-113728

Gandhi, N. J., Barton, E. J., & Sparks, D. L. (2008). Coordination of eye and head components of movements evoked by stimulation of the paramedian pontine reticular formation. *Experimental Brain Research*, *189*(1), 35–47. https://doi.org/10.1007/s00221-008-1401-1

Gaymard, B., Ploner, C. J., Rivaud, S., Vermersch, A. I., & Pierrot-Deseilligny, C. (1998). Cortical control of saccades. *Experimental Brain Research*, *123*(1–2), 159–163. https://doi.org/10.1007/s002210050557

Gerardin, P., Miquée, A., Urquizar, C., & Pélisson, D. (2012). Functional activation of the cerebral cortex related to sensorimotor adaptation of reactive and voluntary saccades. *NeuroImage*, *61*(4), 1100–1112. https://doi.org/10.1016/j.neuroimage.2012.03.037

Gerbella, M., Belmalih, A., Borra, E., Rozzi, S., & Luppino, G. (2010). Cortical connections of the anterior (F5a) subdivision of the macaque ventral premotor area F5. *Brain Structure and Function*, *216*(1), 43–65. https://doi.org/10.1007/s00429-010-0293-6

Gisbergen, J. A. M. van, Opstal, J. van, & Ottes, F. P. (1984). Parametrization of Saccadic Velocity Profiles in Man. In *Theoretical and Applied Aspects of Eye Movement Research, Selected/Edited Proceedings of The Second European Conference on Eye Movements* (pp. 87–94). Elsevier. https://doi.org/10.1016/s0166-4115(08)61822-1

Godschalk, M., Mitz, A. R., Duin, B. van, & Burga, H. van der. (1995). Somatotopy of monkey premotor cortex examined with microstimulation. *Neuroscience Research*, *23*(3), 269–279. https://doi.org/10.1016/0168-0102(95)00950-7

Gold, J. I., & Shadlen, M. N. (2007). The Neural Basis of Decision Making. *Annual Review of Neuroscience*, *30*(1), 535–574. https://doi.org/10.1146/annurev.neuro.29.051605.113038

Goldberg, M. E., & Wurtz, R. H. (1972). Activity of superior colliculus in behaving monkey. I. Visual receptive fields of single neurons. *Journal of Neurophysiology*, *35*(4), 542–559. https://doi.org/10.1152/jn.1972.35.4.542

Goldring, J., Dorris, M., Corneil, B., Ballantyne, P., & Munoz, D. (1996). Combined eye-head gaze shifts to visual and auditory targets in humans. *Experimental Brain Research*, *111*(1). https://doi.org/10.1007/bf00229557

Goonetilleke, S. C., Katz, L., Wood, D. K., Gu, C., Huk, A. C., & Corneil, B. D. (2015). Cross-species comparison of anticipatory and stimulus-driven neck muscle activity well before saccadic gaze shifts in humans and nonhuman primates. *Journal of Neurophysiology*, *114*(2), 902–913. https://doi.org/10.1152/jn.00230.2015

Goossens, H. H. L. M., & Opstal, A. J. Van. (1997). Human eye-head coordination in two dimensions under different sensorimotor conditions. *Experimental Brain Research*, *114*(3), 542–560. https://doi.org/10.1007/pl00005663

Goossens, H. H. L. M., & van Opstal, A. J. (2012). Optimal control of saccades by spatial-temporal activity patterns in the monkey superior colliculus. *PLoS Computational Biology*, *8*(5), e1002508–e1002508. https://doi.org/10.1371/journal.pcbi.1002508

Goossens, H. H. L. M., & Van Opstal, A. J. (2000). Blink-perturbed saccades in monkey. I. Behavioral analysis. *Journal of Neurophysiology*, *83*(6), 3411–3429. https://doi.org/10.1152/jn.2000.83.6.3411

Goossens, H. H. L. M., & Van Opstal, A. J. (2006). Dynamic Ensemble Coding of Saccades in the Monkey Superior Colliculus. *Journal of Neurophysiology*, *95*(4), 2326–2341. https://doi.org/10.1152/jn.00889.2005

Graziano, M. S. A., & Gross, C. G. (1998). Visual responses with and without fixation: neurons in premotor cortex encode spatial locations independently of eye position. *Experimental Brain Research*, *118*(3), 373–380. https://doi.org/10.1007/s002210050291

Graziano, M. S. A., Hu, X. T., & Gross, C. G. (1997). Visuospatial Properties of Ventral Premotor Cortex. *Journal of Neurophysiology*, *77*(5), 2268–2292. https://doi.org/10.1152/jn.1997.77.5.2268

Graziano, M. S. A., Taylor, C. S. R., & Moore, T. (2002). Complex Movements Evoked by Microstimulation of Precentral Cortex. *Neuron*, *34*(5), 841–851. https://doi.org/10.1016/s0896-6273(02)00698-0

Graziano, M. S. A., Yap, G. S., & Gross, C. G. (1994). Coding of Visual Space by Premotor Neurons. *Science*, *266*(5187), 1054–1057. https://doi.org/10.1126/science.7973661

Groh, J. M. (2001). Converting neural signals from place codes to rate codes. *Biological Cybernetics*, *85*(3), 159–165. https://doi.org/10.1007/s004220100249

Guerrasio, L., Quinet, J., Büttner, U., & Goffart, L. (2010). Fastigial Oculomotor Region and the Control of Foveation During Fixation. *Journal of Neurophysiology*, *103*(4), 1988–2001. https://doi.org/10.1152/jn.00771.2009

Haji-Abolhassani, I., Guitton, D., & Galiana, H. L. (2016). Modeling eye-head gaze shifts in multiple contexts without motor planning. *Journal of Neurophysiology*, *116*(4), 1956–1985. https://doi.org/10.1152/jn.00605.2015

Hanes, D. P., & Wurtz, R. H. (2001). Interaction of the Frontal Eye Field and Superior Colliculus for Saccade Generation. *Journal of Neurophysiology*, *85*(2), 804–815. https://doi.org/10.1152/jn.2001.85.2.804

Hardy, O., & Corvisier, J. (1996). Firing properties of preposito-collicular neurones related to horizontal eye movements in the alert cat. *Experimental Brain Research*, *110*(3), 413–424. http://www.ncbi.nlm.nih.gov/pubmed/8871100

Heinze, K., Ruh, N., Nitschke, K., Reis, J., Fritsch, B., Unterrainer, J. M., Rahm, B., Weiller, C., & Kaller, C. P. (2014). Transcranial direct current stimulation over left and right DLPFC: Lateralized effects on planning performance and related eye movements. *Biological Psychology*, *102*, 130–140. https://doi.org/10.1016/j.biopsycho.2014.07.019

Hepp-Reymond, M.-C., Kirkpatrick-Tanner, M., Gabernet, L., Qi, H.-X., & Weber, B. (1999). Context-dependent force coding in motor and premotor cortical areas. *Experimental Brain Research*, *128*(1–2), 123–133. https://doi.org/10.1007/s002210050827

Herman, J. P., Blangero, A., Madelain, L., Khan, A., & Harwood, M. R. (2013). Saccade adaptation as a model of flexible and general motor learning. *Experimental Eye Research*, *114*, 6–15. https://doi.org/10.1016/j.exer.2013.04.001

Herman, J. P., Harwood, M. R., & Wallman, J. (2009). Saccade adaptation specific to visual context. *Journal of Neurophysiology*, *101*(4), 1713–1721. https://doi.org/10.1152/jn.91076.2008

Histed, M. H., Bonin, V., & Reid, R. C. (2009). Direct activation of sparse, distributed populations of cortical neurons by electrical microstimulation. *Neuron*, *63*(4), 508–522. https://doi.org/10.1016/j.neuron.2009.07.016

Hopp, J. J., & Fuchs, A. F. (2004). The characteristics and neuronal substrate of saccadic eye movement plasticity. *Progress in Neurobiology*, *72*(1), 27–53. https://doi.org/10.1016/j.pneurobio.2003.12.002

Huang, X., & Lisberger, S. G. (2009). Noise correlations in cortical area MT and their potential impact on trial-by-trial variation in the direction and speed of smooth-pursuit eye movements. *Journal of Neurophysiology*, *101*(6), 3012–3030. https://doi.org/10.1152/jn.00010.2009

Inaba, N., Iwamoto, Y., & Yoshida, K. (2003). Changes in cerebellar fastigial burst activity related to saccadic gain adaptation in the monkey. *Neuroscience Research*, *46*(3), 359–368. https://doi.org/10.1016/s0168-0102(03)00098-1

Iwamoto, Y., & Kaku, Y. (2010). Saccade adaptation as a model of learning in voluntary movements. *Experimental Brain Research*, *204*(2), 145–162. https://doi.org/10.1007/s00221-010-2314-3

Jagadisan, U. K., & Gandhi, N. J. (2016). Disruption of Fixation Reveals Latent Sensorimotor Processes in the Superior Colliculus. *The Journal of Neuroscience : The Official Journal of the Society for Neuroscience*, *36*(22), 6129–6140. https://doi.org/10.1523/JNEUROSCI.3685-15.2016

Jagadisan, U. K., & Gandhi, N. J. (2017). Removal of inhibition uncovers latent movement potential during preparation. *ELife*, *6*, e29648. https://doi.org/10.7554/eLife.29648

Jagadisan, U. K., & Gandhi, N. J. (2017). *Population temporal structure supplements the rate code during sensorimotor transformations*. Cold Spring Harbor Laboratory. https://doi.org/10.1101/132514

Judge, S. J., Richmond, B. J., & Chu, F. C. (1980). Implantation of magnetic search coils for measurement of eye position: An improved method. *Vision Research*, *20*(6), 535–538. https://doi.org/10.1016/0042-6989(80)90128-5

Jürgens, R., Becker, W., & Kornhuber, H. H. (1981). Natural and drug-induced variations of velocity and duration of human saccadic eye movements: Evidence for a control of the neural pulse generator by local feedback. *Biological Cybernetics*, *39*(2), 87–96. https://doi.org/10.1007/BF00336734

Kaneda, K., Phongphanphanee, P., Katoh, T., Isa, K., Yanagawa, Y., Obata, K., & Isa, T. (2008). Regulation of burst activity through presynaptic and postsynaptic GABA(B) receptors in mouse superior colliculus. *The Journal of Neuroscience : The Official Journal of the Society for Neuroscience*, *28*(4), 816–827. https://doi.org/10.1523/JNEUROSCI.4666-07.2008

Kasap, B., & van Opstal, A. J. (2017). A spiking neural network model of the midbrain superior colliculus that generates saccadic motor commands. *Biological Cybernetics*, *111*(3–4), 249–268. https://doi.org/10.1007/s00422-017-0719-9

Kase, M., Miller, D. C., & Noda, H. (1980). Discharges of Purkinje cells and mossy fibres in the cerebellar vermis of the monkey during saccadic eye movements and fixation. *The Journal of Physiology*, *300*, 539–555. https://doi.org/10.1113/jphysiol.1980.sp013178

Katnani, H. A., & Gandhi, N. J. (2013). Time course of motor preparation during visual search with flexible stimulus-response association. *The Journal of Neuroscience : The Official Journal of the Society for Neuroscience*, *33*(24), 10057–10065. https://doi.org/10.1523/JNEUROSCI.0850-13.2013

Katnani, H. A., & Gandhi, N. J. (2012). The relative impact of microstimulation parameters on movement generation. *Journal of Neurophysiology*, *108*(2), 528–538. https://doi.org/10.1152/jn.00257.2012

Kaufman, M. T., Churchland, M. M., Ryu, S. I., & Shenoy, K. V. (2014). Cortical activity in the null space: permitting preparation without movement. *Nature Neuroscience*, *17*(3), 440–448. https://doi.org/10.1038/nn.3643

Keller, E. L. (1974). Participation of medial pontine reticular formation in eye movement generation in monkey. *Journal of Neurophysiology*, *37*(2), 316–332. https://doi.org/10.1152/jn.1974.37.2.316

Keller, E. L., & Edelman, J. A. (1994). Use of interrupted saccade paradigm to study spatial and temporal dynamics of saccadic burst cells in superior colliculus in monkey. *Journal of Neurophysiology*, *72*(6), 2754–2770. https://doi.org/10.1152/jn.1994.72.6.2754

Keller, E. L., Gandhi, N. J., & Weir, P. T. (1996). Discharge of superior collicular neurons during saccades made to moving targets. *Journal of Neurophysiology*, *76*(5), 3573–3577. https://doi.org/10.1152/jn.1996.76.5.3573

Klier, E. M., Wang, H., & Crawford, J. D. (2001). The superior colliculus encodes gaze commands in retinal coordinates. *Nature Neuroscience*, *4*(6), 627–632. https://doi.org/10.1038/88450

Knight, T. A., & Fuchs, A. F. (2007). Contribution of the Frontal Eye Field to Gaze Shifts in the Head-Unrestrained Monkey: Effects of Microstimulation. *Journal of Neurophysiology*, *97*(1), 618–634. https://doi.org/10.1152/jn.00256.2006

Kojima, Y., Iwamoto, Y., Robinson, F. R., Noto, C. T., & Yoshida, K. (2008). Premotor Inhibitory Neurons Carry Signals Related to Saccade Adaptation in the Monkey. *Journal of Neurophysiology*, *99*(1), 220–230. https://doi.org/10.1152/jn.00554.2007

Kojima, Y., Soetedjo, R., & Fuchs, A. F. (2010). Changes in simple spike activity of some Purkinje cells in the oculomotor vermis during saccade adaptation are appropriate to participate in motor learning. *The Journal of Neuroscience : The Official Journal of the Society for Neuroscience*, *30*(10), 3715–3727. https://doi.org/10.1523/JNEUROSCI.4953-09.2010

Kojima, Y., Soetedjo, R., & Fuchs, A. F. (2011). Effect of inactivation and disinhibition of the oculomotor vermis on saccade adaptation. *Brain Research*, *1401*, 30–39. https://doi.org/10.1016/j.brainres.2011.05.027

Kowler, E., & Blaser, E. (1995). The accuracy and precision of saccades to small and large targets. *Vision Research*, *35*(12), 1741–1754. https://doi.org/10.1016/0042-6989(94)00255-k

Krauzlis, R. J., Basso, M. A., & Wurtz, R. H. (2000). Discharge Properties of Neurons in the Rostral Superior Colliculus of the Monkey During Smooth-Pursuit Eye Movements. *Journal of Neurophysiology*, *84*(2), 876–891. https://doi.org/10.1152/jn.2000.84.2.876

Kurata, K., & Hoffman, D. S. (1994). Differential effects of muscimol microinjection into dorsal and ventral aspects of the premotor cortex of monkeys. *Journal of Neurophysiology*, *71*(3), 1151–1164. https://doi.org/10.1152/jn.1994.71.3.1151

Kustov, A. A., & Robinson, D. L. (1995). Modified saccades evoked by stimulation of the macaque superior colliculus account for properties of the resettable integrator. *Journal of Neurophysiology*, *73*(4), 1724–1728. https://doi.org/10.1152/jn.1995.73.4.1724

Lee, C., Rohrer, W. H., & Sparks, D. L. (1988). Population coding of saccadic eye movements by neurons in the superior colliculus. *Nature*, *332*(6162), 357–360. https://doi.org/10.1038/332357a0

Leigh, R. J., & Zee, D. S. (1999). *The Neurology of Eye Movements*. Oxford University Press. 3rd

Lennerstrand, G., & Bach-Yrita, P. (1976). Basic Mechanisms of Ocular Motility and Their Clinical Implications. *Optometry and Vision Science*, *53*(4), 209. https://doi.org/10.1097/00006324-197604000-00011

Liversedge, S., Gilchrist, I., & Everling, S. (2011). *The Oxford Handbook of Eye Movements*. Oxford University Press.

Livingston, K. (1995). The Cognitive Neurosciences . Michael S. Gazzaniga, Ed. MIT Press, Cambridge, MA, 1994. xiv, 1447 pp., illus., + plates. $95 or £64.95. A Bradford Book. *Science*, *267*(5204), 1670–1671. https://doi.org/10.1126/science.267.5204.1670.b

Lock, T. M., Baizer, J. S., & Bender, D. B. (2003). Distribution of corticotectal cells in macaque. *Experimental Brain Research*, *151*(4), 455–470. https://doi.org/10.1007/s00221-003-1500-y

Logothetis, N. K., Augath, M., Murayama, Y., Rauch, A., Sultan, F., Goense, J., Oeltermann, A., & Merkle, H. (2010). The effects of electrical microstimulation on cortical signal propagation. *Nature Neuroscience*, *13*(10), 1283–1291. https://doi.org/10.1038/nn.2631

Maranesi, M., Rodà, F., Bonini, L., Rozzi, S., Ferrari, P. F., Fogassi, L., & Coudé, G. (2012). Anatomo-functional organization of the ventral primary motor and premotor cortex in the macaque monkey. *European Journal of Neuroscience*, *36*(10), 3376–3387. https://doi.org/10.1111/j.1460-9568.2012.08252.x

May, P. J., Hartwich-Young, R., Nelson, J., Sparks, D. L., & Porter, J. D. (1990). Cerebellotectal pathways in the macaque: Implications for collicular generation of saccades. *Neuroscience*, *36*(2), 305–324. https://doi.org/10.1016/0306-4522(90)90428-7

May, P. J. (2006). The mammalian superior colliculus: laminar structure and connections. *Progress in Brain Research*, *151*, 321–378. https://doi.org/10.1016/S0079-6123(05)51011-2

Mayo, J. P., & Sommer, M. A. (2008). Neuronal adaptation caused by sequential visual stimulation in the frontal eye field. *Journal of Neurophysiology*, *100*(4), 1923–1935. https://doi.org/10.1152/jn.90549.2008

McLaughlin, S. C. (1967). Parametric adjustment in saccadic eye movements. *Perception & Psychophysics*, *2*(8), 359–362. https://doi.org/10.3758/bf03210071

Miller, J. M., Anstis, T., & Templeton, W. B. (1981). Saccadic plasticity: Parametric adaptive control by retinal feedback. *Journal of Experimental Psychology: Human Perception and Performance*, *7*(2), 356–366. https://doi.org/10.1037/0096-1523.7.2.356

Miyashita, N., & Hikosaka, O. (1996). Minimal synaptic delay in the saccadic output pathway of the superior colliculus studied in awake monkey. *Experimental Brain Research*, *112*(2). https://doi.org/10.1007/bf00227637

Monteon, J. A., Constantin, A. G., Wang, H., Martinez-Trujillo, J., & Crawford, J. D. (2010). Electrical Stimulation of the Frontal Eye Fields in the Head-Free Macaque Evokes Kinematically Normal 3D Gaze Shifts. *Journal of Neurophysiology*, *104*(6), 3462–3475. https://doi.org/10.1152/jn.01032.2009

Morén, J., Shibata, T., & Doya, K. (2013). The mechanism of saccade motor pattern generation investigated by a large-scale spiking neuron model of the superior colliculus. *PloS One*, *8*(2), e57134. https://doi.org/10.1371/journal.pone.0057134

Morrow, M. M., Jordan, L. R., & Miller, L. E. (2007). Direct comparison of the task-dependent discharge of M1 in hand space and muscle space. *Journal of Neurophysiology*, *97*(2), 1786–1798. https://doi.org/10.1152/jn.00150.2006

Munoz, D. P., Waitzman, D. M., & Wurtz, R. H. (1996). Activity of neurons in monkey superior colliculus during interrupted saccades. *Journal of Neurophysiology*, *75*(6), 2562–2580. https://doi.org/10.1152/jn.1996.75.6.2562

Munoz, D. P., & Wurtz, R. H. (1995). Saccade-related activity in monkey superior colliculus. I. Characteristics of burst and buildup cells. *Journal of Neurophysiology*, *73*(6), 2313–2333. https://doi.org/10.1152/jn.1995.73.6.2313

Mushiake, H., Inase, M., & Tanji, J. (1991). Neuronal activity in the primate premotor, supplementary, and precentral motor cortex during visually guided and internally determined sequential movements. *Journal of Neurophysiology*, *66*(3), 705–718. https://doi.org/10.1152/jn.1991.66.3.705

Nagy, B., & Corneil, B. D. (2010). Representation of Horizontal Head-on-Body Position in the Primate Superior Colliculus. *Journal of Neurophysiology*, *103*(2), 858–874. https://doi.org/10.1152/jn.00099.2009

Neromyliotis, E., & Moschovakis, A. K. (2017). Response Properties of Motor Equivalence Neurons of the Primate Premotor Cortex. *Frontiers in Behavioral Neuroscience*, *11*, 61. https://doi.org/10.3389/fnbeh.2017.00061

Nichols, M. J., & Sparks, D. L. (1996). Component stretching during oblique stimulation-evoked saccades: the role of the superior colliculus. *Journal of Neurophysiology*, *76*(1), 582–600. https://doi.org/10.1152/jn.1996.76.1.582

Nichols, M. J., & Sparks, D. L. (1995). Nonstationary properties of the saccadic system: new constraints on models of saccadic control. *Journal of Neurophysiology*, *73*(1), 431–435. https://doi.org/10.1152/jn.1995.73.1.431

Noto, C. T., Watanabe, S., & Fuchs, A. F. (1999). Characteristics of Simian Adaptation Fields Produced by Behavioral Changes in Saccade Size and Direction. *Journal of Neurophysiology*, *81*(6), 2798–2813. https://doi.org/10.1152/jn.1999.81.6.2798

Ohtsuka, K., & Noda, H. (1990). Direction-selective saccadic-burst neurons in the fastigial oculomotor region of the macaque. *Experimental Brain Research*, *81*(3), 659–662. https://doi.org/10.1007/bf02423517

Ohtsuka, K., & Noda, H. (1991). Saccadic burst neurons in the oculomotor region of the fastigial nucleus of macaque monkeys. *Journal of Neurophysiology*, *65*(6), 1422–1434. https://doi.org/10.1152/jn.1991.65.6.1422

Ohtsuka, K., & Noda, H. (1995). Discharge properties of Purkinje cells in the oculomotor vermis during visually guided saccades in the macaque monkey. *Journal of Neurophysiology*, *74*(5), 1828–1840. https://doi.org/10.1152/jn.1995.74.5.1828

Ohtsuka, K., Sato, H., & Noda, H. (1994). Saccadic burst neurons in the fastigial nucleus are not involved in compensating for orbital nonlinearities. *Journal of Neurophysiology*, *71*(5), 1976–1980. https://doi.org/10.1152/jn.1994.71.5.1976

Ohtsuka, K., & Noda, H. (1992). Burst discharges of mossy fibers in the oculomotor vermis of macaque monkeys during saccadic eye movements. *Neuroscience Research*, *15*(1–2), 102–114. https://doi.org/10.1016/0168-0102(92)90023-6

Opitz, B., & Kotz, S. A. (2012). Ventral premotor cortex lesions disrupt learning of sequential grammatical structures. *Cortex*, *48*(6), 664–673. https://doi.org/10.1016/j.cortex.2011.02.013

Osborne, L. C., Lisberger, S. G., & Bialek, W. (2005). A sensory source for motor variation. *Nature*, *437*(7057), 412–416. https://doi.org/10.1038/nature03961

Panouillères, M., Habchi, O., Gerardin, P., Salemme, R., Urquizar, C., Farne, A., & Pélisson, D. (2012). A Role for the Parietal Cortex in Sensorimotor Adaptation of Saccades. *Cerebral Cortex*, *24*(2), 304–314. https://doi.org/10.1093/cercor/bhs312

Paré, M., & Munoz, D. P. (2001). Expression of a re-centering bias in saccade regulation by superior colliculus neurons. *Experimental Brain Research*, *137*(3–4), 354–368. https://doi.org/10.1007/s002210000647

Pélisson, D., Alahyane, N., Panouillères, M., & Tilikete, C. (2010). Sensorimotor adaptation of saccadic eye movements. *Neuroscience & Biobehavioral Reviews*, *34*(8), 1103–1120. https://doi.org/10.1016/j.neubiorev.2009.12.010

Philipp, R., & Hoffmann, K.-P. (2014). Arm movements induced by electrical microstimulation in the superior colliculus of the macaque monkey. *The Journal of Neuroscience : The Official Journal of the Society for Neuroscience*, *34*(9), 3350–3363. https://doi.org/10.1523/JNEUROSCI.0443-13.2014

Phongphanphanee, P., Marino, R. A., Kaneda, K., Yanagawa, Y., Munoz, D. P., & Isa, T. (2014). Distinct local circuit properties of the superficial and intermediate layers of the

rodent superior colliculus. *The European Journal of Neuroscience*, *40*(2), 2329–2343. https://doi.org/10.1111/ejn.12579

Prsa, M., Dash, S., Catz, N., Dicke, P. W., & Thier, P. (2009). Characteristics of responses of Golgi cells and mossy fibers to eye saccades and saccadic adaptation recorded from the posterior vermis of the cerebellum. *The Journal of Neuroscience : The Official Journal of the Society for Neuroscience*, *29*(1), 250–262. https://doi.org/10.1523/JNEUROSCI.4791-08.2009

Pruszynski, J. A., King, G. L., Boisse, L., Scott, S. H., Flanagan, J. R., & Munoz, D. P. (2010). Stimulus-locked responses on human arm muscles reveal a rapid neural pathway linking visual input to arm motor output. *European Journal of Neuroscience*, *32*(6), 1049–1057. https://doi.org/10.1111/j.1460-9568.2010.07380.x

Quaia, C., Lefèvre, P., & Optican, L. M. (1999). Model of the control of saccades by superior colliculus and cerebellum. *Journal of Neurophysiology*, *82*(2), 999–1018. https://doi.org/10.1152/jn.1999.82.2.999

Quessy, S., Quinet, J., & Freedman, E. G. (2010). The locus of motor activity in the superior colliculus of the rhesus monkey is unaltered during saccadic adaptation. *The Journal of Neuroscience : The Official Journal of the Society for Neuroscience*, *30*(42), 14235–14244. https://doi.org/10.1523/JNEUROSCI.3111-10.2010

Reina, G. A., Moran, D. W., & Schwartz, A. B. (2001). On the relationship between joint angular velocity and motor cortical discharge during reaching. *Journal of Neurophysiology*, *85*(6), 2576–2589. https://doi.org/10.1152/jn.2001.85.6.2576

Rezvani, S., & Corneil, B. D. (2008). Recruitment of a head-turning synergy by low-frequency activity in the primate superior colliculus. *Journal of Neurophysiology*, *100*(1), 397–411. https://doi.org/10.1152/jn.90223.2008

ROBINSON, F. R., FUCHS, A. F., & NOTO, C. T. (2002). Cerebellar Influences on Saccade Plasticity. *Annals of the New York Academy of Sciences*, *956*(1), 155–163. https://doi.org/10.1111/j.1749-6632.2002.tb02816.x

Robinson, F. R., & Fuchs, A. F. (2001). The Role of the Cerebellum in Voluntary Eye Movements. *Annual Review of Neuroscience*, *24*(1), 981–1004. https://doi.org/10.1146/annurev.neuro.24.1.981

Robinson, F. R., Noto, C. T., & Bevans, S. E. (2003). Effect of Visual Error Size on Saccade Adaptation in Monkey. *Journal of Neurophysiology*, *90*(2), 1235–1244. https://doi.org/10.1152/jn.00656.2002

Rochat, M. J., Caruana, F., Jezzini, A., Escola, L., Intskirveli, I., Grammont, F., Gallese, V., Rizzolatti, G., & Umiltà, M. A. (2010). Responses of mirror neurons in area F5 to hand and

tool grasping observation. *Experimental Brain Research*, *204*(4), 605–616. https://doi.org/10.1007/s00221-010-2329-9

Rodgers, C. K., Munoz, D. P., Scott, S. H., & Paré, M. (2006). Discharge properties of monkey tectoreticular neurons. *Journal of Neurophysiology*, *95*(6), 3502–3511. https://doi.org/10.1152/jn.00908.2005

Sahibzada, N., Dean, P., & Redgrave, P. (1986). Movements resembling orientation or avoidance elicited by electrical stimulation of the superior colliculus in rats. *The Journal of Neuroscience : The Official Journal of the Society for Neuroscience*, *6*(3), 723–733. https://doi.org/10.1523/JNEUROSCI.06-03-00723.1986

Schall, J. D., Morel, A., King, D. J., & Bullier, J. (1995). Topography of visual cortex connections with frontal eye field in macaque: convergence and segregation of processing streams. *The Journal of Neuroscience : The Official Journal of the Society for Neuroscience*, *15*(6), 4464–4487. https://doi.org/10.1523/JNEUROSCI.15-06-04464.1995

Schieber, M. H. (2000). Inactivation of the ventral premotor cortex biases the laterality of motoric choices. *Experimental Brain Research*, *130*(4), 497–507. https://doi.org/10.1007/s002219900270

Schiller, P. H., & Malpeli, J. G. (1977). Properties and tectal projections of monkey retinal ganglion cells. *Journal of Neurophysiology*, *40*(2), 428–445. https://doi.org/10.1152/jn.1977.40.2.428

Schlag, J., Pouget, A., Sadeghpour, S., & Schlag-Rey, M. (1998). Interactions between natural and electrically evoked saccades. III. Is the nonstationarity the result of an integrator not instantaneously reset? *Journal of Neurophysiology*, *79*(2), 903–910. https://doi.org/10.1152/jn.1998.79.2.903

Schmidlin, E., Brochier, T., Maier, M. A., Kirkwood, P. A., & Lemon, R. N. (2008). Pronounced reduction of digit motor responses evoked from macaque ventral premotor cortex after reversible inactivation of the primary motor cortex hand area. *The Journal of Neuroscience : The Official Journal of the Society for Neuroscience*, *28*(22), 5772–5783. https://doi.org/10.1523/JNEUROSCI.0944-08.2008

Scudder, C. A., Batourina, E. Y., & Tunder, G. S. (1998). Comparison of Two Methods of Producing Adaptation of Saccade Size and Implications for the Site of Plasticity. *Journal of Neurophysiology*, *79*(2), 704–715. https://doi.org/10.1152/jn.1998.79.2.704

Scudder, C. A., & McGee, D. M. (2003). Adaptive Modification of Saccade Size Produces Correlated Changes in the Discharges of Fastigial Nucleus Neurons. *Journal of Neurophysiology*, *90*(2), 1011–1026. https://doi.org/10.1152/jn.00193.2002

Semmlow, J. L., GauthieR, G. M., & Vercher, J.-L. (1987). SHORT TERM ADAPTIVE MODIFICATION OF SACCADIC AMPLITUDE. In *Eye Movements from Physiology to Cognition* (pp. 191–200). Elsevier. https://doi.org/10.1016/b978-0-444-70113-8.50031-x

Sergio, L. E., Hamel-Pâquet, C., & Kalaska, J. F. (2005). Motor Cortex Neural Correlates of Output Kinematics and Kinetics During Isometric-Force and Arm-Reaching Tasks. *Journal of Neurophysiology*, *94*(4), 2353–2378. https://doi.org/10.1152/jn.00989.2004

Shadlen, M. N., & Kiani, R. (2013). Decision making as a window on cognition. *Neuron*, *80*(3), 791–806. https://doi.org/10.1016/j.neuron.2013.10.047

Shelhamer, M., & Clendaniel, R. A. (2002). Context-specific adaptation of saccade gain. *Experimental Brain Research*, *146*(4), 441–450. https://doi.org/10.1007/s00221-002-1199-1

Shmiel, T., Drori, R., Shmiel, O., Ben-Shaul, Y., Nadasdy, Z., Shemesh, M., Teicher, M., & Abeles, M. (2006). Temporally precise cortical firing patterns are associated with distinct action segments. *Journal of Neurophysiology*, *96*(5), 2645–2652. https://doi.org/10.1152/jn.00798.2005

Smalianchuk, I., Jagadisan, U. K., & Gandhi, N. J. (2018). Instantaneous Midbrain Control of Saccade Velocity. *The Journal of Neuroscience : The Official Journal of the Society for Neuroscience*, *38*(47), 10156–10167. https://doi.org/10.1523/JNEUROSCI.0962-18.2018

Soetedjo, R., & Fuchs, A. F. (2006). Complex spike activity of purkinje cells in the oculomotor vermis during behavioral adaptation of monkey saccades. *The Journal of Neuroscience : The Official Journal of the Society for Neuroscience*, *26*(29), 7741–7755. https://doi.org/10.1523/JNEUROSCI.4658-05.2006

Soetedjo, R., Kojima, Y., & Fuchs, A. F. (2008). Complex spike activity in the oculomotor vermis of the cerebellum: a vectorial error signal for saccade motor learning? *Journal of Neurophysiology*, *100*(4), 1949–1966. https://doi.org/10.1152/jn.90526.2008

Solman, G. J. F., Foulsham, T., & Kingstone, A. (2017). Eye and head movements are complementary in visual selection. *Royal Society Open Science*, *4*(1), 160569. https://doi.org/10.1098/rsos.160569

Sommer, M. A., & Wurtz, R. H. (2000). Composition and Topographic Organization of Signals Sent From the Frontal Eye Field to the Superior Colliculus. *Journal of Neurophysiology*, *83*(4), 1979–2001. https://doi.org/10.1152/jn.2000.83.4.1979

Sparks, D. L., & Mays, L. E. (1990). Signal transformations required for the generation of saccadic eye movements. *Annual Review of Neuroscience*, *13*(1), 309–336. https://doi.org/10.1146/annurev.ne.13.030190.001521

Sparks, D. L., Mays, L. E. (1981). The role of the monkey superior colliculus in the control of saccadic eye movements: A current perspective. In: Progress in Oculomotor Research, A. Fuchs and W. Becker (Eds.), Elsevier, New York, 1981, pp. 137-144.

Spedden, M. E., Beck, M. M., Christensen, M. S., Dietz, M. J., Karabanov, A. N., Geertsen, S. S., Nielsen, J. B., & Lundbye-Jensen, J. (2020). Directed connectivity between primary and premotor areas underlying ankle force control in young and older adults. *NeuroImage*, *218*, 116982. https://doi.org/10.1016/j.neuroimage.2020.116982

Stanford, T. R., Freedman, E. G., & Sparks, D. L. (1996). Site and parameters of microstimulation: evidence for independent effects on the properties of saccades evoked from the primate superior colliculus. *Journal of Neurophysiology*, *76*(5), 3360–3381. https://doi.org/10.1152/jn.1996.76.5.3360

Steenrod, S. C., Phillips, M. H., & Goldberg, M. E. (2013). The lateral intraparietal area codes the location of saccade targets and not the dimension of the saccades that will be made to acquire them. *Journal of Neurophysiology*, *109*(10), 2596–2605. https://doi.org/10.1152/jn.00349.2012

Straube, A., Fuchs, A. F., Usher, S., & Robinson, F. R. (1997). Characteristics of Saccadic Gain Adaptation in Rhesus Macaques. *Journal of Neurophysiology*, *77*(2), 874–895. https://doi.org/10.1152/jn.1997.77.2.874

Stryker, M., & Schiller, P. (1975). Eye and head movements evoked by electrical stimulation of monkey superior colliculus. *Experimental Brain Research*, *23*(1). https://doi.org/10.1007/bf00238733

Stuphorn, V., Hoffmann, K. P., & Miller, L. E. (1999). Correlation of primate superior colliculus and reticular formation discharge with proximal limb muscle activity. *Journal of Neurophysiology*, *81*(4), 1978–1982. https://doi.org/10.1152/jn.1999.81.4.1978

Takagi, M., Zee, D. S., & Tamargo, R. J. (1998). Effects of Lesions of the Oculomotor Vermis on Eye Movements in Primate: Saccades. *Journal of Neurophysiology*, *80*(4), 1911–1931. https://doi.org/10.1152/jn.1998.80.4.1911

Takeichi, N., Kaneko, C. R. S., & Fuchs, A. F. (2005). Discharge of monkey nucleus reticularis tegmenti pontis neurons changes during saccade adaptation. *Journal of Neurophysiology*, *94*(3), 1938–1951. https://doi.org/10.1152/jn.00113.2005

Takeichi, N., Kaneko, C. R. S., & Fuchs, A. F. (2007). Activity Changes in Monkey Superior Colliculus During Saccade Adaptation. *Journal of Neurophysiology*, *97*(6), 4096–4107. https://doi.org/10.1152/jn.01278.2006

Thompson, K. G., Hanes, D. P., Bichot, N. P., & Schall, J. D. (1996). Perceptual and motor processing stages identified in the activity of macaque frontal eye field neurons during

visual search. *Journal of Neurophysiology*, *76*(6), 4040–4055. https://doi.org/10.1152/jn.1996.76.6.4040

Tian, J., & Zee, D. S. (2010). Context-specific saccadic adaptation in monkeys. *Vision Research*, *50*(23), 2403–2410. https://doi.org/10.1016/j.visres.2010.09.014

van Beers, R. J. (2007). The sources of variability in saccadic eye movements. *The Journal of Neuroscience : The Official Journal of the Society for Neuroscience*, *27*(33), 8757–8770. https://doi.org/10.1523/JNEUROSCI.2311-07.2007

van Beers, R. J. (2008). Saccadic eye movements minimize the consequences of motor noise. *PloS One*, *3*(4), e2070–e2070. https://doi.org/10.1371/journal.pone.0002070

Van Gisbergen, J. A., Robinson, D. A., & Gielen, S. (1981). A quantitative analysis of generation of saccadic eye movements by burst neurons. *Journal of Neurophysiology*, *45*(3), 417–442. https://doi.org/10.1152/jn.1981.45.3.417

van Opstal, A. J., & Goossens, H. H. L. M. (2008). Linear ensemble-coding in midbrain superior colliculus specifies the saccade kinematics. *Biological Cybernetics*, *98*(6), 561–577. https://doi.org/10.1007/s00422-008-0219-z

Van Opstal, A. J., Hepp, K., Suzuki, Y., & Henn, V. (1995). Influence of eye position on activity in monkey superior colliculus. *Journal of Neurophysiology*, *74*(4), 1593–1610. https://doi.org/10.1152/jn.1995.74.4.1593

Vargas-Irwin, C. E., Franquemont, L., Black, M. J., & Donoghue, J. P. (2015). Linking Objects to Actions: Encoding of Target Object and Grasping Strategy in Primate Ventral Premotor Cortex. *The Journal of Neuroscience : The Official Journal of the Society for Neuroscience*, *35*(30), 10888–10897. https://doi.org/10.1523/JNEUROSCI.1574-15.2015

Vargas-Irwin, C. E., Shakhnarovich, G., Yadollahpour, P., Mislow, J. M. K., Black, M. J., & Donoghue, J. P. (2010). Decoding complete reach and grasp actions from local primary motor cortex populations. *The Journal of Neuroscience : The Official Journal of the Society for Neuroscience*, *30*(29), 9659–9669. https://doi.org/10.1523/JNEUROSCI.5443-09.2010

Vokoun, C. R., Jackson, M. B., & Basso, M. A. (2010). Intralaminar and interlaminar activity within the rodent superior colliculus visualized with voltage imaging. *The Journal of Neuroscience : The Official Journal of the Society for Neuroscience*, *30*(32), 10667–10682. https://doi.org/10.1523/JNEUROSCI.1387-10.2010

Waitzman, D. M., Ma, T. P., Optican, L. M., & Wurtz, R. H. (1991). Superior colliculus neurons mediate the dynamic characteristics of saccades. *Journal of Neurophysiology*, *66*(5), 1716–1737. https://doi.org/10.1152/jn.1991.66.5.1716

Wallman, J., & Fuchs, A. F. (1998). Saccadic Gain Modification: Visual Error Drives Motor Adaptation. *Journal of Neurophysiology*, *80*(5), 2405–2416. https://doi.org/10.1152/jn.1998.80.5.2405

Walton, M. M. G., Bechara, B., & Gandhi, N. J. (2007). Role of the primate superior colliculus in the control of head movements. *Journal of Neurophysiology*, *98*(4), 2022–2037. https://doi.org/10.1152/jn.00258.2007

White, B. J., Boehnke, S. E., Marino, R. A., Itti, L., & Munoz, D. P. (2009). Color-related signals in the primate superior colliculus. *The Journal of Neuroscience : The Official Journal of the Society for Neuroscience*, *29*(39), 12159–12166. https://doi.org/10.1523/JNEUROSCI.1986-09.2009

White, B. J., & Munoz, D. P. (2011). Separate visual signals for saccade initiation during target selection in the primate superior colliculus. *The Journal of Neuroscience : The Official Journal of the Society for Neuroscience*, *31*(5), 1570–1578. https://doi.org/10.1523/JNEUROSCI.5349-10.2011

Wilson, J. J., Alexandre, N., Trentin, C., & Tripodi, M. (2018). Three-Dimensional Representation of Motor Space in the Mouse Superior Colliculus. *Current Biology : CB*, *28*(11), 1744-1755.e12. https://doi.org/10.1016/j.cub.2018.04.021

Wolf, W., Deubel, H., & Hauske, G. (1984). Properties of Parametric Adjustment in the Saccadic System. In *Theoretical and Applied Aspects of Eye Movement Research, Selected/Edited Proceedings of The Second European Conference on Eye Movements* (pp. 79–86). Elsevier. https://doi.org/10.1016/s0166-4115(08)61821-x

Wurtz, R. H., & Goldberg, M. E. (1971). Superior Colliculus Cell Responses Related to Eye Movements in Awake Monkeys. *Science*, *171*(3966), 82–84. https://doi.org/10.1126/science.171.3966.82

Xu-Wilson, M., Chen-Harris, H., Zee, D. S., & Shadmehr, R. (2009). Cerebellar contributions to adaptive control of saccades in humans. *The Journal of Neuroscience: The Official Journal of the Society for Neuroscience*, *29*(41), 12930–12939. https://doi.org/10.1523/JNEUROSCI.3115-09.2009

Yamada, J., & Noda, H. (1987). Afferent and efferent connections of the oculomotor cerebellar vermis in the macaque monkey. *The Journal of Comparative Neurology*, *265*(2), 224–241. https://doi.org/10.1002/cne.902650207

Yoshida, K., Iwamoto, Y., Chimoto, S., & Shimazu, H. (2001). Disynaptic inhibition of omnipause neurons following electrical stimulation of the superior colliculus in alert cats. *Journal of Neurophysiology*, *85*(6), 2639–2642. https://doi.org/10.1152/jn.2001.85.6.2639